USP9X CONTROLS DNA REPLICATION FORK STABILITY AND THE REPLICATION STRESS CHECKPOINT THROUGH CLASPIN

Edel McGarry (BSc) (MSc)

Supervisor: Prof Corrado Santocanale

Centre for Chromosome Biology

Biochemistry, School of Natural Science

National University of Ireland Galway, Ireland

A thesis submitted to the National University of Ireland, Galway

for the degree of Doctor of Philosophy

February 2016

Contents

List of figures

List of abbreviations

Alphabetical order

APC	anaphase promoting complex
ATM	ataxia telangiectasia mutated
ATR	ATM Rad-3 related
ATRIP	ATR-interacting protein
BCL2	B-cell lymphoma 2
BECLIN-1	BCL2-interacting protein
CDC	cell division cycle proteins
CDKs	cyclin-dependent kinases
CDT1	chromatin licencing and DNA replication factor 1
CHK1	Checkpoint kinase 1
CI	catalytically inactive
CK1γ1	Casein kinase 1 gamma 1
CKBD	CHK1 binding domain
CMG	CDC45-MCM-GINS
CPC	chromosome passenger complex
CSM3	chromosome segregation in meiosis 3
CUL	cullin
DBF4	dumbbell forming protein 4
DDK	DBF4 dependent kinase
DDR	DNA damage repair pathway
DNA	Deoxyribonucleic acid
dNTPs	deoxyribonucleotides
DSB	double strand breaks
DSB	double strand break
DUB	deubiquitylating enzymes
EGFR	epidermal growth factor receptor
EV	empty vector
FDR	false discovery rates
GINS	Go-Ichi-Ni-San complex
GINS	gravitational constant
HECT	homology E6 C-terminus
HERC2	HECT And RLD domain containing E3 ubiquitin protein ligase 2
hr	hour
HU	hydroxyurea
ITCH	E3 ubiquitin-protein ligase Itchy homolog
JAKs	janus kinases
kDa	kilo dalton
KRAS	V-Ki-ras2 Kirsten rat sarcoma viral oncogene homolog

l	litre
M	mole
mass spectrometry	MS
MCL-1	myeloid cell leukaemia 1
MCM	mini-chromosome maintenance
min	minutes
ml	millilitre
mM	millimole
MRC1	mediator of replication checkpoint
MRN	MRE11-RAD50-NBS1
msec	millisecond
MULE	Mcl-1 ubiquitin ligase
MYC	myelocytomatosis oncogene cellular homolog
NT	non transfected
ORC	origin recognition complex
PCNA	proliferating cell nuclear antigen
PDAC	pancreatic ductal adenocarcinoma
PI	proteasome inhibitors
PIKKs	phosphatidylinositol-3-kinase-like kinase family
PLK1	polo-like kinase 1
PP2A	protein phosphatase 2A
pre-IC	pre-initiation complex
pre-RC	pre-replication complex
PRICKLE1	REST/NRSF-interacting LIM domain protein 1
PTM	post translation modifications
RAD	RF-C/activator 1 homolog
RFB	replication fork barrier
RFC	replication Factor C
RING	really interesting new gene
rNTPs	ribonucleotides
RPA	Replication Protein A
rpm	revolutions per minute
SCF	Skp1/Cul1/F-box protein
SCFFbw7	F-box/WD repeat-containing protein 7
sec	seconds
SMURF1	SMAD Specific E3 ubiquitin protein ligase 1
ssDNA	single strand DNA
STAT	signal transducer and activator of transcription
TGFβ	transforming growth factor beta
TIM	timeless homologue
TIPIN	Timeless-interacting protein

TNR	trinucleotide repeats
TOF1	topoisomerase interacting factor 1
TOPBP1	topoisomerase (DNA) II binding protein 1
TOPI	topoisomerase I
TRIM17	tripartite motif-containing protein 17
UB	ubiquitin
UBAP1	ubiquitin-associated protein 1
UCH	ubiquitin C-terminal hydrolases
USP	ubiquitin specific protease
WT	wild type
β-TrCP	β-transducin repeat containing protein
µl	microlitre
µM	micromole

Most abbreviations, other than commonly used expressions, are also defined at the first point of occurrence in the text.

Declaration

I hereby declare that the work presented in this thesis was carried out in accordance with the regulations of the National University of Ireland Galway. The research is original and entirely my own work, with the exception of the external input listed below. The thesis or any part thereof has not been submitted to the National University of Ireland, Galway or any other institution in connection with any other academic award. Any views expressed herein are that of the author.

Signed:…… Date:……..

External Input

Dr. Michael Rainey generated the Flp-In TREx HEK-293 cell lines used in this study.

Dr. Umberto Restuccia assisted with the mass spectrometry data collection and analysis.

Dr. David Gaboriau assisted with the Operetta quantification detailed in Figure 4.4 (C) and the generation of Figure 4.6 (D).

Dr. Kevin Wu assisted with the generation of Figure 4.8.2 (B) and (C).

Abstract

Cells possess checkpoint pathways which are important for maintaining genome stability and preventing cancer. These signalling pathways include the ATR and CHK1 kinases which are activated in response to DNA damage or replication stress. Activation of CHK1 by ATR requires the mediator protein Claspin. Claspin also regulates the rate of fork progression during DNA replication.

The levels of Claspin are cell cycle regulated and importantly Claspin is stabilised during S-phase. A growing number of ubiquitin ligases and deubiquitylating enzymes (DUBs) have been shown to affect Claspin stability, however how they cooperate in regulating Claspin levels remains unclear.

In this thesis, I have characterised an affinity tagged overexpression system allowing for the induction of Claspin. I extensively optimised a purification protocol for this protein and using, SILAC, a quantitative proteomic approach, I identified several proteins that differentially co-purify with Claspin compared to control cells. Among these, I found a novel DUB, USP9X. I have confirmed by reciprocal immunoprecipitation experiments that it binds to Claspin.

Using siRNA depletion and pharmacological inhibition strategies, I found that USP9X controls Claspin stability in an S-phase specific manner. I have also demonstrated that USP9X protects proteasome-dependent Claspin degradation. Using a DNA fiber spreading approach I have established that USP9X contributes to DNA replication fork stability. I have also established that USP9X contributes to the intra S-phase replication checkpoint response and the ability of a replication fork to recover following replication stress. Further still I have demonstrated that the depletion of USP9X leads to the spontaneous accumulation of DNA damage; however this damage can be significantly rescued with the simultaneous overexpression of Claspin. Therefore I propose that USP9X, through its role in the regulation of Claspin, is a novel player involved in the maintenance of genomic stability and in the DNA replication stress response pathway.

Manuscript submitted to Cancer Research, provisionally accepted December 2015.

Acknowledgements

I would like to begin by acknowledging the unwavering support of my supervisor Corrado. From my initial interview panel, through some tougher times, to now, the almost end, your advice professionally and friendship personally have helped me survive. For this and so much more I cannot thank you enough. Do not worry Galway is still a happy place for me. One last thing it was C-dawg, never Sea-Dog.

To members of the Santocanale lab past and present, Aga, Alex, Ais, Anna, Ashton, David, Edel, Gemma, Guan-Nan, Huong, Jennifer, Karolina, Kevin, Lorraine Mike and Rachel. Thank you guys, I sincerely doubt I would have got through this without the chats, tears, shops, cakes and pints. We got this! A special thank you to Mike for inflicting, I mean gifting Claspin upon me. Without your guidance and endless rounds of Mike questions, I would still be at my bench trying to get that Bradford right.

To my collaborators in the IFOM, Angela and Umbe, I must express huge gratitude for the expertise and kindness you showered me with, especially through those soapy samples. To all members of the Bachi group, thanks for the laughs along the way.

Undoubtingly one of the best experiences of this time was the opportunity to teach others. Thanks to my 'lab children,' Rachel and Karolina, for your enthusiasm, our mistakes and the questions you asked me for which I had no answer. You have taught me more than you can ever imagine.

To our lab neighbours, the PCI's and the Lahue's, who truly became friends, thank you. It makes such a difference to your day knowing that the people beside you are as mad as the people around you. Thanks also to the NCBES, REMEDI and CCB families, many of whom are not just colleagues, but friends.

I would like to acknowledge Molecular Medicine Ireland for funding my research but more importantly for introducing me to the other scholars of the CTRSP programme, who I now call friends. It is with great sadness that one such dear friend has since passed. Wesley, you truly were the best of us.

To the ladies of 6 Costello Rd, Ais, Marie and Steph. Over three years of madness, MKR, convents, hair-dryers and table topping parties. Although the lease is up, I know our friendships will endure.

To my dearest friends the 'Mercy Minxs', Ann, Brady, Claire, Emma, Grainne, Miriam and Sarah. I can barely remember a time without you lot making my life happier. Now as we grow older, emigrate, co-habitat and marry, our circumstances may change, but our love for each other will last.

To my family, Aoife, Mum and Dad, the last few years have been far from easy but we got through it, like I always knew we would. To Aoife, the world is still yours for the taking. Remember this, even without a doctorate you will always be the clever sibling! To my Mum and Dad, Jennifer and Liam, it is difficult to express in words what to say. You have always supported me (and no Dad I am not talking about the Bank of Mum and Dad, although for that and the Blue Bullet, thanks) and been my strongest allies. Yes the McGarry bunch may be slightly crazy, but would we have it any other way!

Finally to my late Granny May, you were and remain the best person I have ever known, our English lady. I will always remember your voice among the crowd, asking was I sure I even wanted to go to college. Well I must have Granny, as ten years later I'm still here!

CHAPTER 1 INTRODUCITON

1.1 - DNA replication initiation

1.1.1 - Introduction to DNA replication

DNA replication is required for complete transmission of genetic material during each cell division (Mechali, 2010). The sequence of events and many of the proteins involved in DNA replication are conserved throughout the eukaryotic world (Duderstadt et al., 2014). DNA replication requires the precise synthesis of large amounts of DNA. Errors occurring in replication can be amplified and accumulate over time, leading to genome instability, a hallmark of cancer (Macheret and Halazonetis, 2015). To help prevent this, cells possess numerous mechanisms to preserve genome integrity which include ensuring the fidelity of DNA replication at replication forks (Fragkos et al., 2015). The processes of replication and replication stress signalling, with particular focus on Claspin, a protein essential for both activities, are discussed in this introduction.

1.1.2 - DNA replication initiation: origin licensing

To facilitate duplication, a DNA double helix must open and unwind, which permits DNA synthesis machinery to copy both strands of DNA (Renard-Guillet et al., 2014). In humans these opening sites are called DNA replication origins, and are defined as the region on the genome from which replication can begin (Siddiqui et al., 2013). In every cell division, 30,000–50,000 DNA replication origins are activated (Mechali, 2010).

In eukaryotes, replication origins are determined in two discreet steps, first the assembly of the pre replication complex (pre-RC) site. This is a process known as replication origin licensing (Siddiqui et al., 2013; Yekezare et al., 2013). The second stage involves the activation of DNA synthesis, known as origin firing. This process is tightly regulated as once any origin is activated, it should not be activated a second time, in the same cell cycle (Fragkos et al., 2015).

DNA replication initiates with the assembly of pre-RCs, at the replication origins located on the genome (Renard-Guillet et al., 2014). Origin licensing is strictly confined to G1 and occurs following the sequential loading of pre-RC proteins on all potential origins present in the genome (Costa et al., 2013). The origin recognition complex (ORC), which is composed of the six subunits ORC1–6, is recruited to the DNA sequences of replication origins (Siddiqui et al., 2013). This event mediates the binding of cell division cycle protein 6 (CDC6) and chromatin licencing and DNA replication factor 1 (CDT1) to the origins. The loading of the mini-chromosome maintenance (MCM) helicase complex, which is comprised of the six subunits MCM2–7, is the final stage of the licensing process. Loading of MCM can only occur if ORC, CDC6 and CDT1 are already present on the origins (Yekezare et al., 2013) (Figure 1.1).

1.1.3 - DNA replication initiation: origin firing

Origin activation involves the formation of a pre-initiation complex (pre-IC) coupled with the activation of the MCM helicase complex. Assembly of the pre-IC occurs at the G1/S transition, and is triggered by the DBF4-CDC7 complex, also referred to as the DBF4 dependent kinase (DDK), as well as cyclin-dependent kinases (CDKs) (Mechali, 2010; Renard-Guillet et al., 2014). In human cells, the deregulation of origin firing can have deleterious effects, as demonstrated by the increased expression of CDC7 found in many cancer cell lines (Montagnoli et al., 2008).

The DDK and CDKs can phosphorylate several replication factors including MCM10, (RECQL4), Treslin, CDC45, Go-Ichi-Ni-San complex (GINS), topoisomerase DNA II binding protein 1 (TOPBP1) and DNA polymerase ε (Pol ε) (Figure 1.1). The phosphorylation of these factors promotes their loading on origins (Renard-Guillet et al., 2014; Siddiqui et al., 2013; Yekezare et al., 2013). DDK and CDKs can also directly phosphorylate several residues within the MCM2–7 complex, which enables helicase activation and DNA unwinding (Montagnoli et al., 2006).

When the MCM complex is initially loaded to form the pre-RC, it is an inactive head-to-head double hexamer that environs double-stranded DNA (Sun et al., 2014). During helicase activation the MCM2–7 double hexamer splits into two hexamers. Each hexamer can function at one of the two replication forks initiating from a single replication origin (Figure 1.1). This step is facilitated by the transient binding of DDK to chromatin. This allows DDK dependent phosphorylation of the MCM complex (Fragkos et al., 2015; Heller et al., 2011).

Helicase activation facilitates the recruitment of other proteins, such as replication factor C (RFC), proliferating cell nuclear antigen (PCNA), replication protein A (RPA) and DNA polymerases (Sherstyuk et al., 2014) (Figure 1.1). These convert the pre-IC into two functional replication forks that move in opposite directions away from the activated origin, with a protein complex, known as the replisome, at each fork, unless a replication fork barrier (RFB) is present (Jones and Petermann, 2012; Sun et al., 2014). This functional helicase found at each fork consists of CDC45, the MCM complex and the DNA replication complex GINS (referred to as the CMG complex) (Sun et al., 2015) is essential for the actual initiation of replication and fork progression (Jones and Petermann, 2012).

Typically, only one out of every three origins is activated, with the nearby origins remaining silent, although they have been licensed. Therefore, a replisome can only be formed in an activated origin (Yamazaki et al., 2013). Whereas factors involved in the DNA licensing and firing steps are relatively well understood, the exact mechanisms that are responsible for origin inhibition remain unclear. Similarly, it is not understood how origins are preferentially selected for activation or silencing. However multiple factors including, chromatin context and epigenetic information have been implicated in these processes (Renard-Guillet et al., 2014).

Following origin activation, cells are prevented from re-licensing during S-phase, which guarantees that chromosomes replicate only once per cell cycle (Siddiqui et al., 2013).

The interaction of CDT1 with its inhibitor geminin coupled with CDT1 degradation prevents re-licensing, as well as the phosphorylation of other initiation factors (Cayrou et al., 2010).

1.1.4 - DNA replication forks

A DNA replication fork has been defined as 'the branch point structure that forms during DNA replication, between two template DNA strands, at which nascent DNA synthesis is ongoing' (Branzei and Foiani, 2010).

Origin firing generates two bi-directional forks, each of which are associated with a multi component complex referred to as the replisome (Marheineke et al., 2005). Replisomes can unzip the helix and duplicate the separated DNA strands during genome replication (Yao and O'Donnell, 2009). Considering the importance of accurate replication, the assembly and activity of the replisome must be tightly regulated (Macheret and Halazonetis, 2015).

The movement of the functional helicase away from the origin occurs concurrently with the dissociation of the helicase loader and recruitment of primase in complex with DNA polymerase α (Foiani et al., 1997; Marini et al., 1997). Primase is the protein which mediates the synthesis of RNA primers on DNA strand templates (Duderstadt et al., 2014). Recruitment of the primase permits the loading of other components of the replisome including the elongation factors DNA polymerases ε and δ and polymerase accessory factors such as the clamp loader RFC and the processivity clamp PCNA (Branzei and Foiani, 2010; Duderstadt et al., 2014) (Figure 1.1). Claspin, the focus of this study is also associated with the replisome (Lee et al., 2003a; Osborn and Elledge, 2003) and its role in replication is discussed in further detail in Introduction Section 1.4.3.

The chemistry of DNA synthesis dictates that the elongation of replicating DNA strands occurs in the direction of 5′ to 3′ (Duderstadt et al., 2014). The anti-parallel nature of DNA allows continuous synthesis only in the strand elongated in the same direction as

the movement of the replication fork. This strand is referred to as the leading strand and is replicated by polymerase ε (Pursell et al., 2007; Yao and O'Donnell, 2009).

Simultaneously, copying of the complementary strand, known as the lagging strand, happens discontinuously, with the formation of short DNA fragments known as Okazaki fragments (Okazaki et al., 1967; Smith and Whitehouse, 2012). To overcome this disjoint, the lagging strand requires cycles of priming, clamp loading, polymerase δ loading and polymerase release at every Okazaki fragment (Yao et al., 2009) (Smith and Whitehouse, 2012).

Replication of the lagging strand can expose stretches of single stranded DNA (ssDNA). ssDNA binding proteins such as RPA, have to surround and protect such stretches until they are displaced by polymerase and the Okazaki fragments are processed and then ligated to the previous fragment (Jones and Petermann, 2012).

Other processes occurring at replication forks, including the removal of RNA primers and ligation of Okazaki fragments are mediated by proteins not generally thought of as part of the replisome. However these auxiliary activities are essential to the generation of an uninterrupted copy of DNA and the maintenance of genome integrity (Branzei and Foiani, 2010).

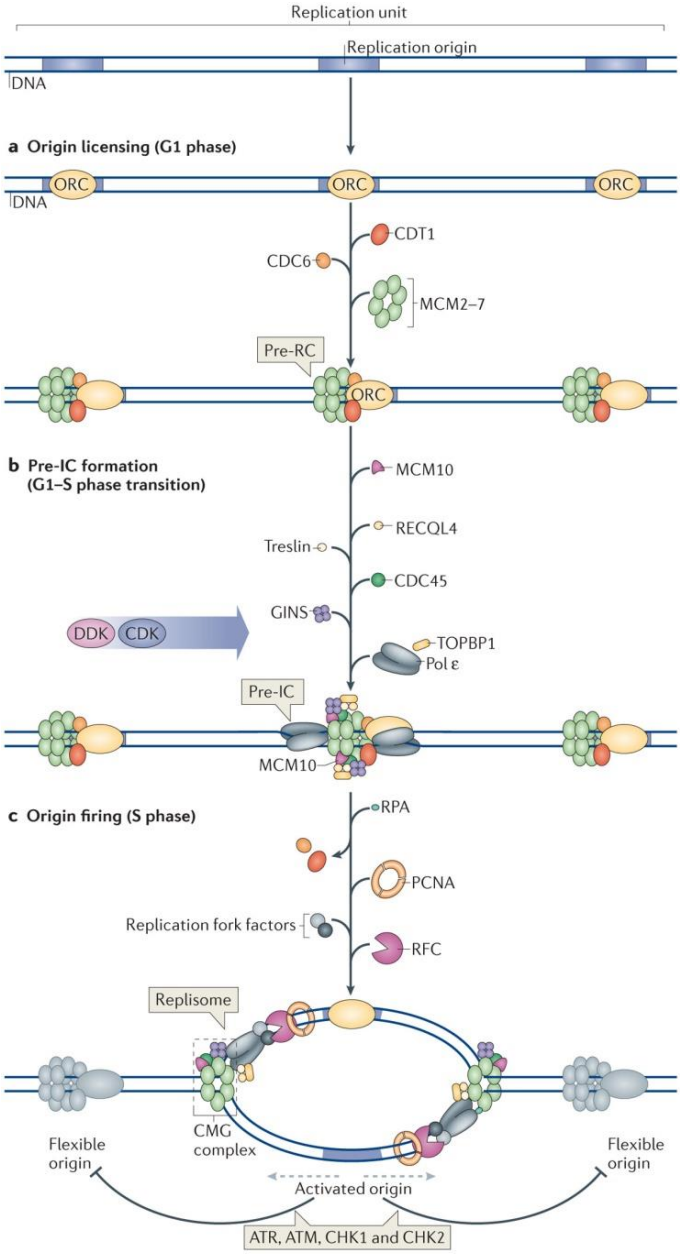

Figure 1.1. DNA replication initiation. (A) Replication origin licensing occurs following loading of pre-RC proteins on all potential origins. (B)(C) Origin activation involves the formation of a pre-IC and activation of the MCM helicase complex. Assembly of the pre-IC is triggered by DDK and CDKs at the G1–S phase transition, and its activation into a functional replisome occurs in the S phase. DDK and CDKs phosphorylate several replication factors to promote their loading on origins. DDK and CDKs can directly phosphorylate residues within the MCM2–7 complex, resulting in helicase activation and DNA unwinding. During helicase activation the MCM2–7 double hexamer divides into two hexamers that function at the two replication forks emanating from the replication origin. Figure taken from (Fragkos et al., 2015)

1.2 - Replication stress

1.2.1 - Causes

The DNA contained in mammalian cell is susceptible to both exogenous and endogenous sources of damage, which can directly attack its three billion bases or break the phosphodiester backbone on which the bases reside (Wang et al., 2015a). Damage to DNA is a serious threat as the information needed to synthesis RNA and proteins is contained within DNA. Unlike proteins or metabolites, DNA is the only cellular component that cannot be replenished upon damage and exclusively relies on repair (Pearl et al., 2015). During the S-phase of the cell cycle DNA is particularly vulnerable to insult. Throughout replication, cells detect and repair DNA damage, as if replication is corrupted, it will affect the normal function of the cell leading to genomic instability (Polo and Jackson, 2011).

Replication stress is caused by a variety of insults (Besteiro and Gottifredi, 2015), with unrepaired DNA lesions providing one of the most common sources of replication stress, acting as a physical barrier to fork progression. However, many other sources of stress have also been described (Besteiro and Gottifredi, 2015; Jones and Petermann, 2012; Marechal and Zou, 2013; Zeman and Cimprich, 2014).

Nicks and gaps are endogenous intermediates resulting from DNA repair pathways and therefore represent symptoms, but also sources of replication stress and when encountered by replication machinery can be converted to double strand breaks (DSBs) (Ayares et al., 1987).

The misincorporation of ribonucleotides is another cause of replication stress (Jones and Petermann, 2012; Potenski and Klein, 2014). While the replicative polymerases are highly specific at pairing bases, both Pol δ and Pol ε are less rigorous at discriminating deoxyribonucleotides (dNTPs) from ribonucleotides (rNTPs), which they incorporate at an extremely high rate. Misincorporated rNTPs can be recognised and removed through

ribonucleotide excision repair by the specialised enzyme RNase H2. Loss of RNase H2 is lethal in mammalian cells and demonstrates that the removal of misincorporated rNTPs is vital for cell survival (Potenski and Klein, 2014). Misincorporated rNTPs can stall the replicative polymerases, and additionally can be aberrantly processed into non-ligatable ssDNA nicks by topoisomerase I (TOPI), which results in replication stress (Williams et al., 2013).

There are a number of DNA sequences that are inherently difficult for cells to replicate. For example, trinucleotide repeats (TNRs), which can form secondary DNA structures such as hairpins, are proposed to block replication fork progression or encourage replication slippage (McMurray, 2010). This leads to expansion or contraction of the TNR sequence resulting in gene dysfunction, through replication-dependent mechanisms (McMurray, 2010).

The overexpression or activation of oncogenes such as Myelocytomatosis oncogene cellular homolog (MYC) and cyclin E are emerging sources of replication stress, although the mechanism remains unclear. These oncogenes promote increased replication initiation or origin firing. This can enhance the depletion of nucleotide pools, adversely effecting replication (Zeman and Cimprich, 2014).

Obstructions on the DNA that specifically affect the progression of the replication fork can lead to uncoupling of the replicative polymerase and helicase activities (Zeman and Cimprich, 2014). The helicase then continues unwinding the DNA which leads to the generation of extremely long stretches of ssDNA (Jones and Petermann, 2012). If the obstruction or stress is not efficiently dealt with, forks can collapse into DNA DSBs. This is a highly mutagenic and the most deleterious form of DNA damage (Zeman and Cimprich, 2014) which can contribute to genome instability, mutation and ultimately disease (Wang et al., 2015a).

1.2.2 - DNA damage response pathways

Importantly, cellular surveillance mechanisms, collectively known as the DNA damage response (DDR) pathways, which overlap with the DNA damage repair pathways detect, stabilise and resolve stalled replication forks or DNA breaks (Branzei and Foiani, 2010; Macheret and Halazonetis, 2015). This prevents cell death or massive mutagenesis which helps preserve genome integrity. The response from the DDR pathways promotes DNA repair, translesion synthesis, cell cycle arrest or apoptosis in a timely and accurate fashion (Polo and Jackson, 2011).

Two central players in the DDR signalling pathways are the ataxia telangiectasia mutated (ATM) and ATM Rad-3 related (ATR) protein kinases. These large Serine/Threonine kinases are members of the phosphatidylinositol-3-kinase-like kinase family (PIKKs). The ATR and ATM kinases are activated preferentially depending on the source of genomic insult, although there is considerable cross talk between the two pathways (Marechal and Zou, 2013).

Like classic signal transduction pathways, the DDR uses signal sensors, transducers, and effectors. However, the DDR is not activated by ligands of receptor kinases, but instead aberrant DNA structures induced by DNA damage or DNA replication stress (Marechal and Zou, 2013) (Figure 1.2.2).

ATM and ATR preferentially phosphorylate serine (S) and threonine residues (T), followed by glutamine residues (Q) (SQ/TQ motifs) on target proteins. Their substrates often have clusters of SQ/TQ motifs (Walker et al., 2009). While the ATM kinase is mainly activated in response to double-strand DNA breaks, ATR signalling is activated in response to replication stress and will be discussed in greater detail in Introduction Section 1.2.3 (Cimprich and Cortez, 2008).

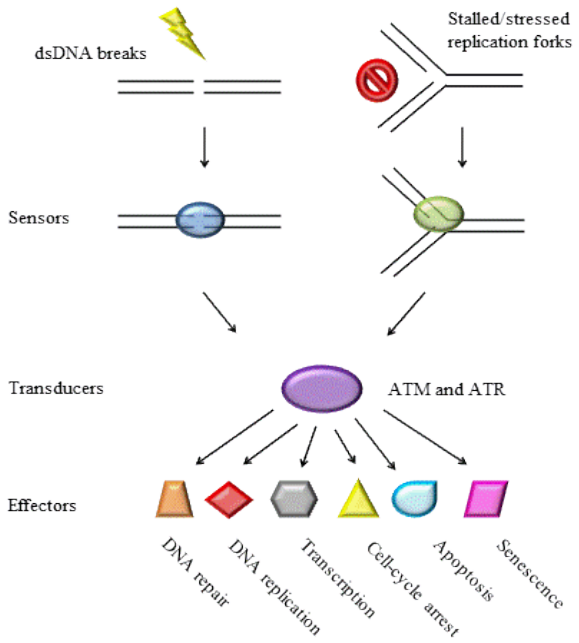

Figure 1.2.2. DDR signalling pathways. The DDR signalling pathways are composed of signal sensors, transducers, and effectors. Sensors proteins recognise DNA structures induced by DNA damage such as dsDNA breaks and DNA replication stress. Transducers consist of kinases, including ATM, ATR, and their downstream kinases. The effectors are target proteins of ATM and ATR. They are responsible for numerous cellular processes that are important for maintenance of genomic integrity. Figure adapted from (Marechal and Zou, 2013).

1.2.3 - Replication checkpoint signalling

The detection of ssDNA leads to the recruitment of RPA, to coat and to protect the DNA strands and the activation of the replication stress response (Jones and Petermann, 2012). This event serves as a signalling platform, facilitating the recruitment of a number of replication stress response proteins. The most important of which is the ATR protein kinase and its interacting protein ATRIP (ATR-interacting protein) (Cimprich and Cortez, 2008).

The ATR/ATRIP complex, in coordination with the RF-C/activator 1 homolog 17 (RAD17) and the 9–1–1 (RAD9-HUS1-RAD1) complex, also known as the RAD17-RFC complex recruits an essential ATR activator, TOPBP1 to sites of damage (Besteiro and Gottifredi, 2015). TOPBP1 contains the ATR activation domain which is responsible for

stimulation of ATR kinase activity. Recruitment of TOPBP1 is mediated by the interaction of RAD9 to the BRCT domains of TOPBP1. Following replicative stress, TOPBP1 is phosphorylated by ATR which enhances the ATR-TOPBP1 interaction, further promoting the activation of ATR (Cimprich and Cortez, 2008). Activated ATR can phosphorylate target proteins on SQ/TQ sites to facilitate signal transmission to downstream effector proteins, enabling control of cell cycle progression (Walker et al., 2009). One well characterised substrate of ATR is checkpoint kinase 1 (CHK1).

CHK1 was initially identified by the Beach laboratory in 1993 as a Serine/Threonine kinase that regulates the G2/M transition in response to DNA damage in the fission yeast *Schizosaccharomyces pombe* (Walworth et al., 1993). Subsequently orthologues of CHK1 have been identified from *Drosophila* to human (Flaggs et al., 1997). Following the discovery in 1996 that CHK1 is phosphorylated in response to DNA damage in yeast, and later in humans, over the succeeding 20 years it has become apparent that CHK1 plays an essential role in the response to DNA damage (Sanchez et al., 1997; Walworth and Bernards, 1996) with ATR mediated phosphorylation of CHK1 conserved from yeast to human (Zhang and Hunter, 2014).

ATR mediated phosphorylation of CHK1 on Serine 317 and 345, activates CHK1 on the chromatin. Fully activated CHK1 is released from chromatin and can phosphorylate downstream effectors to appropriate an effective DNA damage response. Efficient phosphorylation of CHK1 by ATR is promoted by several other replication and checkpoint proteins, including RAD9, RAD17, TOPBP1 as well as the complex of TIM (timeless homologue) and TIPIN (TIMELESS-interacting protein) (Jones and Petermann, 2012). Claspin contributes to this process by binding to CHK1 which facilitates ATR mediated CHK1 activation and is discussed in further detail in Introduction Section 1.5.2.

Activated CHK1 in turn phosphorylates the cell cycle phosphatases CDC25-A, CDC25-B and CDC25-C to prevent activation of cyclin E/A-CDK2 and cyclin B-CDK1. This slows progression through S-phase and prevents mitotic entry, delaying cell cycle progression (Cimprich and Cortez, 2008; Zeman and Cimprich, 2014). Suppression of late origin firing by activated CHK1 also provides additional time for resolution of the

replicative stress (Zeman and Cimprich, 2014). This offers the cell time to restart or repair the stalled replication forks and permits the preservation of resources to finish DNA synthesis adjacent to stalled replication forks. Replication forks that are stabilised by the ATR pathway can be restarted once the replicative stress has been removed (Zeman and Cimprich, 2014). Indeed ATR helps stabilise and restart the stalled fork and suppress recombination (Besteiro and Gottifredi, 2015).

In response to DNA damage, ATM requires the MRE11-RAD50-NBS1 (MRN) complex in co-ordination with the mediator of DNA-damage checkpoint 1 (MDC1) along with p53 binding protein 1 (53BP1) and other signalling protein, for its activation. CHK2, its downstream effector kinase, can then target CDKs and p53. Although considered much less important in the response to replication stress, ATM can be phosphorylated and activated by ATR in response to replication blockage (Stiff et al., 2006). ATM can also slow cell cycle progression in response to DNA damage, through inhibition of origin firing and contributes to the stabilisation and repair of damaged replication forks (Trenz et al., 2006).

Despite the complex response initiated by ATR and to a much lesser extent ATM to stabilise and restart a stalled fork, the fork may fail to restart, and collapse. This occurs if replication stress persists or if important replication stress response proteins are lost (Besteiro and Gottifredi, 2015). Fork collapse is also associated with the formation of a DSB at the stalled fork (Duderstadt et al., 2014; Zeman and Cimprich, 2014). A DSB may result from a cells attempt to resolve a fork that has been difficult to resolve, by using endonucleolytic cleavage and recombination based restart pathways (Yu et al., 2014). Secondly, DSBs can result from the persistence of ssDNA located in gaps left behind the stalled fork which can be targeted by endonucleases and which are prone to double strand breakage (Branzei and Foiani, 2010; Langston et al., 2009).

Several diseases are linked to defects in replication stress signalling including Seckel syndrome which is characterised by developmental delay, microcephaly, mental retardation, is associated with a mutation of ATR or ATRIP (Ogi et al., 2012). However

the most common disease related to replication stress is cancer (Aze et al., 2013; Macheret and Halazonetis, 2015). Indeed genome instability, associated with replicative stress defects, is a hallmark of the disease (Macheret and Halazonetis, 2015).

1.3 - Attenuation of replication stress signalling

1.3.1 - Attenuation of CHK1 signalling

If DNA damage has been successfully repaired, the attenuation of checkpoint signalling is needed to facilitate resumption of DNA replication and to prevent cell death resulting from trapping of cells in S-phase (Besteiro and Gottifredi, 2015; Duderstadt et al., 2014; Sun et al., 2015; Zeman and Cimprich, 2014). CHK1 is subject to strict regulation, with CHK1 inactivated directly by proteasomal mediated degradation and dephosphorylation, or indirectly by the destruction of Claspin, the latter of which is discussed briefly in Introduction Section 1.5.2.

1.3.2 - Proteasomal mediated degradation of CHK1

Post-translation regulation, contributes to the reduction in CHK1 levels, observed after replication stress. Added to this accumulation of CHK1 in normal cycling cells is reported following the addition of proteasome inhibitors, indicating that the protein is subject to constant degradation (Besteiro and Gottifredi, 2015).

A degron-like region found in the C-terminal domain of CHK1 flags the protein for ubquitylation and degradation and predominantly contributes to the regulation of CHK1 levels. Two Cullin-RING E3 ubiquitin ligases (CRLs), cullin 1 (CUL1) and CUL4A, mediate CHK1 ubiquitylation. Ubquitylation of CHK1 requires dephosphorylation of Serine 345 by ATR but not Serine 317 (Duderstadt et al., 2014).

1.3.3 - Dephosphorylation of CHK1

Dephosphorylation of CHK1 occurs in both normal cycling cells and in cells subjected to replicative stress. In unperturbed cells, the Serine/Threonine phosphatase, protein phosphatase 2A (PP2A) dephosphorylates Serine 317 and 345 which requires CHK1 kinase activity (Leung-Pineda et al., 2006). During replication stress when CHK1 activity

is increased, PP2A mediated dephosphorylation of CHK1 is prevented (Freeman and Monteiro, 2010).

A second phosphatase is involved in S-phase checkpoint recovery, the p53-regulated PP2C Serine/Threonine protein phosphatase WIP1 (PPM1D) (Besteiro and Gottifredi, 2015). *In vitro*, PPM1D contributes to CHK1 dephosphorylation and inactivation but does not appear to contribute to CHK1 destruction during unperturbed replication (Lu et al., 2005).

1.4 - Termination of replication

DNA replication is terminated in eukaryotic cells when two opposing replication forks collide. This results in local completion of DNA synthesis, decatenation of daughter molecules and replisome disassembly (Dewar et al., 2015). In *Xenopus* egg extracts it had been proposed that termination occurs at random sites which made the process difficult to capture and study. Recent, a study in *Xenopus* egg extracts, by the Walter laboratory, paused converging replisomes with a site-specific barrier. After removing the barrier, forks could undergo synchronous and site-specific termination. The study demonstrated that DNA synthesis does not slow down as forks approach one another, and that leading strands pass each other unimpeded before undergoing ligation to downstream lagging strands. Dissociation of the replicative CDC45-MCM-GINS (CMG) helicase occurs only after ligation is complete, and is not needed for completion of DNA synthesis. This indicated that converging CMGs pass each other and dissociate from dsDNA. (Dewar et al., 2015).

1.5 – Claspin, critical for both replication and the replication checkpoint

1.5.1 - Initial description of Claspin

Claspin was first identified in *Xenopus* egg extracts as a novel protein that interacted with CHK1, upon activation of replication stress signalling (Kumagai and Dunphy, 2000). Claspin is evolutionarily conserved amongst higher eukaryotes and the subsequently identified human homologue shares 49% identity with *Xenopus* Claspin (Kumagai and

Dunphy, 2000). A functional yeast homologue has also been identified, and named mediator of replication checkpoint (MRC1) but this protein contains little sequence similarity to Claspin (Tanaka and Russell, 2001).

In its initial description, Claspin was demonstrated to be a large (1339 amino acids long) and very acidic (pI 4.5) protein. Although the predicted molecular weight of Claspin is between 150-160 kDa, in SDS-PAGE the protein migrates to ~250 kDa and this has been attributed to the acidic nature of the protein. Claspin contained no previously defined motifs found on other DNA damage response proteins such as FHA or BRCT domains (Kumagai and Dunphy, 2000), or indeed shared motifs with any other protein except between other Claspin homologues in other organisms. However SQ/TQ sites were contained within the protein, which are known to be preferentially targeted by the ATM/ATR kinases as discussed previously (Cimprich and Cortez, 2008). Electron microscopy studies have revealed that Claspin is a ring-like structure that appears to circle DNA and bind with high affinity to branched DNA molecules specifically at single-stranded structures (Chini and Chen, 2004; Sar et al., 2004).

Since its initial description, two broadly defined roles for Claspin, briefly eluded to in the preceding text, have emerged, one to mediate CHK1 activation and deactivation, and the other as a component of the replication fork.

1.5.2 - Claspin a mediator of the replication checkpoint activation and deactivation

As mentioned, Dunphy's laboratory was first to implicate a role for Claspin in the replication checkpoint in *Xenopus* (Kumagai and Dunphy, 2000). Thereafter, human Claspin was also shown to be required for activation of CHK1 in response to replication stress (Chini and Chen, 2003, 2004). Owing to its ring like structure and ability to bind to ssDNA structures that may form at stalled replication forks, Claspin provides a frontline damage sensor in the mammalian checkpoint response (Sar et al., 2004). Depletion of Claspin can attenuate CHK1 activation in response to replication stress. Further still, in human cells the down-regulation of Claspin enhances the premature chromatin condensation induced by Hydroxyurea, prevents the UV-induced reduction of DNA synthesis and decreases cell survival, indicating the critical role for Claspin in

replication checkpoint control in mammalian cells (Chini and Chen, 2003, 2004). This demonstrates the crucial function Claspin plays in maintaining genomic integrity.

Further investigation into the mechanism of CHK1 activation mediated by *Xenopus* Claspin revealed that an evolutionarily conserved, 57 amino acid region of Claspin, called the CHK1 binding domain (CKBD) is vital for CHK1 binding and activation (Kumagai and Dunphy, 2003). Human Claspin CKBD is phosphorylated in a similar fashion to the *Xenopus* homologue, however it contains three repeat sequences, only two of which are required for CHK1 activation (Clarke and Clarke, 2005). These phosphoserines were initially described as induced by the checkpoint, allowing Claspin to bind to the catalytic domain of CHK1, which mediates CHK1 activation by ATR, accumulating in the release of activated CHK1 from the chromatin (Jeong et al., 2003) (Kumagai et al., 2004). Although originally proposed that Claspin interacted with CHK1 in response to damage, it has now been shown that the Claspin and CHK1 can interact continually (Rainey et al., 2013).

However, this phosphorylation may not be directly attributed to ATR as these conserved sites do not represent ATM/ATR consensus phosphorylation motifs (SQ/TQ) (Kumagai and Dunphy, 2003). Nevertheless two other SQ residues on Claspin, identified by phospho-proteomic analysis, Serine 839 and 950, are phosphorylated in response to IR and UV irradiation, proposing that ATM/ATR could regulate additional sites to those in the CKBD (Matsuoka et al., 2007).

Alternative kinases have also been proposed to be responsible for the phosphorylation of Claspin including CHK1 itself. CHK1 is reported to phosphorylate Claspin on Serine 916 which regulates the Claspin-CHK1 interaction (Chini and Chen, 2006). However, this was later disputed, with studies demonstrating that Claspin phosphorylation at this site was CHK1 independent (Bennett et al., 2008). Casein kinase 1 gamma 1 (CK1γ1) has been identified to be essential for Claspin phosphorylation as well as its interaction with, and activation of CHK1 (Meng et al., 2011).

CDC7 kinase has also been implicated in Claspin phosphorylation (Kim et al., 2008). Studies from our group have demonstrated that inhibition of CDC7 kinase contributes to diminished Claspin phosphorylation, following Hydroxyurea (HU) treatment. This may contribute to the associated delay in the induction of CHK1 phosphorylation observed, following replicative stress (Rainey et al., 2013). Using a mass-spectrometry approach, multiple putative CDC7 phosphorylation sites on Claspin were also identified (Rainey et al., 2013). Further still CDC7 kinase activity helps mediate the interaction between Claspin and the DNA helicase subunit MCM2, demonstrating that CDC7 dependent phosphorylation is important in the regulation of critical Claspin protein interactions (Rainey et al., 2013).

Given the importance of the phosphorylation induced Claspin-CHK1 interaction, the complete elucidation of the kinase mediated Claspin phosphorylation in the CKBD will provide an important discovery. A study to recapitulate the ATR mediated phosphorylation of CHK1 using recombinant proteins ATR, TOPBP1, Claspin and CHK1, indicated that Claspin greatly stimulates the kinase activity of ATR towards CHK1 but no other ATR substrates (Lindsey-Boltz et al., 2009). This confirms the specificity of Claspin for ATR mediated phosphorylation of CHK1.

Claspin also plays a role in the deactivation of the replication checkpoint which is needed to re-enter the cell cycle once damaged DNA has been repaired. This is critical for the completion of replication. Phosphorylation of Claspin by polo-like kinase 1 (PLK1), which targets Claspin for degradation, contributes to the termination of CHK1 signalling (Mailand et al., 2006). The extinction of active Serine 317 and 345 phosphorylated CHK1 is promoted by the destruction of Claspin (Gewurz and Harper, 2006). The proteasomal mediated regulation of Claspin will be discussed in further detail in Introduction Section 1.6.2.

1.5.3 - The role of Claspin at replication forks

After the revelation of Claspin's role as a mediator protein of the replication checkpoint, numerous studies have demonstrated a role for Claspin in replication.

In *Xenopus* egg extracts Claspin was first described to associate with the replication fork during S-phase (Lee et al., 2003a). This association was dependent upon CDC45 and S-CDK but not replication protein A (RPA), indicating that Claspin is loaded onto the chromatin at the DNA unwinding stage of initiation, similar to Pol ε (Lee et al., 2003a). The absence of Claspin in these extracts resulted in the slowing down of replication, suggesting that Claspin is needed to promote normal replication (Lee et al., 2003a).

This hypothesis was confirmed by DNA fibre analysis which examined replication kinetics in the absence of Claspin in human cells (Petermann et al., 2008). Depletion of Claspin slowed the progression of replication forks, a singularity that had also been observed upon CHK1 depletion (Petermann et al., 2006). This indicated that Claspin works by facilitating CHK1 mediated replication fork progression. However, when Claspin and CHK1 were simultaneously depleted from cells, there was a greater decrease in replication fork progression observed than when the proteins were depleted individually (Petermann et al., 2008). This suggested that Claspin and CHK1 have distinct and independent roles in promoting normal replication.

This was later confirmed by a study that showed that in the absence of either Claspin or CHK1, replicating cells displayed a higher number of stalled forks and a higher number of fired origins, as examined by DNA combing (Scorah and McGowan, 2009). Subsequent to replication stress CHK1 can inhibit origin firing by suppressing the CDC25-CDK2 pathway, but Claspin does not appear to be needed for CHK1 activation in this context. Following replicative stress, Claspin depletion did not lead to an increase in origin firing, suggesting that Claspin is not required to suppress origin firing under such conditions. Therefore, CHK1 but not Claspin is needed to inhibit origin firing under replication stress (Scorah and McGowan, 2009). How exactly Claspin regulates origin firing and fork stalling during normal replication is not yet completely understood.

Claspin, as well as interacting proteins TIM and TIPIN, may promote replication fork progression through direct interactions with the replication machinery. As well as TIM and TIPIN, Claspin can interact with multiple replication fork proteins such as CDC45,

replication factor C (RFC), RPA, and polymerase ε (Pol ε) (Tanaka, 2010). The yeast orthologues of Claspin, TIM and TIPIN, (mediator of replication checkpoint (MRC1), topoisomerase interacting factor 1 (TOF1) and chromosome segregation in meiosis 3 (CSM3), respectively) can form a complex that promotes both replication fork progression and stability. One way in which the MRC1–TOF1–CSM3 complex is thought to achieve this is by coupling polymerase and helicase activities to prevent excessive unwinding and ssDNA formation. A similar function has been proposed for its vertebrate homologues (Jones and Petermann, 2012). Taken together this suggests that the Claspin-TIM-TIPIN interaction may be important for the regulation of DNA replication.

Consistent with a role in contributing to normal replication and mirroring what is seen for ATR down regulation, Claspin depletion leads to increased fragile site instability. Fragile sites are regions in the genome that are extremely sensitive to replication stress and due to the difficulty in replicating through such regions, often leads to chromosomal abnormalities (Focarelli et al., 2009).

1.6 - Claspin regulation by ubiquitylation and deubiquitylation

While studying the subcellular localisation of Claspin, the Lukas group observed that Claspin levels varied, among individual cells, in a cell cycle dependent manner (Mailand et al., 2006). This study demonstrated that in mammalian cells, the levels of Claspin oscillate, with protein levels high in S-phase but supressed in G2/M and G1 phases (Mailand et al., 2006). This fluctuation was subsequently attributed to Claspin regulation by the post translation modifications (PTMs) of ubiquitylation and deubiquitylation (Freire et al., 2006; Mamely et al., 2006).

1.6.1 - Ubiquitylation

PTMs help to regulate protein function by influencing localisation, activity, signal transduction cascade and stabilisation. A hallmark of PTMs is that they are rapid and reversible, which facilitates cellular regulation of various signalling pathways depending

on environmental conditions (Hutchins et al., 2013; Murtaza et al., 2015; Sowa et al., 2009). Among the PMTs ubiquitylation is one of the best studied.

During this process proteins are covalently linked to ubiquitin, a 76 amino acid (8.5 kDa) protein (Berndsen and Wolberger, 2014; Sahtoe and Sixma, 2015). Ubiquitin is encoded by four genes UBC, UBB, UBA52 and UBA80. It can be transcribed and translated as a linear fusion consisting of multiple copies of ubiquitin or ubiquitin fused to the amino terminus of two ribosomal proteins, 40S ribosomal protein L40 and 60S ribosomal protein S27a (Komander et al., 2009). Whilst attachment of ubiquitin was initially described as a process of tagging proteins for degradation, study of the process has evolved to reveal more dynamic and versatile functions which contribute to the regulation of the majority of cellular processes (Berndsen and Wolberger, 2014).

Ubiquitylation is a sequential enzymatic reaction mediated by the ubiquitin-activating enzymes (E1s), ubiquitin-conjugating enzymes (E2s) and ubiquitin ligases (E3s) (de Bie and Ciechanover, 2011) (Figure 1.6.1). In the first step, E1 activates the carboxy-terminal glycine of the ubiquitin molecule. The ubiquitin molecule is bound to the E1 enzymes on a cysteine residue. This activated ubiquitin is then transferred to the E2 ubiquitin carrier protein. In the final stage the E3 enzyme catalyses the carboxy terminal linkage of the ubiquitin molecule to a lysine residue on the substrate protein. E2 and E3 ligases are evolutionarily highly conserved, having been identified in yeasts, *Drosophila* and mammals (Berndsen and Wolberger, 2014). E2 ligases show specificity for particular E3 ligases and E3 ligases can impact on substrate recognition specificity (de Bie and Ciechanover, 2011). There are 2 major classes of E3 ligases, defined by their ubiquitin-associated domains, the HECT (Homology E6 C-terminus) family and the RING (Really Interesting New Gene) family (de Bie and Ciechanover, 2011). One subfamily of the RING E3 ligases is the Cullin-ring ubiquitin ligases, one member of which is among the main mediators of Claspin ubiquitylation and will be discussed in further detail in in Introduction 1.6.2.

Substrates can be ubiquitylated in a variety of ways, mono- ubiquitylation with a single ubiquitin molecule, multi- ubiquitylation where a single ubiquitin can bind to multiple residues on a single substrate and poly- ubiquitylation, consisting of a chain linkage of at least 4 ubiquitin molecules on a single residue on the target protein. Ubiquitylation primarily involves lysine residues (Lys6, Lys11, Lys27, Lys29, Lys33, Lys48 or Lys63) as well as the ubiquitin amino terminus. This facilitates an isopeptide linkage to a substrate protein (Figure 1.6.1). All these chain linkages have been described in eukaryotic cells, however, only Lys48 and Lys63 linked chains, largely associated with protein degradation, by the proteasome or lysosome, respectively, have been extensively studied (Wu et al., 2010). The other types of poly-, multi and mono- ubiquitinylation have also been implicated in the regulation of protein interactions, activity and cellular localisation (Hutchins et al., 2013). Defects within the ubiquitin system have been described as contributing to multiple cancers as well as multiple neuro-generative diseases (Devoy et al., 2005; Hutchins et al., 2013).

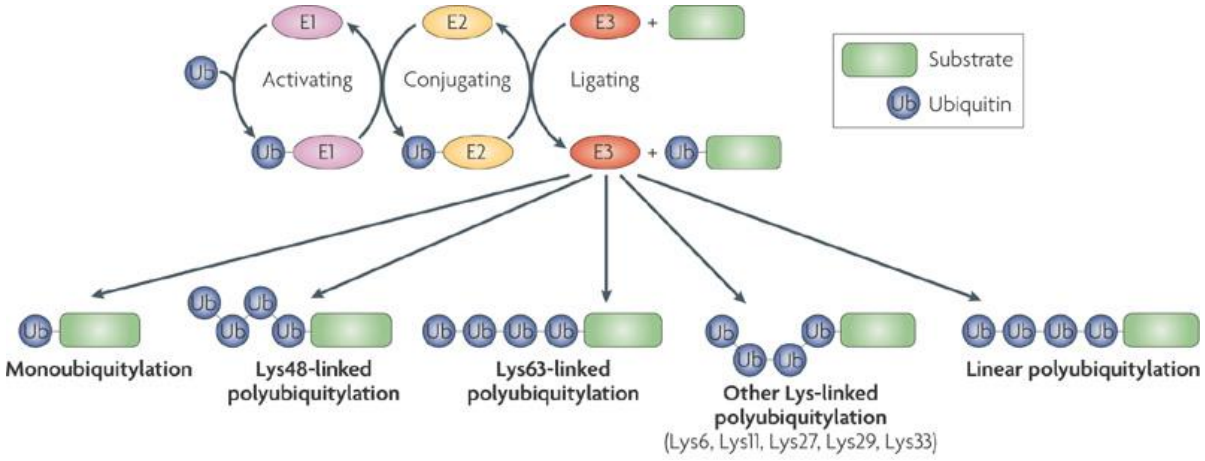

Figure 1.6.1. Enzymatic cascade that leads to substrate ubiquitylation. The activity of three enzymes is required for ubiquitylation, the ubiquitin-activating enzyme (E1), the ubiquitin-conjugating enzyme (E2) and the ubiquitin-ligating enzyme (E3), which recognises the substrate. The completion of one ubiquitylation cycle results in a monoubiquitylated substrate. However, the cycle can be repeated to form polyubiquitylated substrates. Additional ubiquitin molecules can be ligated to a Lys residue (Lys6, Lys11, Lys27, Lys29, Lys33, Lys48 or Lys63) in a previously attached ubiquitin to form Lys-linked chains. Alternatively, ubiquitin molecules can be linked head to tail to form linear chains. Figure taken from (Dikic et al., 2009).

1.6.2 - Claspin proteasomal mediated degradation

The Lukas group noted that the downregulation of Claspin in early mitosis resembled the expression profile of WEE1, a known target for proteasomal degradation, mediated by the E3 ligase SKP1/CUL1/F-box protein (SCF) (Mailand et al., 2006). Therefore, they examined the effects of depletion of β-transducin repeat containing protein (β-TrCP), the substrate adaptor for the SCF, and observed an increase of Claspin protein levels in G2, when it is normally present at low levels (Mailand et al., 2006) (Mamely et al., 2006). Claspin was shown to interact with β-TrCP and importantly, the SCF-β-TrCP- dependent degradation of Claspin was required for the efficient and timely termination of the DNA replication checkpoint (Peschiaroli et al., 2006). Furthermore, in response to DNA damage in G2, Claspin proteolysis is inhibited to allow the prompt reestablishment of the checkpoint (Peschiaroli et al., 2006). Cells expressing Claspin, lacking the SCFβ-TrCP ubiquitylation site, exhibit delayed entry into the cell cycle after replication stress due to prolonged activation of CHK1 (Peschiaroli et al., 2006) (Mailand et al., 2006; Mamely et al., 2006).

Although β-TrCP depletion increased Claspin in G2, no increase was observed in G1 (Faustrup et al., 2009). Mailand and colleagues subsequently reasoned that the anaphase promoting complex (APC), which promotes the degradation of numerous regulatory proteins in late mitosis and G1, may be driving Claspin degradation in G1. Indeed, upon depletion of CDH1, the substrate-specific activator of the APC in G1, Claspin levels were restored (Faustrup et al., 2009).

The APC-mediated degradation of Claspin in G1 provides an important means of suppressing inappropriate CHK1 activation during this window of the cell cycle. This study also highlighted that the control of Claspin stability was more complex than previously anticipated involving both ubiquitylation and deubiquitylation (Faustrup et al., 2009).

1.6.3 - Deubiquitylation

As mentioned ubiquitylation is a reversible process with a family of enzymes termed deubiquitylating enzymes (DUBs) responsible for the deconjugation of ubiquitin from tagged substrates by isopeptide bond cleavage (Sahtoe and Sixma, 2015; Sowa et al., 2009). This regulates ubiquitinylation homeostasis as well as contributing to ubiquitin-precursor processing (Grou et al., 2015).

There are close to 100 DUBS encoded by the human genome predicted to be active and oppose the function of E3 ligases. DUBs can be subdivided into 5 families; ubiquitin specific proteases (USPs), ubiquitin C-terminal hydrolases (UCHs), ovarian tumour proteases (OTUs), Josephins, and JAMMs (Nishi et al., 2014). The first families are cysteine proteases whereas the JAMMs family members are zinc metalloproteases. The cysteine proteases are likely to be more "druggable" than E3 ligases as cysteine residues in the active sites of DUBs are expected to be reactive to various electrophiles (Sahtoe and Sixma, 2015). The FDA approval of proteasome inhibitors (PIs) including Bortezomib and Carfilzomib, for treatment of haematological malignancies, has firmly established proteasomal regulation as an anti-cancer target. Unfortunately, numerous patients are inherently resistant or quickly develop resistance to such compounds. One proposed strategy to tackle PI resistance is the targeting of upstream components of the proteasome such as DUBs. While considerable efforts have been undertaken to develop DUB modulators, significant advancements are necessary to move DUB inhibitors into the clinical setting (Farshi et al., 2015).

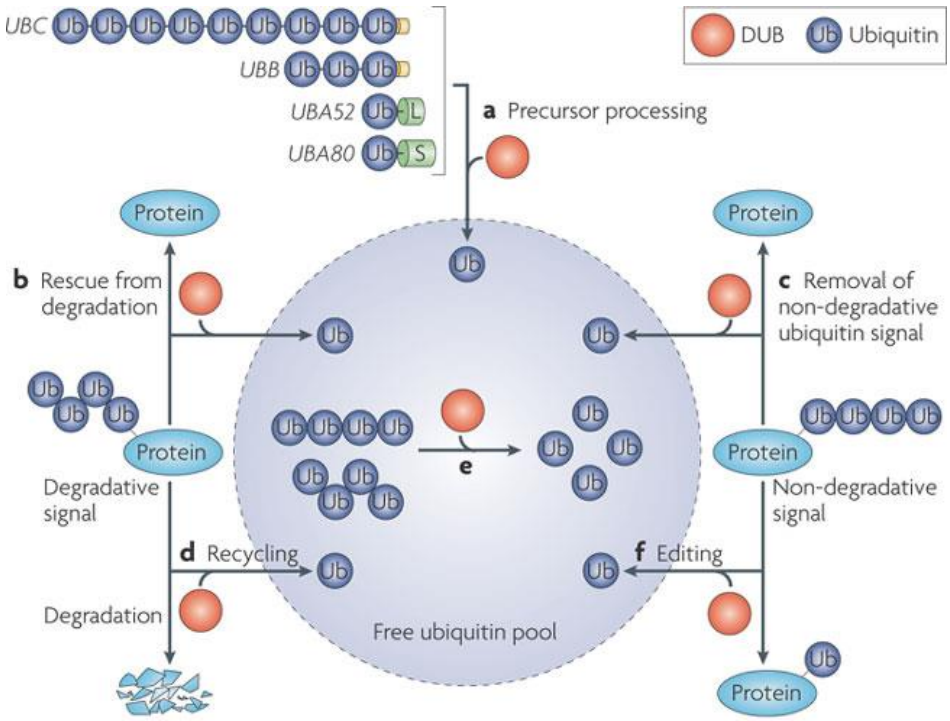

Figure 1.6.3. General role of DUBs. (A) Ubiquitin is encoded by four genes and is transcribed and translated as a linear fusion consisting of multiple copies of ubiquitin or ubiquitin fused to the amino terminus the 40S ribosomal protein L40 (L) and 60S ribosomal protein S27a (S). Generation of free ubiquitin from these precursors is a key function of DUBs. (B) Deubiquitylation can rescue proteins from degradation. (C) Alternatively, deubiquitylation can remove a non-degradative ubiquitin signal. (D) DUBs have a crucial role in maintaining ubiquitin homeostasis and preventing degradation of ubiquitin together with substrates of the 26S proteasome and lysosomal pathways (recycling of ubiquitin). (E) Disassembly of ubiquitin chains generated by removal from substrates ensures that recycled ubiquitin re-enters the free ubiquitin pool. (F) Some DUBs function to edit ubiquitin chains and help to exchange one type of ubiquitin signal for another (Komander et al., 2009) .

1.6.4 - Ubiquitin Specific Proteases (USPs): The largest DUB family

The largest DUB family, the USPs, have particular relevance to Claspin stability and this is further discussed in Introduction 1.6.5. This diverse family shares a catalytic domain of between 300 and 800 amino acids containing 2 short conserved cysteine and histidine catalytic motifs (Komander et al., 2009). Intervening these motifs are long stretches of non-conserved sequences. Flanking the catalytic domain are non-conserved N- and C-terminal extensions which influence substrate specificity (Murtaza et al., 2015). Apart

from the motifs mentioned USPs share little similarity however all USPs are ‘post-post translational’ modifiers acting down stream of ubiquitylation. Therefore the activity of all USPs is highly context dependent and specific to upstream enzymes such as the E3 ligases (Berndsen and Wolberger, 2014). Although DUB activity is found at the end of a chain of PTMs, USPs are far from redundant with deregulation of nearly all USPs associated with severe consequences and disease (Nishi et al., 2014).

1.6.5 - Claspin regulation by USPs

1.6.5.1 - Claspin and USP28

The first reported regulation of Claspin exerted by a DUB was described almost a decade ago (Zhang et al., 2006). As mentioned Claspin levels oscillate in the cell cycle and the protein is degraded by the proteasome in G1, mediated by the E3 ubiquitin ligase complex APC (Gao et al., 2009). USP28 was shown to interact with and regulate Claspin stability by reversing APC dependent proteasomal degradation. This was one of the first reports to demonstrate a role for DUBs in DNA damage (Zhang et al., 2006).

1.6.5.2 - Claspin and USP7

As mentioned in the Introduction Section 1.3, the termination of CHK1 signalling is needed for entry into mitosis and checkpoint recovery. For this SCF-βTrCP mediated Claspin destruction is essential and required to maintain steady-state levels of Claspin (Faustrup et al., 2009). USP7 mediated deubiquitylation can significantly increase the half-life of Claspin, which in turn can increase the duration and magnitude of CHK1 signalling in response to replication stress. Specifically, USP7 was shown to oppose SCF-βTrCP mediated degradation, which differs from the role of USP28 in the regulation of Claspin which reverses Claspin degradation mediated through the APC complex (Faustrup et al., 2009).

1.6.5.3 - Claspin and USP29

Whilst USP28 and USP7 seemed to counteract the two ubiquitin mediated Claspin degradation pathways, the finding that another DUB, USP29, can play a role in Claspin

deubiquitylation regulation begun to unravel the complex control of DUBs on Claspin regulation and ultimately genomic stability (Martin et al., 2015) (published online ahead of Claspin and USP20 reports). USP29 depletion was shown to destabilise Claspin, whereas its overexpression promoted an increase in Claspin levels. Similar to the previous Claspin-DUB papers, Claspin interacted with USP29 and USP29 was able to deubiquitylate Claspin both *in vivo* and *in vitro.* This demonstrated that Claspin is a direct substrate of this DUB and that the depletion of USP29 also impaired CHK1 activation. Overexpression of USP29 was able to reverse SCF-βTrCP mediated degradation of Claspin, indicating a similar function for USP29, as that described for USP7 in Claspin regulation (Martin et al., 2015).

1.6.5.4 - Claspin and USP20

Two concurrent reports demonstrated a role for USP20 in the regulation of the DNA damage checkpoint by modulating Claspin stability (Yuan et al., 2014; Zhu et al., 2014). In these studies, the E3 ligase HECT and RLD domain containing E3 ubiquiting protein ligase 2 (HERC2) was found to bind to and regulate the stability of USP20. HERC2 mediates continuous ubiquitylation of the substrate which promotes USP20 proteasomal degradation. However in response to replication stress, ATR-mediated phosphorylation of USP20 results in USP20-HERC2 disassociation. This facilitates an increased interaction between USP20 and Claspin. USP20 contributes to the deconjugation of K48-linked polyubiquitylated chains on Claspin (Zhu et al., 2014). This protects and stabilises Claspin, ultimately promoting CHK1 signalling and checkpoint activation. These studies reveal a third independent DUB which can regulate Claspin stability in S-phase, along with USP7 and USP29 (Yuan et al., 2014).

USP20 was identified by the Lou group who used a colony formation assay, examining cell viability in response to a panel of USPs siRNA and Hydroxyurea treatment to screen hypersensitivity to replication stress (Yuan et al., 2014). Intriguingly, within this screen USP9X, a focus of this study, emerged as another DUB that resulted in hypersensitivity to Hydroxyurea treatment (Yuan et al., 2014). This study focuses on USP9X and its role in genome stability.

1.7- Introduction to USP9X

1.7.1 - Structure and conservation of USP9X, from fly to human

One member of the USP family USP9X, a large protein, encoded by a 45 exon gene, displays a high degree of conservation across species but relatively little is known about its structure (Brown et al., 1998). The large size of USP9X (2550 amino acids in size) may reflect its ability to interact with multiple substrates. Apart from the catalytic motifs found in all USPs only a ubiquitin like module (UBL) in USP9X's N-terminal extension, has been identified (Murtaza et al., 2015; Nijman et al., 2005). The USP9X protein sequence displays a high degree similarity from *Drosophila* to mammals and is comparable to the conservation reported for developmental master-regulatory genes such as PAX6 (Khut et al., 2007).

In a search for mutations affecting eye development in *Drosophila*, the first USP9X homologue was identified by the Lehmann laboratory and named *fat facets (Faf)* (Fischervize et al., 1992). *Faf* was shown to be essential for the development of the eye and oocyte and to be expressed in other tissues where it is non-essential. Lehmann's laboratory later identified *Faf* as a DUB that displayed little sequence homology to other identified *Drosophila* USPs (Chen et al., 2000).

Expression of the mouse USP9X homologue *fat facets in mouse* (*Fam*) was discovered in gene-trap experiments to identify genes expressed in mouse embryonic development (Wood et al., 1997). The *Fam* protein shares 50% identity and 70% similarity to *Faf*. *Fam* expression is able to rescue defects in *Faf* mutants demonstrating functional conservation from flies to mammals (Chen et al., 2000). The *faf* homologue identified in humans was originally named *DFFRX* but was later recalled *USP9X* to reflect its USP classification, number 9, within the class and the X chromosomal location in both human and mouse. Human USP9X could alleviate defects in neurons derived from *Fam* conditionally deleted mice further demonstrating the high degree of conserved evolutionary functions of USP9X (Homan et al., 2014).

1.7.2 - The cellular localisation of USP9X

Immunofluorescence studies have predominantly detected USP9X in the cytoplasm, however, other studies have reported small portions of USP9X in the nucleus as well as the mitochondria (Mouchantaf et al., 2006; Theard et al., 2010; Trinkle-Mulcahy et al., 2008; Urbe et al., 2012). The existence of multiple pools of USP9X is likely to reflect the variety of USP9X functions which may be influenced by localisation. For example, exchange factor for ARF6 (EFA6), which is essential for tight junction formation, is a USP9X substrate detected in multiple cellular localisations but only a small portion of USP9X and EFA6 colocalise (Theard et al., 2010).

1.8 - The cellular functions of USP9X

1.8.1 - USP9X and development: The first description of USP9X

Since its initial description USP9X has been associated with development, as mentioned, with *Faf* implicated in cell fate of developing *Drosophila* eyes with subsequent mice studies identifying *Fam* as a gene expressed during early embryonic development (Fischervize et al., 1992) (Wood et al., 1997). Since these studies, USP9X has been shown to be essential for embryogenesis. USP9X depletion in mice results in embryonic lethality with development stopping at the blastocyst stage (Nagai et al., 2009).

USP9X has been shown to mediate regulation of transforming growth factor beta (TGFβ) signalling pathway (Stegeman et al., 2013). The TGFβ signalling pathway is involved in many key cellular processes in both the adult organism and in the developing embryo including cell growth, differentiation, apoptosis and homeostasis. USP9X promotes TGFβ signalling by facilitating SMAD4 deubiquitylation, allowing it to form a complex with phosphorylated receptor SMADs, which can then shuttle into the nucleus and enable transcriptional responses to TGFβ family ligands (Dupont et al., 2009).

On the contrary USP9X can stabilise the E3 ligase SMAD specific E3 ubiquitin protein lisase 1 (SMURF1), which can promote the down regulation of TGFβ receptors and therefore counteract signalling, once again demonstrating the complexity and duality of USP9X functions (Xie et al., 2013).

The recently described inducible LoxP knockout cell mouse, which disrupted aspects of CNS development, will no doubt offer invaluable insight in the role of USP9X during development (Stegeman et al., 2013).

1.8.2 - USP9X in embryonic and adult stem cells

USP9X has been found to be expressed in both mouse and human embryonic, neural and hematopoietic stem cells, as well as adult epidermal stem cells (Murtaza et al., 2015). As mentioned, USP9X knockout is embryonic lethal but depletion of the protein from cultured mouse ESCs did not affect growth and implicates a more predominant role in the regulation of early differentiation (Nagai et al., 2009). USP9X has also been identified in the interaction network of the critical stem cell proteins SRY box 2 (SOX2) and octamer binding transcription factor 4 (OCT4) (Cox et al., 2013). In muscle stem cells the regulation of the mTOR pathway by USP9X demonstrates its contribution to control of proliferation and differentiation (Agrawal et al., 2012).

USP9X in stem cells and neural development has been more extensively studied by one of the forefathers of USP9X research, Stephen Wood (Stegeman et al., 2013). USP9X is highly expressed in neural stem cells in mice, however, in the adult brain the expression is reduced but retained in neural progenitors, influencing both organisation and fate of these cells (Jolly et al., 2009). Deletion of USP9X in mice neural progenitors affects both the cortical and hippocampal architecture. On the contrary, in cell culture, the overexpression of USP9X promotes polarised clusters of neural progenitors which can increase their self-renewing capabilities, demonstrating the diverse consequences of altered USP9X expression in the regulation of neural progenitor cells (Jolly et al., 2009).

1.8.3 - USP9X contributes to chromosome segregation through Survivin

The attachment of sister kinetochores to microtubules from opposite spindle poles leading to the formation of bi-oriented chromosomes on the metaphase spindle is essential for complete and proper chromosome segregation (Carmena et al., 2012). Errors in chromosome segregation can cause aneuploidy, cancer and various diseases (Silkworth et al., 2009). Regulating this process from the centromeres is the chromosome passenger

complex (CPC) which contains Survivin and the Aurora B kinase (Carmena et al., 2012). USP9X can influence chromosome segregation by controlling the dynamic interaction of Survivin with centromeres and the correct targeting of Survivin and Aurora B to centromeres (Vong et al., 2005). USP9X can deconjugate the Lys-63 ubiquitin linkages which is needed for the dissociation of Survivin from centromeres which counteracts the ubiquitin mediated Survivin-centromere association (Vong et al., 2005). This demonstrates a dynamic role for USP9X in chromosome segregation where it can help mediate protein-protein interaction independent of protein degradation.

1.8.4 - USP9X can regulate pro- and anti- apoptotic pathways

One type of programmed cell death, apoptosis, is an important cellular mechanism highly implicated in disease (Favaloro et al., 2012; Gorman, 2008). USP9X has been demonstrated to be involved in the regulation of both pro- and anti- apoptotic pathways (Murtaza et al., 2015).

In *Drosophila,* the products of the Grim-Reaper genes are required for the induction of apoptosis (Goyal et al., 2000). *Faf* can enhance Grim-Reaper mediated apoptosis through regulation of ubiquitylation processes (Wing et al., 2002). In mammalian cells USP9X can regulate pro-apoptotic kinases such as ASK-1 (Nagai et al., 2009).

On the contrary, USP9X has been shown to promote the stability of the anti-apoptotic B-cell lymphoma 2 (BCL2) family member myeloid cell leukemia 1 (MCL-1), through removal of K48 linked poly-ubiquitylated chains, thus protecting MCL-1 from proteasomal degradation (Boise, 2015; Peterson et al., 2015; Schwickart et al., 2010; Vucic et al., 2011).

USP9X is the only identified DUB, which, along with four different E3 ubiquitin ligases, MCL-1 ubiquitin ligase (MULE), SCFβ-TrCP, F-box/WD repeat-containing protein 7 (SCFFbw7) and tripartite motif-containing protein 17 (TRIM17), can influence MCL-1 ubiquitination (Mojsa et al., 2014). It has been proposed that USP9X competes with these E3 ligases for binding to a crucial phosphodegron domain on MCL-1 to mediate their opposing affects (Mojsa et al., 2014). Studies have demonstrated that siRNA-mediated

depletion of USP9X can induce MCL-1 polyubiquitylation (Gomez-Bougie et al., 2011). Further still USP9X depletion leads to an increased MCL-1-MULE interaction underlying the essential role of USP9X in MCL-1 protein turnover (Gomez-Bougie et al., 2011).

It has been observed that elevated levels of MCL-1 are associated with chemo-resistance to BCL2 antagonists in multiple myeloma, B- and mantle-cell lymphomas and chronic myeloid leukaemia. A direct correlation between levels of USP9X and MCL-1 was identified in these carcinomas. Chemical or genetic inhibition of USP9X in these carcinomas resulted in decreased MCL-1 levels and importantly a resensitisation to BCL2 antagonists (Schwickart et al., 2010).

A reciprocal relationship involving USP9X between pro- and anti- apoptotic proteins, MCL-1 and BCL2-interacting protein 1 (BECLIN-1) has been recently demonstrated (Elgendy et al., 2014). BECLIN-1 was proposed to be the first tumour-suppressor gene associated with autophagy. Subsequent reports have indicated that the proximity of *BECN1* to the ovarian and breast tumour suppressor gene *BRCA1* on chromosome 17q21 has decreased the certainty of BECLIN-1's role as a *bona fide* tumour suppressor gene (Rebecca and Amaravadi, 2015). However there is evidence to indicate that BECLIN-1 can contribute to multiple processes that effect tumour restraining mechanisms (Elgendy et al., 2014).

USP9X contributes to the regulation of BECLIN-1, where MCL-1 and BECLIN-1 compete for binding to USP9X. This interaction is directly responsible for the regulation of their ubiquitinylation status and consequential protein degradation. (Elgendy et al., 2014). These results demonstrate the complex role of USP9X in cell death where it can impart stabilisation of both a tumour suppressor and a tumour promoter within the same pathway.

1.8.5 - A role for USP9X in the regulation of endocytosis

Endocytosis is the uptake of extracellular material in vesicles formed by invaginations from the plasma membrane towards the inner cytosol of a cell (Maxfield, 2014). This process has critical roles in normal cell physiology, with disruption of endocytic

processes implicated in many diseases such as Alzheimer's disease and tumour invasiveness (Maxfield, 2014).

Regarding endocytosis, USP9X has been shown to deubiquitylate the endocytic E3 ligase ITCH (Mouchantaf et al., 2006). ITCH antagonises the trafficking of the activated epidermal growth factor receptor (EGFR) to the lysosome by promoting the proteasome mediated degradation of endophilin and another E3 ligase CB1. E3 ubiquitin-protein ligase Itchy homolog (ITCH) also auto-ubiquitylates itself following the activation of EGFR and depends on USP9X deubiquitylation to protect itself (Mouchantaf et al., 2006).

A recent report has implicated USP9X in membrane trafficking of integrins, which play a pivotal role in cell proliferation and migration (Kharitidi et al., 2015). This report demonstrated that fibronectin (FN) binding to α5β1 integrin prompts ubiquitylation and internalisation of the receptor complex. Acidification allows FN dissociation from integrin α5β1 in early endosomes, triggering receptor complex deubiquitylation which is mediated by USP9X and recycling to the cell surface. Depending on residual ligand occupancy of receptors, some α5β1 integrins remain ubiquitylated and are directed for proteolysis by the histidine domain-containing protein tyrosine phosphatase (HD-PTP) and ubiquitin-associated protein 1 (UBAP1). This limits receptor downstream signalling and cell migration. Therefore, HD-PTP or UBAP1 depletion causes a pro-invasive phenotype (Kharitidi et al., 2015). USP9X deubiquitylation of the activated integrin α5β1 is required for receptor resensitisation and cell migration whereas ubiquitylation lessens cell migration which leads to the proposal that USP9X depletion is a potential target to modulate tumour invasiveness (Kharitidi et al., 2015).

1.8.6 - USP9X influences cellular inflammation through JAK-STAT signalling

Janus kinases (JAKs) are tyrosine kinases involved in signal transducer and activator of transcription (STAT) signalling. Deregulation of these kinases is associated with numerous inflammatory diseases such as rheumatoid arthritis and various cancers such as acute lymphoblastic leukaemia (Stark and Darnell, 2012). Therefore a huge effort has been exerted to pharmacologically target the JAK-STAT pathway however the generation

of selective inhibitors has remained elusive (Stark and Darnell, 2012). Due to their partial selectivity, clinically used JAK kinase inhibitors have numerous off target effects (O'Shea et al., 2015). Further still, kinase inhibition of JAK may not target important scaffolding properties of this kinase which can influence important protein interactions that influence JAK deregulation. As such the development of chemicals which target the JAK-STAT pathway independent of kinase function may provide an attractive alternative option to classic kinase inhibition (Chou et al., 2015).

A recent report identified the compound, BRD0476, which targets USP9X deubiquitinase activity, as able to inhibit interferon-gamma (IFN-γ)-induced JAK-STAT1 signalling (Chou et al., 2015). This promoted B-cell survival in a mouse model of type 1 diabetes. These results indicate that competition between phosphorylation and ubiquitylation on JAK can account for the compounds ability to protect B-cells from death (Chou et al., 2015). This data demonstrated a novel mechanistic role of USP9X in an apparently well-understood cell signalling pathway.

1.8.7- USP9X contributes to ubiquitin precursor recycling

Two pathways, recycling of ubiquitin from ubiquitin conjugates and the processing of ubiquitin precursors synthesised *de novo* are required for an adequate pool of free ubiquitin, ensuring a state of cellular homeostasis (Grou et al., 2015). DUBs are known to be involved in these pathways but our knowledge is still limited. Recently, USP9X has been demonstrated to be an active DUB which can act on ubiquitin precursors, along with USP7, UCHL3 and USP5, amongst others. This demonstrates that each ubiquitin precursor can be processed by different manners which accounts for the robustness of the ubiquitin *de novo* synthesis pathway (Grou et al., 2015).

1.9 - USP9X deregulation and disease

1.9.1 - USP9X deregulation is associated with multiple neurological disorders

It has hardly surprising that deregulation of USP9X, a DUB implicated in a dynamic and diverse range of molecular processes, has been described to have an underlying contributory role in numerous human diseases, namely neurological disorders, cancers,

and a recent report has resurfaced a role for USP9X in male infertility (Lee et al., 2003b; Murtaza et al., 2015; Vieweg et al., 2015).

The identification of two missense and one truncating mutation in USP9X have been implicated in X-linked intellectual disability (Homan et al., 2014). Studies showed these to be loss of function mutations, all found in the C-terminal region of the protein, suggesting its significance in neural development (Homan et al., 2014).

A pathological feature of Parkinson's disease (PD) and diffuse Lewy body disorder is α-synuclein aggregation with Lewy bodies. Unravelling the mechanisms that regulate α-synuclein levels is key to understanding the pathophysiology of the disease. USP9X colocalise with these aggregations in the brain tissue of PD patients (Rott et al., 2011). Studies have also demonstrated an interaction between α-synuclein and USP9X and have shown that USP9X mediated deubiquitylation of α-synuclein determines the partition of α-synuclein between the proteasomal and autophagy pathways (Engelender, 2012). By manipulating USP9X levels, mono- ubiquitylated α-synuclein can be degraded by the proteasome, whereas deubiquitination of α-synuclein favours its degradation by autophagy. As USP9X levels and activity are decreased in α-synucleinopathy brains, USP9X may now represent a novel target for PD (Rott et al., 2011).

Recent studies have revealed a role of USP9X in epileptic seizure regulations where USP9X is shown to deubiquitylate the REST/NRSF-interacting LIM domain protein 1 also known as PRICKLE1 protein and prevent its degradation (Paemka et al., 2015). PRICKLE proteins are characterised by PET and LIM domains. The PRICKLE proteins function in the non-canonical WNT signalling pathway, which regulates intracellular calcium release and planar cell polarity (PCP) (Tao et al., 2011). Mutations in PRICKLE are associated with seizure predisposition with this pathway evolutionary conserved from flies to humans but as of yet this protein has not been targeted therapeutically (Tao et al., 2011). In a seizure prone *Drosophila* model associated with PRICKLE mutation, inhibition of USP9X with WP1130 can suppress seizures (Paemka et al., 2015). Interestingly mutations in USP9X have also been observed in a small number of seizure

patients. This study suggests that USP9X inhibition is a potential anti-seizure treatment option (Paemka et al., 2015).

To date the role of USP9X in neurodegenerative and synchronous neuronal activity disorders has been mainly associative. The data collected warrants further investigation using animal models and human samples to elucidate functional understanding and to allow therapeutic advantage.

1.9.2 - The role of USP9X in cancer is highly context dependent

Deubiquitinase inhibition as a cancer therapeutic strategy is receiving much attention in the literature (Farshi et al., 2015; McClurg and Robson, 2015). The dependency of cancer cells on a functioning DUB has made these proteins an attractive target for the development of drugs that impart a high degree of selectivity for tumour cells and as mentioned cysteine proteases provide 'druggable' targets (Sahtoe and Sixma, 2015). Considering the contribution of USP9X to maintain homoeostasis and signalling pathways, the increasing relevance of USP9X in both the initiation and progression of cancer is hardly surprising. Numerous studies have reported the deregulation of USP9X function as contributing to several cancers including non-small cell lung, hepatocellular, and bladder carcinomas (Cui et al., 2015; Harris et al., 2012; Liu et al., 2015; Perez-Mancera et al., 2012; Wang et al., 2015c).

USP9X can contribute to cancer development and tumour progressive through various mechanisms with roles in emerging integrin processing (Kharitidi et al., 2015) and JAK-STAT signalling (Chou et al., 2015). However, the majority of the USP9X oncology literature focuses on its role as an oncogene, with USP9X overexpressed in multiple carcinomas including lymphomas and cervical cancers (Murtaza et al., 2015; Zhou et al., 2015).

The best described oncogenic function of USP9X is derived from its role in stabilising the anti-apoptotic protein MCL1, as briefly discussed in Introduction Section 1.8.4. Overexpression of MCL1 is found in numerous cancers and it is associated with resistance to chemotherapy (Schwickart et al., 2010). Overexpression of USP9X in patient samples

correlates with high MCL1 levels. Pharmacological inhibition of USP9X increases sensitivity of certain chemo resistant colon carcinoma and leukaemia cells lines to BCL-2/BCL-xL inhibitors including ABT-737 and ABT-263 (Schwickart et al., 2010). This finding led to multiple publications which examined the benefit of targeting USP9X in various carcinomas, with depletion of USP9X overcoming glucocorticoid resistance in B-ALL cells, inhibiting the growth of hepatocellular carcinoma cells as well as inducing apoptosis in human bladder cancer cells (Cui et al., 2015; Liu et al., 2015; Zhou et al., 2015).

These studies add precedence to the development of novel USP9X chemical inhibitors with increased bioactivity and selectivity as the USP9X inhibitor WP1130 used in many of these studies is only partially selective and has solubility issues rendering the compound unsuitable for clinical trials. Chemicals with better pharmacokinetic properties such as G9 have since been developed, offering promising therapeutic options (Peterson et al., 2015).

Recently two reports using two drugs previously evaluated clinically, namely TRAIL-inducing compound 10 (TIC10/ONC201) and a known small molecule inhibitor of MCL-1, GX15-070, were found when combined with ABT263 to offer a potentially new therapeutic strategy in the treatment of glioblastomas (Karpel-Massler et al., 2015a; Karpel-Massler et al., 2015b). Prognosis with this carcinoma is currently grim, with current therapeutic strategies sparse. They attribute the ability to overcome apoptotic resistance in these cells through enhanced apoptosis by post translational down-regulation of USP9X leading to a sustained depletion of MCL-1 protein levels. This in turn enhances apoptosis induced through BCL-2/BCL-xL inhibition. These studies demonstrate that compounds that are already clinically evaluated can effectively target USP9X deregulation. Using such combinatorial approaches could greatly increase patient outcomes (Karpel-Massler et al., 2015b).

Other reports have demonstrated a role for USP9X as a tumour suppressor. A study demonstrated a novel role for USP9X in ERGα-positive breast cancers with

downregulation of USP9X associated with resistance to one of the most commonly used drugs in the management of ERGα-positive breast cancers, Tamoxifen (Oosterkamp et al., 2014).

The tumour suppressor role of USP9X has been reported in particular in pancreatic ductal adenocarcinoma (PDAC), with low expression associated with poor patient outcome and widespread metastasis (Perez-Mancera et al., 2012). Using a murine PDAC model, depletion of USP9X lead to a more rapid onset of cancer in these animals. These studies urge caution with the use of USP9X inhibitors for cancer therapy. Some of the USP9X tumour suppressor functions is attributed to a genetic interaction with mutated V-Ki-ras2 Kirsten rat sarcoma viral oncogene homolog (KRAS) but the molecular link between the two remains to be revealed. (Perez-Mancera et al., 2012).

However, little has been documented at the molecular level about USP9X tumour suppression function. This work suggests that USP9X is epigenetically downregulated in PDAC and hints that treatment of PDAC cells with a DNA methyltransferase inhibitor coupled with a histone deacetylase inhibitor can increase USP9X mRNA and protein levels. This indicates that chromatin-modulating drugs may be able to promote re-expression of USP9X in PDAC patients (Perez-Mancera et al., 2012).

Even within the poorly understood role of USP9X as a tumour suppressor in PDAC there is conflicting literature, with inhibition of USP9X in a KRAS wild type PDAC cell tumour xenograft model line leading to a decrease in tumour volume (Schwickart et al., 2010). This observation has since been extended to four PDAC cell lines that express mutated KRAS as well as wild type KRAS and point to a more complex role of USP9X in PDAC (Cox et al., 2014). USP9X may behave as a tumour suppressor in the early stages of disease progression and function as an oncogene during later stages and progression of the cancer, which mirrors the behaviour of TGF-β in some cancers (Cox et al., 2014).

Overall, studies indicate that the function of USP9X in cancer is highly tissue specific. Elucidating complete understanding of USP9X function will undoubtingly aid the development of the most effective USP9X mediated therapies that could benefit patients.

1.10 - Thesis Aims

- The identification of putative Claspin interacting proteins
- The confirmation of a novel protein-protein interaction
- The investigation of the functional relationship between the two proteins

CHAPTER 2
MATERIALS AND METHODS

2.1 - Commonly used buffers

Materials used were generally obtained from Sigma and were of the highest purity available unless otherwise stated.

Ponceau S Protein Stain: 1 g Ponceau S, 5 ml acetic acid, dH_2O to 100 ml.

SDS-Gel Running Buffer: 3 g Tris base, 14.4 g glycine, 1 g SDS, dH_2O to 1 L.

Transfer Buffer: 18.9 g Glycine, 3.02 tris base, 200 ml methanol, dH_2O to 1 L.

TE Buffer: 10 mM Tris-HCl pH 8.0, 1 mM EDTA pH 8.0.

10% SDS: 50 g SDS, dH_2O to 500 ml.

10% APS: 1 g APS, dH_2O to 10 ml.

1 M Tris pH 8.8: 121.14 g Tris, adjust pH to 8.8 using HCl dH_2O to 1000 ml.

1 M Tris pH 8.8: 121.14 g Tris, adjust pH to 6.8 using HCl dH_2O to 1000 ml.

PBS: Tablets from Sigma, made as per manufacturer's recommendations.

PBST: PBS with 0.05% tween-20.

PBS-TX: PBS with 0.1% triton-X.

5% Milk: 2.5 g Dried semi-skimmed milk, PBS to 50 ml.

5% Milk-PBST: 2.5 g Dried semi-skimmed milk, PBST to 50 ml.

1% BSA-PBS: 0.5 g BSA, PBS to 50 ml.

1% BSA-PBST: 0.5 g BSA, PBST to 50 ml.

Buffer A: 50 mM Tris-HCl, pH 7.4, 300mM NaCl, 1 mM EDTA, 1% triton-X.

2.2 - Basic DNA methods

2.2.1 - USP9X WT, CI and HA-ubiquitin cDNA

Full length HA tagged cDNA of wild type USP9X (cat no. DU10171) and catalytically inactive USP9X (C1566A) (cat no. DU10685) were obtained via a MTA from MRC-PPU Reagents at the University of Dundee. HA-ubiquitin was provided by Dr Stephen Rea.

2.2.2 - E.coli transformations

A 50 µl aliquot of Mach1 competent bacterial cells were allowed to thaw on ice. Once thawed 1 µl of DNA was added to the bacterial cells and mixed. The cells were incubated on ice for 30 min, heat shocked at 42 °C for 45 s and replaced on ice for 2 min. Cells recovered with the addition of a 100 µl aliquot of LB media and incubation at 37 °C with rotation at 250 rpm for 1 hr. Cells were plated onto LB/Amp (100 µg/ml) plates and incubated, overnight at 30 °C.

2.2.3 - DNA preparation and enzymatic reactions

Qiagen kits were used for mini or maxi DNA preparation, as per the manufacturer's recommendations. Restriction digests were performed with buffers and protocols supplied with the enzymes from NEB. For the preparation of CI USP9X, following transformations, a colony was picked for a maxi preparation and the usual intermediate step of preparation of a small culture was bypassed to avoid a prolonged culture.

2.2.4 - Agarose gels

Agarose gels (0.6 %) were prepared in 1X TE, gels were run at 80 V for 2 hr. The gels were stained with Sybr-Safe for 30 min and imaged on the PharosFX scanner (Bio-Rad)

2.2.5 - DNA sequencing

DNA sequencing (Eurofins) was performed to confirm the sequence identity of the USP9X constructs used in this study.

2.3 - Cell culture methods

2.3.1 - Maintenance of U2OS cells

Osteosarcoma (U2OS) cells from Prof Noel Lowndes laboratory were first authenticated by STR analysis and subsequently certified by transposon profiling. Cells were cultured at 37°C, 5% CO_2 in DMEM supplemented with 1% penicillin-strep and heat inactivated 10% fetal bovine serum (FBS).

2.3.2 - Generation of Strep-Claspin Flp-In TREx HEK-293 cells

Generation of Flp-In TREx cell lines was conducted by Dr Michael Rainey.

To generate a cell line in which tagged Claspin could be inducibly expressed, the full-length Claspin coding sequence was PCR amplified from an image clone (IMAGE:9021657) using forward (5'GCCACAGCCGCCACCATGGGAACAGGCGAGGTGGGTTCTG-3') and reverse (5'-CCGGCAGCGCCTCCGCTCTCCAAATATTTGAAGATG-3') primers and cloned in-frame with a dual C-terminal Flag/OneSTrEP tag contained within a modified version of the pcDNA5/FRT/TO plasmid (pAB1) using ligation independent cloning. Stable cell lines conditional expressing tagged-Claspin were generated by co-transfection of pAB1-Claspin plasmid and pOG44 plasmid into the Flp-In T-REx human embryonic kidney (HEK) 293 cell line (Life technologies) using FuGENE HD (Promega). Cells that underwent FRT-directed recombination of the pAB1-Clapsin plasmid were selected using Hygromycin (100 μg/ml) and individual clones were isolated and are referred to as Strep-Claspin cells.

2.3.3 - Induction of Strep-Claspin

Conditional expression of Strep-Claspin was routinely induced by the addition of Doxycycline (1 μg/ml) to cell culture media, to alleviate TET-repression. Control cells were generated as above using an empty pAB1 plasmid and are referred to as empty-vector cells.

2.3.4 - Maintenance of Claspin Flp-In TREx and empty vector HEK-293 cells

Cells were cultured at 37°C, 5% CO_2 in DMEM supplemented with 1% penicillin-strep and heat inactivated 10% FBS. Every 8 passage, cells were placed in selection with Hygromycin (50 μg/ml) and Blasticidin (5 μg/ml).

2.3.5 – Labelling cells for SILAC

Empty vector and Strep-Claspin cells were grown for 5 passages in medium (R6K4) or light (R0K0) (Dundee Cell Products, cat no. LM016 and LM014) respectively.

2.3.6 - Growth curves

Empty vector, Strep-Claspin cells treated with Doxycycline and Strep-Claspin cells untreated, were plated at $2x10^5$ cells, in triplicate, and allowed to grow for 24, 48, 72 and 96 hr. At each time point the cells were harvested and counted using the automated cell counter Countess (Invitrogen), which also determined cell viability via trypan blue exclusion. Samples were also taken for immunoblotting.

2.3.7 - siRNA transfection

All siRNA were purchased from Sigma. Sequences and references are detailed in Table 2.3.7. U2OS or HEK-293 cells were transfected with 25 nM, 50 nM or 100 nM of siRNA as indicated for 48 hr using JetPrime transfection reagent (Polyplus), according to manufacturer's instructions. As control, 100 nM of the Ambion negative control # 1 (Ambion) was used. Depletion of protein was confirmed by immunoblotting and immunofluorescence.

siRNA	Sequence	Reference
siUSP9X(a)	AGAAAUCGCUGGUAUAAAUUU	(Schwickart et al., 2010)
siUSP9X(b)	GCAGUGAGUGGCUGGAAGUTT	(Dupont et al., 2009)
siClaspin	GCACAUACAUGAUAAAGAA	(Semple et al., 2007)
siHERC2	GCGGAAGCCUCAUUAGAAA	(Zhu et al., 2014)
siUSP20	CCAUAGGAGAGGUGACCAA	(Zhu et al., 2014)
siUSP29	CCAAAGUGUUUGUUUGCCCUGUUGU	(Liu et al., 2011)
siUSP7	ACCCUUGGACAAUAUUCCU	(Khoronenkova et al., 2011)

Table 2.3.7. Sequences and references of all siRNA used in this study.

2.3.8 - Colony formation assay

Following treatment with siCTRL or siUSP9X for 30 hr, cells were treated with different concentrations of Hydroxyurea, as indicated. 18 hr later, control and Hydroxyurea treated cells were typsinised, counted and replated at a density of 10,000 cells/10-cm dish. Ten days later colonies resulting from the surviving cells were fixed overnight with methanol, stained with crystal violet and counted. Statistical analysis of three independent experiments was performed using Prism (GraphPad Software).

2.3.9 – Drug treatments

When mentioned in this study drugs were used at the concentrations in Table 2.3.9

Name of drug	Abbreviation	Concentration (μM)	Source
Cycloheximide	CHX	10 μM	Sigma
Hydroxyurea	HU	2 μM	Sigma
Leptomycin B	LMB	0.1 μM	Sigma
MG132	-	10 μM	Sigma
Nocodazole	Noc	1 μM	Sigma
WP1130	-	5 μM	SelleckChem

Table 2.3.9. Details of drugs used in this study.

2.4 – Protein manipulation methods

2.4.1 - Protein extraction and quantitation methods

2.4.1.1 - Trichloroacetic acid (TCA) protein extraction

Adapted from (Foiani et al., 1994). Cell pellets were re-suspended in 20% TCA. Twice the volume of 5% TCA was then added and the samples were centrifuged at 3,000 rpm for 10 min. The supernatant was discarded and the cell pellet was re-suspended in Laemmli buffer. 1 M Tris was added in a dropwise fashion until the mixture turned blue. The sample was then placed at 99°C for 1 min and centrifuged at 300 rpm for 10 min. The supernatant was then removed and ready to load onto SDS-PAGE gel.

2.4.1.2 - Laemmli Protein Extraction

Cell pellets were re-suspended in 5x Laemmli buffer (60 mM Tris-Cl pH 6.8, 2% SDS, 10% glycerol, 5% β-mercaptoethanol, 0.01% bromophenol blue) (Laemmli, 1970), sonicated into solution, with the use of a probe sonicator for 1 s on 1 s off with 10% amplitude with 10 repeat cycles and placed at 95° for 5 min, after which the sample was ready to be loaded onto a SDS-PAGE gel.

2.4.1.3 - Soluble cell extraction

Cells pellets were re-suspended in buffer A, containing protease and phosphatase inhibitors, and placed on ice for 10 min. Samples were then centrifuged at 13,000 rpm for 10 min and the soluble fraction moved to a fresh tube. The soluble fraction was quantified using a Bradford assay (as described in 2.4.1.5). Typically, 20 μg of soluble extract was prepared per sample. Following the addition of Laemmli buffer to a dilution of 1x, samples were placed at 95° for 5 min, after which the sample was ready to be loaded onto a SDS-PAGE gel.

2.4.1.4 - Insoluble protein extraction

Buffer A was added to an insoluble cell pellet and the pellet was sonicated into solution following the use of a probe sonicator for 1 s on 1 s off with 10% amplitude with 10 repeat cycles. Following the addition of Laemmli buffer to a dilution of 1x, samples were placed at 95° for 5 min, after which the sample was ready to be loaded onto a SDS-PAGE gel.

2.4.1.5 – Protein quantification using the Bradford assay

Adapted from the original Bradford assay description (Bradford, 1976). Protein concentration was determined by adding 1 µl of protein extract to a well of a 96 well plate. 180 µl of Bradford protein reagent was then added to the samples. The absorbance at 595 nm of each sample was measured using a Wallac Victor 3 1420-012 (Perkin-Elmer). A standard curve was prepared with a known range of concentrations of bovine serum albumin (1 mg/ml – 5 mg/ml).

2.4.2 - Protein detection

2.4.2.1 – SDS-PAGE protein gels

Protein gels were run using either the Bio-Rad mini-PROTEAN system or XCell SureLock™ Mini-Cell Electrophoresis System (Invitrogen). When using the XCell SureLock system Nu-PAGE 4-12 % Bis-Tris (with MES buffer) pre-cast gels (Invitrogen) were used, as per manufacturer's instructions. For the Bio-Rad mini PROTEAN system, different percentage gels were routinely used and the gels were made in house. Table 2.4.2.1 details the different components for the resolving and stacking gels used to make a single Bio-Rad mini-gel of varying acrylamide percentage.

	Resolving Gels (µl)			Stacking Gel (µl)
Gel %	6%	10%	15%	5%
ddH_20	4100	2760	4140	3605
30% Bis-acrylamide	2000	3340	1960	665
1M Tris-HCL pH 8.8	3750	3750	3750	-
1M Tris-HCL pH 6.8	-	-	-	625
10% SDS	100	100	100	50
10% APS	50	50	50	25
TEMED	5	5	5	5

Table 2.4.2.1. Components of the SDS-PAGE resolving and stacking gels

Resolving gels were allowed to set for 45 min at room temperature with isopropanol overlaying the gel. This was removed when the resolving gel had set and stacking gels were poured and either 10 well or 15 well combs were added immediately. Stacking gels were allowed to set for 20 min at room temperature. Combs were then removed and wells washed with SDS gel running buffer. Typically 20 µg of protein was loaded per lane alongside 5 µl of a pre-stained protein molecular weight marker (PageRuler™ Plus Prestained Protein Ladder - 10 to 250 kDa). Gels were either transferred to a nitrocellulose membrane using wet transfer to facilitate immune detection of proteins or fixed and stained for protein.

2.4.2.2 - Protein transfer

The SDS-PAGE gels were placed on a piece of nitrocellulose membrane which was pre-equilibrated in transfer buffer. This was sandwiched between 2 sheets of pre-equilibrated 2 mm blotting paper, contained in a transfer cassette and placed in a Mini Trans-Blot system (Bio-Rad) transfer apparatus surrounded with transfer buffer and an ice pack. Transfers of proteins between 100 kDa and 290 kDa was conducted for 3 hr at 250 mA constant, for proteins below 100 kDa the transfer was conducted for 2 hr at 250 mA constant and for proteins above 290 kDa the transfer was conducted for 18 hr at 20 V constant at 4°C. Following transfer, the nitrocellulose was stained with Ponceau S stain to confirm protein transfer and provide an approximate loading control (Nakamura et al., 1985). The Ponceau S stain was removed prior to immunoblotting by rinsing with PBS.

2.4.2.3 - Immunoblotting

Prior to antibody incubation, the nitrocellulose was blocked in 5% milk-PBS for 1 hr at room temperature, with constant rocking. Exact conditions for primary antibody preparation depended on the antibody being used, details are contained in the Table 2.4.2.3 (A).

Primary antibody incubation occurred at 4ºC for 18 hr. Primary antibody was removed from the nitrocellulose with three 10 min washes in PBS-T, following which the membrane was incubated with infrared-labelled secondary antibodies, detailed in Table 2.4.2.3 (B), at room temperature for 1 hr. Secondary antibody was removed from the nitrocellulose with two 10 min washes in PBS-T and a final 10 min wash in PBS. Immunoreactive bands were visualized and quantified using Odyssey Infrared Imaging Systems (Li-Cor Biosciences).

Primary Antibody	Gel (%)	Species	Antibody Source	Primary Conditions
Caspase-3	10%	Mu	Cell Signalling 9668	(1:1000) 5% Milk-PBST
CDC45	10	Rat	(Broderick et al., 2013)	(1:10) 1% BSA-PBST
CHK1	15	Mu	Santa Cruz sc-8408	(1:1000) 5% Milk-PBST
Claspin	6/10	Rb	(Rainey et al., 2013)	(1:1000) 5% Milk-PBST
Cyclin B1	10	Mu	Santa-Cruz sc-245	(1:1000) 5% Milk-PBST
GAPDH	10	Rb	Santa Cruz sc-25778	(1:5000) 5% Milk-PBST
H2A	15	Rb	Abcam ab18255	(1:2000) 5% Milk-PBST
HA-11	6/10	Mu	Covance 901501	(1:2000) 5% Milk-PBST
HERC2	6	Rb	Bethyl A30-905A	(1:2000) 5% Milk-PBST
p21	15	Rb	Santa Cruz sc-397	(1:1000) 5% Milk-PBST
pCHK1 ser131	15	Rb	Cell Signaling 2344L	(1:1000) 1% BSA-PBST
Strep	6/10	Mu	Qiagen 34850	(1:2000) 5% Milk-PBST
Ubiquitin	6/10	Mu	Abcam ab7254	(1:1000) 5% Milk-PBST
USP20	6/10	Rb	Bethyl A301-189A	(1:1000) 5% Milk-PBST
USP29	6/10	Rb	Abcam ab108056	(1:1000) 5% Milk-PBST
USP7	6/10	Rb	Bethyl A300-033A	(1:2500) 5% Milk-PBST
USP9X	6/10	Rb	Bethyl A201-351A	(1:1000) 5% Milk-PBST
γH2AX	15	Rb	Cell Signaling 9718S	(1:1000) 1% BSA-PBST

Table 2.4.2.3 (A). Details of primary antibodies used for immunoblotting.

Secondary Antibody	Species	Antibody Source	Secondary Conditions
Anti- Rb (680 LT)	Rb	Li-Cor 926-68021	(1:10,000) 5% Milk-PBST
Anti- Rb (800 CW)	Rb	Li-Cor 926-32211	(1:10,000) 5% Milk-PBST
Anti- Mu (680 LT)	Mu	Li-Cor 926-68020	(1:10,000) 5% Milk-PBST
Anti- Mu (800 CW)	Mu	Li-Cor 926-32210	(1:10,000) 5% Milk-PBST
Anti- Rat (800 CW)	Rat	Li-Cor 925-32219	(1:10,000) 5% Milk-PBST

Table 2.4.2.3 (B). Details of secondary antibodies used for immunoblotting.

2.4.2.4 - Coomassie staining

Prior to staining, a fixing solution (45 ml methanol, 5 ml acetic acid, 50 ml dH_2O) was added to the gel for 20 min with gentle rocking, the fixing solution was decanted and replaced with ultrapure water to rehydrate the gel. The gel was rinsed 3 times in ultrapure water and left overnight in ultrapure water or until the smell of acid was no longer detectable. Gels were transferred into a clean plastic box and Coomassie stained using Instant Blue (Expedeon) stain, was added to cover the gel (Eaton et al., 2013). This was incubated at room temperature with shaking for a minimum of 15 min, with maximum staining achieved after 60 min staining. The stain was then decanted and the gel was washed several times with ultrapure water and imaged on the Odyssey Infrared Imaging Systems (Li-Cor Biosciences) and stored at 4°C.

2.4.2.5 - Silver staining

Adapted from (Chevallet et al., 2006). Gels were fixed as described in 2.4.2.4. Sensitizer solution (0.1 g of $Na_2S_2O_3$ dH_2O to 500 ml) was then added to the gel for 2.5 min, decanted and the gel was rinsed twice with ultrapure water. Silver solution (0.5 g $AgNO_3$ dH_2O to 500 ml) was added to the gel for 20 min at 4°C, decanted and the gel washed twice with ultrapure water. Developer solution (12.5 g Na_2CO_3 dH_2O to 500 ml) was added in a fume hood with gentle shaking and 150 µl of 37% formaldehyde was added gradually, until staining began. Formaldehyde was continually added until optimal staining was achieved, that is visible bands with low background. Development was stopped with the addition of 5% acetic acid. The gel was then washed in ultrapure water, imaged and stored at 4°C.

2.4.3 - Protein purification, precipitation and pulldown

2.4.3.1 - Flag immunoprecipitation

Protein extracts were lysed in buffer A, with protease and phosphatase inhibitors, and rotated for 20 min at 4°C. Lysates were clarified with centrifugation at 13000 rpm, for 20 min, at 4°C and the supernatant moved to a fresh tube. The protein was quantified using a Bradford assay.

FlagM2 resin was washed 3 times in buffer A and the clarified supernatant was added to the FlagM2 resin and incubated for 2 hr, on rotation, at 4°C. The lysate was then centrifuged at 2000 rpm, for 3 min, at 4°C and the subsequent flow through removed. The resin was then washed 3 times with buffer A and during the final wash the resin was moved to a fresh tube. Flag-fusion protein was eluted under native conditions by competition with 3XFlag peptide (5 μg/μl) in buffer A added to the resin and incubated with rotation, for 2 hr, at 4°C. Samples were centrifuged for 3 min, at 2000 rpm and the eluate was moved to a fresh tube and stored at -20°C until further examination.

2.4.3.2 - Strep purification: Column

Protein extracts were lysed in buffer A, with protease and phosphatase inhibitors, and rotated for 20 min at 4°C. Lysates were clarified with ultracentrifugation at 100000 g, for 1 hr, at 4°C and the supernatant removed to a fresh tube. The protein was quantified using a Bradford assay and Avidin (100 μg/10 mg) was added to the clarified lysate for 30 min at 4°C. The lysates was then centrifuged at 13000 rpm, for 10 min and the clarified, Avidin treated supernatant was loaded on a 4b Sepharose column. The pre-cleared lysate was then added to the Strep-Tactin Sepharose column (IBA) which had been equilibrated with buffer A. The flow through was collected and reapplied to the column. The column was then washed 5 times with 10 times the column volume with buffer A. Tagged proteins were eluted in 5 fractions with 10 mM biotin dissolved in buffer A.

2.4.3.3 - Strep pulldown: Magnetic beads

Protein extracts were lysed in buffer A, with protease and phosphatase inhibitors, and rotated for 20 min at 4°C. Lysates were clarified with centrifugation at 13000 rpm, for 10 min, at 4°C and the supernatant removed to a fresh tube. As described in the Strep column purifications the lysate was quantified, treated with Avidin and precleared on a Sepharose column. The precleared lysate was added to Strep magnetic beads which had been washed in buffer A. The lysate and bead mixture was incubated at 4°C, with rotation, for 1 hr. The beads were then separated from the lysate using a magnet and the beads were washed 5 times with buffer A, each time using the magnet to separate the liquid from the beads. The tagged protein was eluted using 10 mM biotin dissolved in buffer A, with rotation at 1000 rpm, for 30 min, at 37°C. The eluate was separated from the beads using the magnet and the eluate was stored at -20°C until further examination.

Strep affinity purification in cells expressing HA-Ubiquitin was conducted with the assistance of Dr David Gaboriau.

For small scale Strep affinity pulldowns in cells expressing HA-Ubiquitin, HEK-293 cells expressing inducible Strep-Claspin or the empty vector were transfected with cDNA HA-ubiquitin using JetPrime, according to the manufacturer's instructions. The expression of Strep-Claspin was induced as described, 6 hr post transfection. 24 hr after transfection cells were treated with Hydroxyurea for 18 hr. Cells were then treated with WP1130 and/or MG132. 6 hr post drug treatment cells and subjected to small scale Strep pulldown as described.

2.4.3.4 – Immunoprecipitations

For immunoprecipitation experiments, IgG or antibody were pre-bound to protein A/G beads (Santa-Cruz) by the addition of IgG or antibody (1 mg/ml) to buffer A and added to the beads for 2 hr, on rotation, at 4°C. Concurrently, cell pellets were lysed in buffer A and clarified at 13000 rpm, for 10 min, at 4°C. The clarified lysate was added to protein A/G beads and rotated for 2 hr, at 4°C. The lysate was then removed from the beads and added to prepared antibody bound A/G beads. This mixture was rotated for 2 hr, at 4°C.

After extensive washing with buffer A, proteins were recovered in Laemmli by boiling for 4 min at 95°C. The eluate was stored at -20°C until further examination.

2.4.4- Mass spectrometry sample clean-up protocols

2.4.4.1 - Acetone precipitation

To precipitate proteins, 100 % ice-cold acetone was added to the purified protein material at a ratio of 3:1 of acetone to elution volume. The mixture was placed at -20°C for 12 hr to allow precipitation of protein from the sample. Sample was then centrifuged at 13000 rpm, for 10 min, at 4°C and the resulting pellet was re-suspended in denaturing buffer (10 mM HEPES, pH 8.0, 6 M Urea, 2 M Thiourea) and stored at -20°C until further analysis.

2.4.4.2 - Protein dialysis

Dialysis tubing (cut off < 10 kDa) was soaked in ultrapure water before being clamped and rinsed out with buffer A. A small volume of purified protein was added to the clamped tubing and examined for leaks. If secure, all the eluate was added and the majority of air was removed, however as the sample contained moderate levels of NaCl, a little slack was left in the tubing to allow for sample expansion.

Dialysis buffer (ammonium carbonate 50 mM), 20 times the volume of the eluate was added to a beaker and the tubing was added, with continuous stirring at 4°C. After 4 hr the dialysis buffer was removed and replenished and after another 12 hr this process was repeated. After 36 hr the tubing was removed and the clamp released and the dialysed eluate was collected and stored at -20°C until further analysis.

2.4.4.3 - Desalting column

The desalting column was centrifuged at 1000 g, for 2 min, to remove storage buffer. Ammonium carbonate buffer (50 mM) was added to column and centrifuged at 1000 g, for 2 min, to wash column, this was repeated twice. Eluate material was then added to the desalting column and the sample was allowed absorb into the washed resin. A fresh collection tube was placed under the desalt column to collect the sample and the column

was spun at 1000 g, for 2 min. The collected desalted sample is stored at -20°C until further analysis.

2.4.4.4 - Centrifugal filtration

The Amcion filter (<10 kDa cut-off) was washed with buffer A, centrifuged at 2000 rpm, for 2 min, after repeating 3 times, the eluate was added to the filter and the sample was centrifuged at 13000 rpm, for 20 min. The collection tube was then discarded and a fresh tube used to collect the concentrated sample by inversion of the filter into a fresh collection tube and centrifugation at 13000 rpm, for 3 min. This process concentrated the sample volume 10 fold. The concentrated sample was stored at -20 until further analysis.

2.5 - SILAC mass spectrometry and data analysis

Mass spectrometry was conducted with the assistance of Dr Umberto Restuccia

2.5.1 – Mass spectrometry sample preparation

Protein lysates were prepared from labelled cells (as described in 2.3.5) and loaded onto individually pre-equilibrated Strep-Tactin Sepharose columns (as described in 2.6.2). Proteins were recovered using biotin displacement competition then mixed at 1:1 ratio, concentrated on a centrifugal filter (<10 kDa cut off) and resolved on a 4-12% pre-cast gel (Bio-Rad) as previously described in 2.4.2.1. Gels were stained by Instant Blue (Expedeon) as described in 2.4.2.4 and lanes were cut into 10 slices each of which was subject to reduction, alkylation and trypsin digestion as described (Restuccia et al., 2009).

Briefly, the 10 gel slices were washed twice in ammonium bicarbonate (ABC), followed by the addition of acetonitrile (ACN) to shrink the slices. This was then removed and dithiothreitol (DTT) was added at 56 °C for 30 min. ACN was then added to reshrink the slices. Iodoacetamide (IAA) was added for 20 min in dark and slices were again shrank with ACN before being dried by vacuum. Trypsin (diluted in ABC and containing $CaCl_2$) was then added to the slices for 20 min after which the samples were spun down and liquid removed. ABC was then added in excess and the samples were left overnight at 37

°C. Peptide mixtures were desalted and concentrated on home-made C_{18} desalting tips before being injected onto a UHPLC (Easy-nLC 1000 Proxeon, Denmark).

2.5.2 - Mass spectrometry spectra acquisition

Peptide separation occurred on a home-made 25 cm long reverse-phase spraying fused silica capillary column (75 µm i.d.) packed with 1.7 µm ReproSil AQ C18 (Dr Maisch GmbH, Germany). A gradient of eluents A (pure water with 2% v/v ACN, 0.1% v/v formic acid) and B (ACN with 20% v/v pure water with 0.1% v/v formic acid) was used to achieve separation, from 12% to 50% of B over 20 min, at a constant flow rate of 250 nl/min. The LC system was connected to a QExactive mass spectrometer (Thermo Scientific, Bremen, Germany) equipped with a nanoelectrospray ion source (Proxeon Biosystems, Odense, Denmark). Full scan mass spectra were acquired in the mass spectrometer with the resolution set to 70,000 (at 200 m/z) to a target value of 1e6 for a maximum injection time of 120 msec. The acquisition mass range for each sample was from m/z 300 to 1750 Da and samples were run in duplicate. The ten most intense doubly and triply charged ions were automatically selected and HCD fragmented after accumulation to a 'target value' of 1e5 for a maximum injection time of 120 msec, and recorded with resolution of 35000 (at 200 m/z). Normalized Collision energy was set to 25 % and isolation width to 3.0 m/z. Target ions already selected for the MS/MS were dynamically excluded for 5 sec.

2.5.3 - Mass spectrometry analysis

Identification and quantification of peptides and proteins were performed with MaxQuant 1.5.1.2 against the human Uniprot complete proteome set using the Andromeda search engine in which trypsin specificity was used with up to two missed cleavages allowed (Cox and Mann, 2008). Criteria for high-confidence protein identification were at least 2 peptides (1 unique), 6 amino acids of minimal length for high-confidence protein identification and quantified with at least 2 ratio counts. Cysteine carbamidomethylation was used as fixed modification, methionine oxidation and protein N-terminal acetylation as variable modifications. Mass deviation for MS/MS peaks was set at 4.5 ppm. The peptides and protein false discovery rates (FDR) were set to 0.01. The lists of identified

proteins were filtered to eliminate reverse hits and known contaminants. For quantitative analysis the options Re-quantify and second peptide were selected. Significant outliers scores were calculated using Perseus 1.5.1.6 (Cox and Mann, 2008) and those with a p-value < 0.05 have been selected for further analysis. Proteins were selected to be interactors and further investigated if they display a fold change higher than 3, based on the ratio distribution of all the quantified proteins.

Selected proteins were further filtered by the CRAPome (Mellacheruvu et al., 2013), to eliminate probable purification contaminants. Proteins detected in > 70% of CRAPome control experiments were eliminated from further analysis. The remaining protein list was subjected to biological network clustering using EnrichR (Chen et al., 2013) and Panther (Mi et al., 2013) analysis tools, to select a candidate for further functional investigation.

2.6 – Flow cytometry

Table 2.6 details the conditions for which primary and secondary antibodies were used for flow cytometry in this study.

2.6.1 - DNA content profiles: Propidium iodide staining

Empty vector and Strep-Claspin cells treated with Doxycycline and Strep-Claspin cells untreated were plated at $2x10^5$ cells and allowed to grow for 24, 48 and 72 hr. At each time point cells were typsinised and fixed with 70% ethanol prior to staining with propidium iodide (PI) for 30 min prior to analysis on a BD FACS Canto A cytometer (BD Biosciences). Using the Watson pragmatic model feature on the FlowJo software v10, DNA content percentages for each sample was calculated.

2.6.2 – Detection of Strep-Claspin by flow cytometry

Empty vector and Strep-Claspin cells were plated at $2x10^5$ cells and allowed to grow for 24 hr and treated with Doxycycline (1 μg/μl) for a further 24 hr. Cells were fixed in 4% paraformaldehyde (PFA) and permeablised with PBS-TX and blocked in 1% BSA-PBS, after which the cells were incubated with primary mouse anti-Strep antibody for 2 hr in 1% BSA-PBS-TX. Cells washed with 1 % BSA-PBS and then incubated with Alexa Fluor

488 goat anti-mouse antibody for 30 min in 1% BSA-PBS-TX. DNA was stained with 1 µg/ml DAPI for 30 min and samples were measured on a BD FACS Canto II cytometer (BD Biosciences) and analysed with FlowJo software v10.

2.6.3 – Detection of γH2AX by flow cytometry

For the analysis of DNA damage, cells were fixed with 1% PFA, washed with PBS containing 1% BSA, permeablised with PBS containing 0.05% saponin and 1% BSA. Cells were stained with primary rabbit anti-pSer139 γH2AX antibody and mouse anti-Strep antibody in 0.05% Saponin, followed by incubation with secondary Alexa Fluor 647 donkey anti-rabbit antibody and Alexa Fluor 488 goat anti-mouse antibody in 0.05% Saponin. DNA was stained with 1 µg/ml DAPI and samples were measured on a BD FACS Canto II cytometer (BD Biosciences) and analysed with FlowJo software v10. Statistical analysis of three independent experiments was performed using Prism (GraphPad Software).

Primary Antibody	**Species**	**Antibody Source**	**Primary Conditions**
pSer139 γH2AX	Rb	Cell Signaling 9718S	(1:1000) 0.05% Saponin
Strep	Mu	Qiagen 34850	(1:1000) 1% BSA-PBS-TX / (1:1000) 0.05% Saponin
Secondary Antibody	**Species**	**Antibody Source**	**Secondary Conditions**
Alexa Fluor 488	Mu	Invitrogen A-11001	(1:500) 1% BSA-PBS-TX / (1:500) 0.05% Saponin
Alexa Fluor 647	Rb	Invitrogen A-31573	(1:500) 0.05% Saponin

Table 2.6. Details of antibodies used for flow cytometry.

2.7 - Microscopy

2.7.1 – Routine immunofluorescence microscopy protocol

Routinely for immunofluorescence, $5x10^4$ U2OS cells were plated on 12 mm no 1.5 UV sterilised coverslips and left to settle overnight prior to 48 hr siRNA or 24 hr DNA transfection. If cells were subjected to shorter treatments, $1x10^5$ U2OS cells were plated and left to settle overnight prior to fixation.

When using HEK-293 cells, $2x10^5$ cells were plated on Poly-L-Lysine (PLL) coated, UV sterilised cover slips and left to settle overnight prior to 48 hr siRNA transfection. If cells were not subjected to treatment, $4x10^5$ cells were plated and left to settle overnight prior to fixation.

On the day of fixation, media was removed and cells washed with PBS before fixation with 4 % paraformaldehyde (PFA) for 15 min at room temperature. Cells were then washed with PBS and permeablised, with incubation with PBS-TX, for 3 min. Cells were then blocked in 1 % BSA PBS-TX for 30 min at room temperature. Primary and secondary antibodies were prepared in 1 % BSA PBS-TX at an appropriate dilution. Table 2.7 details the conditions for which primary and secondary antibodies were used in this study, for immunofluorescence. Primary antibodies were added to the cells for 1 hr before 2 washes in PBS-TX after which the secondary antibody was added for 1 hr at room temperature in the dark. After antibody incubation, cells were washed in PBS-TX, PBS and finally dH_2O to remove salt. The coverslips were allowed air dry at room temperature. Nuclei were counterstained stained with DAPI and coverslips were mounted using Slow Fade reagent (Invitrogen). Cells were examined using an IX71 Olympus microscope under a 100x, 60x or 40x oil immersion objective.

2.7.2 Operetta quantification

Operetta quantification was conducted with the assistance of Dr David Gaboriau

USP9X nuclear signal was quantified with Operetta high content microscopy (Perkin Elemer). Slides were scanned under 40x air immersion. The nuclear and cytoplasmic signals were automatically selected. The USP9X nuclear signal was normalised to total USP9X cellular signal and graphed using Prism (GraphPad Software).

Primary Antibody	Species	Antibody Source	Primary Conditions
HA-11	Mu	Covance 901501	(1:1000) 1% BSA-PBS-TX
HERC2	Rb	Bethyl A30-905A	(1:1000) 1% BSA-PBS-TX
Strep	Mu	Qiagen 34850	(1:1000) 1% BSA-PBS-TX
USP9X	Rb	Bethyl A201-351A	(1:1000) 1% BSA-PBS-TX
γH2AX	Rb	Cell Signaling 9718S	(1:1000) 1% BSA-PBS-TX
Secondary Antibody	**Species**	**Antibody Source**	**Secondary Conditions**
Alexa Fluor 488	Mu	Invitrogen A-11001	(1:300) 1% BSA-PBS-TX
Alexa Fluor 488	Rb	Invitrogen A-11034	(1:300) 1% BSA-PBS-TX
Alexa Fluor 647	Rb	Invitrogen A-31573	(1:300) 1% BSA-PBS-TX
Alexa Fluor 647	Mu	Invitrogen A-21238	(1:300) 1% BSA-PBS-TX

Table 2.7. Details of antibodies used for microscopy.

2.8 - DNA fiber analysis

Following siRNA treatment U2OS cells were pulse-labelled with 25 μM IdU (Alpha Technologies) for 30 min, rapidly rinsed 3 times with pre-equilibrated media, and pulse-labelled with 200 μM CldU (Alpha Technologies) for 30 min.

Alternatively, after the first IdU pulse, cells were treated with 2 mM Hydroxyurea for 2 hr, before being washed 3 times with media and labelled with CldU for 30 min. Labelled cells were harvested at 2000 rpm for 10 min, counted and diluted to $2.5x10^5$. Labelled cells were then mixed 1:8 with unlabelled cells and a 2.5 μl aliquot of this mixture was placed on a coverslip and 7.5 μl of spreading buffer (0.5% SDS, 200mM Tris-HCl, pH7.4, 50mM EDTA) was added to the cells. The cells were left to incubate for 10 min, at room temperature and the coverslip was tilted at 15° to allow DNA to run down the glass. When completely dried, fibers were fixed by immersing in methanol/acetic acid (3:1) overnight at 4°C, denatured with 2.5 M HCl for 1 hr at room temperature, washed with PBS, and blocked for 30 min with 0.1% Tween 20 in 1% BSA/PBS. This protocol was adapted from (Merrick et al., 2004) and (Jackson and Pombo, 1998).

All antibodies were diluted in blocking before and in between each antibody incubation, slides were washed with PBS and blocking buffer. CldU tracks were detected with rat

anti-BrdU monoclonal antibody clone no BU1/75 (ICR1) (Thermo Scientific, cat n. MA1-82088) and AlexaFluor 488–conjugated chicken anti–rat IgG (Invitrogen, cat n. A21470). IdU was detected using mouse anti-BrdU monoclonal antibody (BD Biosciences, cat n. 347580) and AlexaFluor 546–conjugated goat anti–mouse IgG (Invitrogen, cat n. A21123). Fibers were examined using an IX71 Olympus microscope with a 40× oil immersion objective. For quantification at least 150 tracks were scored in each sample and three independent experiments performed. Statistical analysis was performed using Prism (GraphPad Software).

2.9 - Statistical analysis

Where indicated statistical analysis was performed using GraphPad Prism software. Three experimental repeats were performed for each dataset. Data are presented using standard deviation (s.d). Student's t-test was used to determine statistical significance between two groups.

CHAPTER 3

CHARACTERISATION AND PURIFICATION OPTIMISATION OF THE FLP-IN TREX HEK-293 CELLULAR SYSTEM FOR THE INDUCIBLE EXPRESSION OF TAGGED CLASPIN

3.1 – Introduction: Claspin regulation, the search continues

Although it has been well established that Claspin is essential for both replication and CHK1 activation, as discussed in the introduction, the mechanism by which Claspin achieves these functions in mammalian cells remains somewhat unclear.

Solving the architecture and assembly of protein complexes is key to understanding the molecular mechanisms underpinning any cellular operations. Therefore, in this study a mass spectrometry based approach was used to discover novel protein partners of Claspin.

The identification of novel Claspin protein-protein interactions will help unravel complete molecular understanding of the crucial protein.

3.2 – Preliminary characterisation of the Flp-In TREx cellular system for the inducible expression of Claspin

The Flp-In T-Rex human embryonic kidney (HEK) 293 cell line contains a tagged-Claspin (Strep-Claspin) fusion protein conditionally expressed from a TET-controlled promoter upon the addition of Doxycycline to the culture medium as described in Materials and Methods Section 2.3.3. This system was generated by Dr Michael Rainey prior to commencement of this study.

To begin the characterisation of the Flp-In TREx cellular system the expression kinetics of the Strep-Claspin protein following induction by Doxycycline was examined (Figure 3.2 A). The empty vector was used as a control cell line for all experiments involving the Flp-In TREx cellular system. Claspin was induced and 24 hr after Doxycycline addition Claspin reached a maximum level, as increased time of induction failed to increase

Claspin levels as observed up to 72 hr (Figure 3.2 A). Approximately 5 times more Claspin is expressed upon induction compared to the empty vector control cells. Also apparent is the leaky expression of the Flp-In TREx system, with a low amount of the Strep tag detectable in cells which have not been subjected to induction (Figure 3.2 A: lanes 9-12). The empty vector samples contained no detectable Strep tag confirming that the system itself is somewhat leaky, as opposed to a non-specific band associated with antibody detection (Figure 3.2 A).

To examine whether the inducibly expressed Claspin caused any cell growth or cell cycle aberrations, growth curves and DNA content analysis were conducted using the Flp-In TREx cells plus or minus Claspin induction with Doxycycline, as well as empty vector cells. To analyse cell growth, cell number was examined by trypan blue exclusion using the Countess automated cell counter at time of induction, (time 0 hr, Figure 3.2 B) and every 24 hr up to hr 96. This was repeated 3 times to generate average counts with standard deviation bars (Figure 3.2 B). The induction of Claspin didn't appear to affect cell growth at the time points examined and the kinetics were almost identical to that of the empty vector cells (Figure 3.2 B).

To determine DNA content, the cells were fixed at the time of induction (time 0 hr, Figure 3.2 C) and every 24 hr up to 72 hr and stained with propidium iodide. Flow cytometry was then used to assess the DNA content (Cecchini et al., 2012). Flow cytometry demonstrated that, at each time-point examined, the induction of Strep-Claspin did not affect the distribution of cells within the different phases of the cell cycle, compared to the empty vector control. (Figure 3.2 C).

As discussed in the introduction, Claspin levels are highly regulated in the cell cycle and at their highest in S-phase (Aze et al., 2013). To examine whether the inducible system was replicating this oscillation, cells plus or minus Doxycycline induction were co-stained with DAPI and the Strep antibody and subjected to flow cytometry analysis (Figure 3.2 D). The Strep-Claspin cells minus induction were used to select and gate the Strep negative cellular population, with Strep intensity plotted against DAPI content. The

induced Strep-Claspin cells were then analysed and the true Strep positive population was detected. The use of co-staining with DAPI, another marker of DNA content (Darzynkiewicz et al., 2001), demonstrated that the majority of Strep positive cells were detected in S-phase (Figure 3.2 D). As 40% of the cells subjected to induction were detected to be Strep positive, this demonstrated that whilst overexpression of Claspin has been induced, overexpression is not occurring in every cell. This reveals the retention of cell cycle control within the inducible system, as induction of Claspin is predominantly restricted to S-phase.

Further confirming this observation, an immunofluorescence experiment was conducted to analyse Strep positive cells after induction. This allowed the visualisation of Strep detection at a single cell level (Figure 3.2 E). In agreement with the flow cytometry analysis, Strep expression was detected in many but not all cells. Strep expression was only detected in Promyelocytic Leukaemia Protein nuclear bodies (PML-NBs) (Lallemand-Breitenbach and de The, 2010). Strep-Claspin was never detected in a mitotic cell, as discriminated by DAPI staining of chromosome condensation (Kireeva et al., 2004), a stage of the cell cycle were Claspin is heavily degraded (Bennett and Clarke, 2006).

Preliminary characterisation of the Flp-In TREx cellular system for the inducible expression of Claspin supported the use of this system for further studies, as Claspin expression didn't appear to cause any aberrant changes to the cell.

(A)

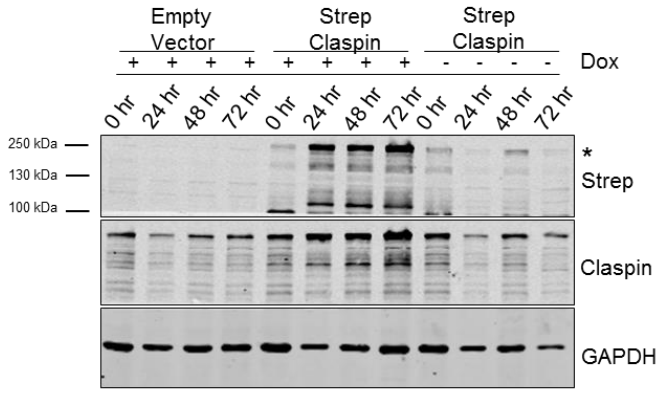
Empty Vector
Strep Claspin
Strep Claspin
Dox
0 hr
24 hr
48 hr
72 hr
250 kDa
130 kDa
100 kDa
*
Strep
Claspin
GAPDH

(B)

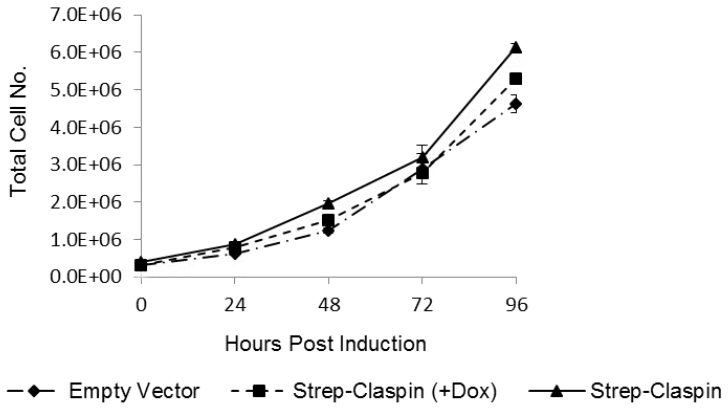
Total Cell No.
Hours Post Induction
Empty Vector
Strep-Claspin (+Dox)
Strep-Claspin

(C)

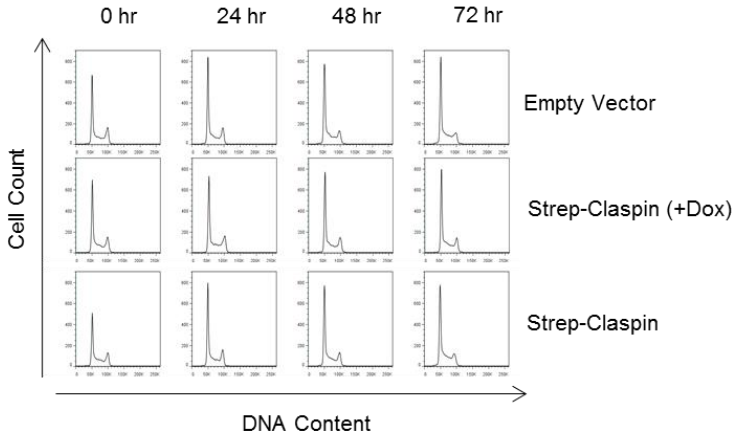
0 hr
24 hr
48 hr
72 hr
Cell Count
DNA Content
Empty Vector
Strep-Claspin (+Dox)
Strep-Claspin

(D)

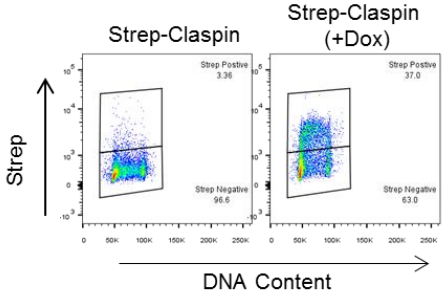
Strep-Claspin
Strep-Claspin (+Dox)
Strep
DNA Content

(E)

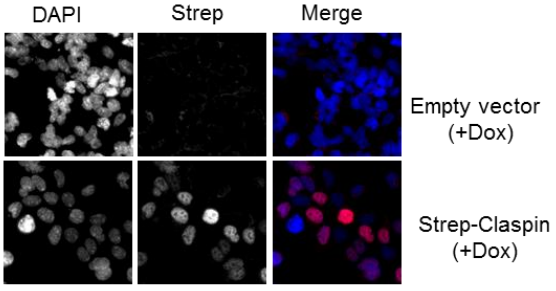
DAPI
Strep
Merge
Empty vector (+Dox)
Strep-Claspin (+Dox)

Figure 3.2. Characterisation of inducible Strep-Claspin HEK-293 cellular system. HEK-293 cells containing empty vector or Strep-Claspin were either induced with Doxycycline or left untreated. (A) Immunoblot of Claspin expression up to 72 hr post induction. The asterisk marks the immunoreactive band for Strep-Claspin at ~250 kDa. (B) Growth curves were generated from total cell number, as determined by trypan blue exclusion at time of induction (0 hr) and 24 hr, 48 hr, 72 hr and 96 hr post induction. (C) Cells were fixed at 0 hr, 24 hr, 48 hr and 72 hr post induction and DNA content was determined with PI staining and flow cytometry analysis. (D) Cells were fixed and stained with primary anti-Strep antibody and the secondary Alexa Fluor 488 nm goat anti-mouse antibody and DAPI was used to examine DNA content. Cells were then analysed by flow cytometry. (E) As in D, but cells were subject to immunofluorescence analysis.

3.3 – Examination of buffer conditions to extract chromatin bound Claspin

Claspin can bind to the chromatin, where it performs important functions. As the inherent aim of this study was to identify relevant novel Claspin interacting proteins, possibly occurring on the chromatin, it was important to establish buffer conditions that facilitated the maximal extraction of Claspin from the chromatin.

To determine optimal buffer conditions for Strep-Claspin chromatin extraction, experiments examining the solubility of Claspin in three different buffers was first performed. buffer 1 and 2, a NP40 based and TGN buffer respectively, have been documented in Claspin literature as suitable for extraction of Claspin from the chromatin (Broderick et al., 2013; Liu et al., 2006; Liu et al., 2012; Rainey et al., 2013). Buffer 3, containing Triton, had been effectively applied in our laboratory (data not shown) as compatible for purification of tagged proteins by not interfering with binding or protein elution.

Following 24 hr induction of Strep-Claspin, cells were harvested and lysed in one of the 3 buffers and fractionated into soluble and insoluble fractions, as described in Materials and Methods Section 2.4.1.3 and 2.4.1.4. The samples were than subjected to analysis by immunoblotting. It appeared that all three buffers could extract the majority of Strep–Claspin from the chromatin (Figure 3.3 A) but buffer 3 seemed to be most effective, as the levels of insoluble Claspin were lowest in this buffer. The inclusion of GAPDH and

H2A in the immunoblot confirmed the successful fractionation of the lysate and equal protein loading (Figure 3.3 A).

To establish optimal NaCl conditions for Claspin extraction in buffer 3, a variety of NaCl concentrations were used to examine Claspin chromatin extraction. Soluble and insoluble samples were then analysed by immunoblotting. Whilst 100 mM NaCl could extract a reasonable fraction of Claspin, increasing NaCl concentrations could better release Claspin from the chromatin, with 300 mM NaCl extracting the majority of Claspin with little detectable in the insoluble fraction (Figure 3.3 B). Here after in this study this buffer is referred to as buffer A (50 mM Tris-HCl, pH 7.4, 300 mM NaCl, 1 mM EDTA, 1% Triton-X) and was used routinely for all protein studies unless otherwise stated.

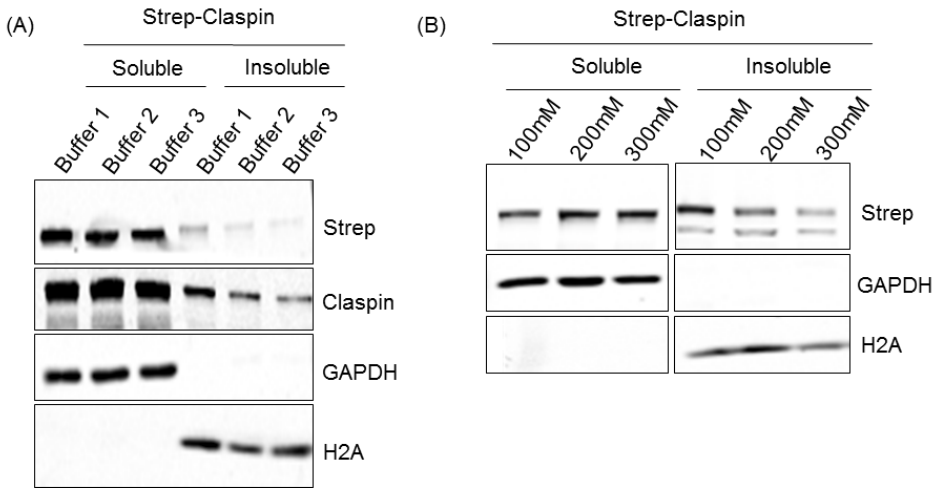

Figure 3.3. Extraction of Strep-Claspin from the chromatin. HEK-293 cells Strep-Claspin were induced with Doxycycline and harvested 24 hr post induction and (A) lysed in buffer 1, 2 or 3 or (B) buffer 3 (50 mM Tris-HCl, pH 7.4, 1 mM EDTA, 1% Triton-X) with varying concentrations of NaCl ranging 100 mM, 200 mM and 300 mM. Proteins were separated into soluble and chromatin enriched fractions by and analysed by immunoblotting.

3.4 – Method development for the isolation of Claspin and interacting proteins

3.4.1 - Small scale Flag precipitation and Strep pulldowns

Owing to the dual affinity tagging of Claspin on its C-terminus, either a Flag precipitation or Strep affinity protocol could be applied to isolate Claspin. To examine which protocol was most efficient, small scale purifications were performed to attempt capture Claspin and known protein interactions.

The Flag precipitation involves the use of an antibody coupled resin and a peptide competition based elution. For small scale precipitations, typically 2 mg of protein was prepared from both Strep-Claspin induced cells and empty vector control cells. The cell lysate was then added to a resin conjugated with Flag antibody and after extensive washing, Flag tagged proteins were eluted by peptide competition as described in Materials and Methods Section 2.4.3.1. Using this procedure isolation of tagged Claspin in the pulled down (PD) fraction was confirmed by immunoblot (Figure 3.4.1 A), with no protein isolated from the empty vector control. The isolated material from the induced cells could interact with a known Claspin partner CDC7 (Rainey et al., 2013).

The Strep tag is a short amino acid peptide which can bind with high selectivity to an engineered Strep-Avidin; Strep-Tactin. For small scale Strep pulldowns, 2 mg of protein from both Strep-Claspin and empty vector cells were added to Strep-Tactin magnetic beads. Following lysate binding, Strep tagged proteins were displaced by biotin as described in Materials and Methods Section 2.4.3.3. The detection of tagged Claspin in the PD material was observed by immunoblot (Figure 3.4.1 B). Again this purified material could interact with CDC7.

Both Flag and Strep small scale isolation experiments confirmed the effectiveness of the affinity tags as a means of protein purification. Importantly, exogenously expressed Claspin behaved like endogenous Claspin and could interact with a known binding partner CDC7.

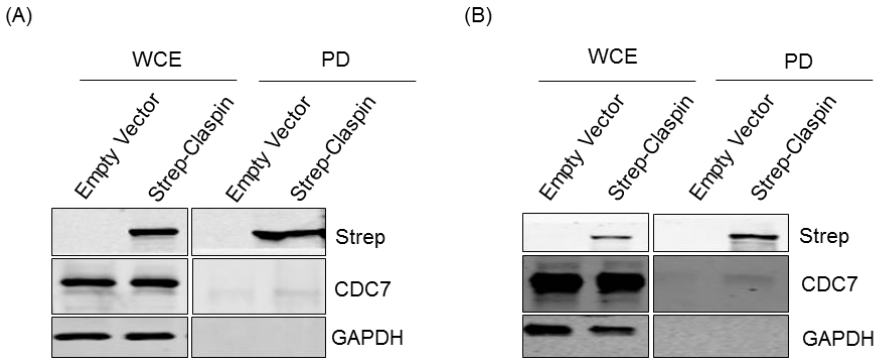

Figure 3.4.1. Small scale Flag precipitation and Strep pulldown can isolate Claspin and known partner CDC7. Strep-Claspin or empty vector cells were induced with Doxycycline and harvested 24 hr post induction and (A) subjected to Flag precipitation or (B) Strep pulldown. Proteins were analysed by immunoblotting

3.4.2 - Large scale Flag purifications

To facilitate the identification of novel Claspin interacting partners, large quantities of purified protein were required for proteomic studies. Both small Flag and Strep scale protocols appeared to isolate Claspin and a known interactor with a similar efficacy. However, limited by the binding capacity of the Strep-Tactin magnetic beads, up-scaling the Strep purification procedure involved switching the binding matrix to the Strep-Tactin gravity flow columns, which have a higher binding capacity. Up-scaling the Flag purification protocol involve no change in tools but simply an increase in lysate concentration and resin volumes, therefore the Flag purification was selected for large scale purification studies.

For initial large scale purifications, typically 15 mg of protein was prepared from both Strep-Claspin and empty vector cells. This lysate was then added to Flag resin and following peptide elution as described in Materials and Methods Section 2.4.3.1. The purified material was examined by immunoblotting and silver staining.

The success of the large scale Flag purification was confirmed by immunoblotting, where a small fraction of the purified material was analysed and tagged Claspin was easily detectable (Figure 3.4.2 A). To examine whether material purified from Strep-Claspin

cells differed from material purified from the empty vector control cells, a small fraction of the purified material from both were subjected to silver staining.

The material from the Strep-Claspin PD had a differential banding pattern to the empty vector control, with more bands visible, indicative of more protein (Figure 3.4.2 B: lanes 1 and 3). Importantly a strong band running at 250 kDa, the expected molecular weight of our bait protein Claspin in SDS-PAGE, was observed (Uno and Masai, 2011).

Considering that mass spectrometry analysis was the final destination of the purified material, it was important to eliminate the high salt concentration and detergent from the sample as these contaminants can interfere with proteomic analysis.

To this end, acetone precipitation, a method of protein precipitation commonly applied for proteomic studies, was performed. To analyse the efficiency of this strategy, a fraction of the samples post acetone precipitation were also subjected to sliver staining alongside the initial purified material from the Strep-Claspin and control empty vector cells. However, upon acetone precipitation, huge sample loss was evident (Figure 3.4.2 B: compare lanes 1 and 2, 3 and 4). The only faint band visible in the Strep-Claspin post acetone precipitation lane was likely the bait protein itself (Figure 3.4.2 B: lane 4).

Problems with low protein yield post acetone precipitation can be overcome by increasing the amount of protein to be precipitated. However increasing the protein amount subjected to Flag purification from 15 mg to 30 mg led to problems.

Although higher amounts of protein were visible by silver staining from our bait protein after Claspin isolation (Figure 3.4.2 C: lane 2), the increased protein amount led to a much greater level of background from the empty vector control (Figure 3.4.2 C: lane 1). The banding pattern between the empty vector control and Strep-Claspin, as examined by silver staining, were almost identical. Increased wash steps prior to elution did not alleviate this problem (data not shown).

Whilst a change of buffer conditions may have overcome the problem of high background, the extensive optimisation of the Claspin extraction buffer conditions had

been confirmed to be optimal for the protein of interest. Instead, the use of the second affinity tag, Strep, for large scale purification was examined.

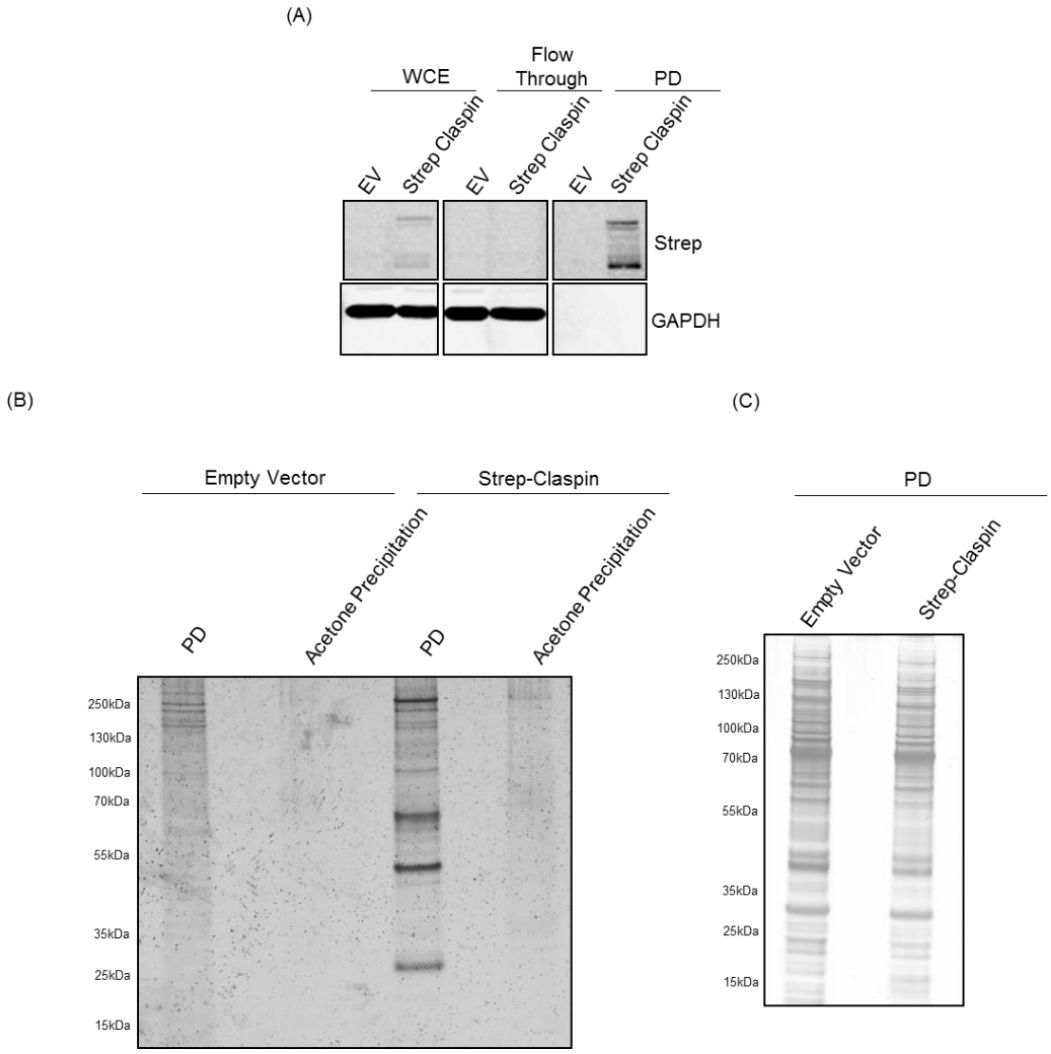

Figure 3.4.2. Examination of large scale Flag purifications. Strep-Claspin or empty vector cells were induced with Doxycycline and harvested 24 hr post induction and (A) subjected to Flag purification. Proteins were analysed by immunoblotting. (B) The PD material from A was subjected to acetone precipitation and an aliquot of the material pre and post precipitation was subjected to silver staining. (C) Increasing the amount of protein subjected to Flag purification led to increased background levels from empty vector cells as observed by silver staining of PD material from cells.

3.4.3 - Large scale Strep purifications

Large scale Strep purifications utilise gravity flow columns, which are packed with high binding capacity resin, to facilitate high yields of pure Strep tagged proteins as described in Materials and Methods Section 2.4.3.2. Typically 30 mg of protein from both Strep-Claspin and empty vector cells were prepared for column purification. After lysate application to 2 separate Strep-Tactin columns, proteins were displaced by biotin. The purified material was collected across 6 separate fractions, each 100 µl in volume. Each fraction was then analysed by immunoblot and the fractions containing the bait protein were further examined by silver staining.

Immunoblot detection confirmed the successful purification of tagged Claspin (Figure 3.4.3 A) in multiple fractions, typically fractions 2-5. When fractions 2 and 3 of purified material from both Strep-Claspin and empty vector cells were stained, first with Coomassie blue and subsequently silver, a different banding pattern was visualised between the two samples (Figure 3.4.3 B). Importantly the level of staining visible from the empty vector cells was minimal, indicating that the large scale Strep purification protocol afforded low levels of non-specific binding. This protocol proved robust and reproducible, overcoming the problems encountered with large scale Flag purification and was selected for future studies.

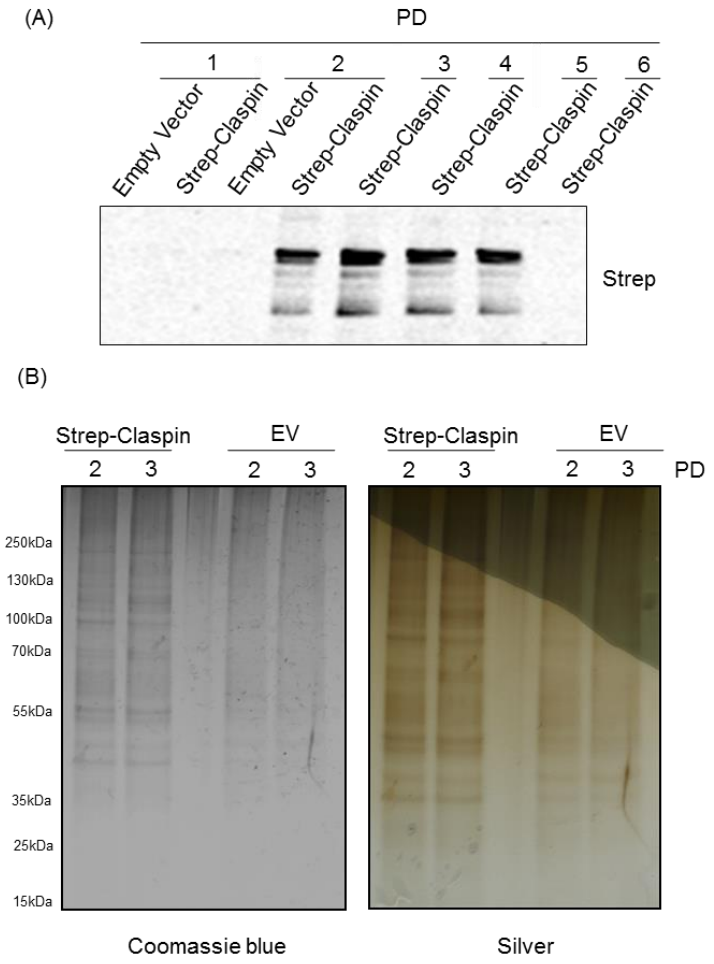

Figure 3.4.3. Large scale Strep purification can purify proteins with differential banding pattern to control. Strep-Claspin or empty vector cells were induced with Doxycycline and harvested 24 hr post induction and (A) subjected to Strep purification. 1-6 refer to the elution fraction. Proteins were analysed by immunoblotting. (B) Two PD fractions (fractions 2 and 3) from (A) were subjected to Coomassie blue and silver staining.

3.5 – Sample preparation for SILAC analysis

3.5.1 - Optimisation of sample preparation for proteomic studies

The large scale Strep gravity flow protocol, whilst generating a highly pure sample, generates multiple fractions of such material, accumulating in a large sample volume ~300 µl per purification. Further still, the purified material contained salts and detergents that are not compatible with the downstream proteomic analysis.

Ideally for mass spectrometry, samples should be concentrated to minimise sample injections and thus variability, as well as being free of potential reagents that interfere with analysis.

To address this problem several sample clean-up protocols, routinely used for proteomic analysis; acetone precipitation, centrifugal filtration, desalting columns and dialysis, were tested, as described in Materials and Methods Section 2.4.4. These protocols can both concentrate and purify samples.

To examine which method was the most efficient, a large scale Strep purification was performed using 30 mg of Strep-Claspin cells. The purified material was then equally divided into 4 and subjected to a method of sample clean-up. Dividing the purified material from a single purification ensured that each method received the same quality and quantity of purified protein.

An immunoblot examining each of the clean-up protocols identified centrifugal filtration as the most efficient method, with high levels of Strep-Claspin recovered (Figure 3.5.1 A: lane 8). Substantial loss of protein was observed in all other sample clean-up protocols tested.

A subsequent large scale Strep purification was performed using 30 mg of both Strep-Claspin and empty vector cells. The purified material from each purification was then subjected to centrifugal filtration. An equal aliquot of this material before and after centrifugal filtration clean-up was analysed by immunoblot (Figure 3.5.1 B). Importantly,

this immunoblot demonstrated that the cleaned up protein sample, which had also been concentrated, showed no loss of the bait Claspin and could still interact with a known partner CDC45 (Figure 3.5.1 B) with the same efficacy as the material initially isolated from the large scale Strep purification (Figure 3.5.1 B: compare lane 2 and lane 4).

When the cleaned up material from the Strep-Claspin and empty vector cells were examined by silver staining a differential banding pattern was observed (Figure 3.5.1 C). A strong band at 250 kDa, the expected molecular weight of Claspin in SDS-PAGE gels was visualised and there was minimal bands identified in the empty vector control.

These results demonstrated that the combination of the large scale Strep purification with centrifugal filtration provided a suitable approach to generate a sample of highly pure material that is free of any containments that could interfere with mass spectrometry analysis.

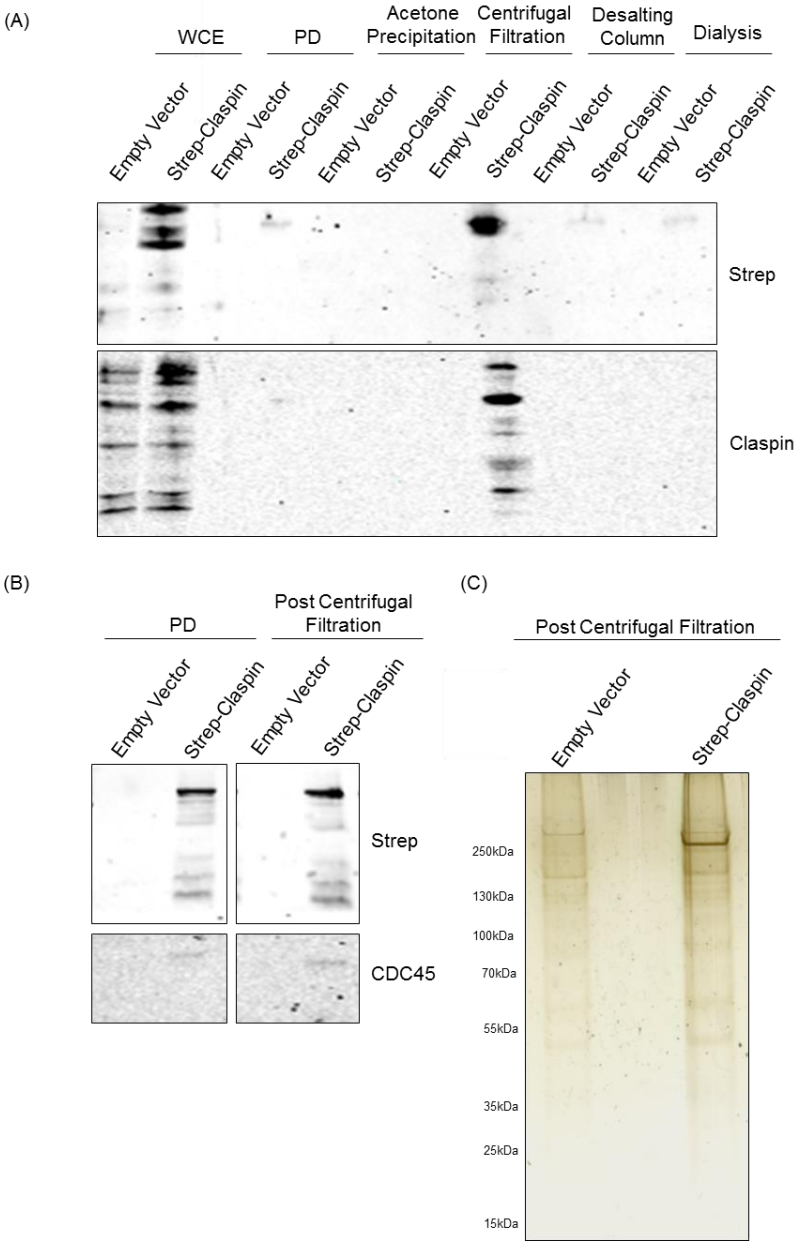

Figure 3.5.1. Optimisation of a sample preparation for mass spectrometry. (A) Strep-Claspin or empty vector cells were induced with Doxycycline and harvested 24 hr post induction and subjected to Strep purification before being subjected to the sample clean-up strategies indicated. Proteins were analysed by immunoblotting. (B) As in (A) but all the PD material was subjected to centrifugal filtration. (C) The PD cleaned up fractions from control and Strep-Claspin cells in (B) were subjected to silver staining.

3.5.2 – Purification of Claspin for SILAC analysis

Strep-Claspin and empty vector cells were metabolically labelled for SILAC as described in Material and Methods Section 2.3.5. Following 5 passages in heavy and light SILAC media and confirmation that the cells had undergone complete labelling with <95% incorporation (performed by Dr Umberto Restuccia, data not shown) the Strep-Claspin and empty vector cells were induced with Doxycycline. After 24 hr the cells were harvested and 30 mg of lysate from both cell types was prepared for purification.

These lysates were then applied to 2 separate Strep-Tactin columns and the tagged protein was eluted by biotin displacement. The purified material was collected in 6 separate fractions. Fractions 2-5 from the Strep-Claspin and empty vector purifications were then subjected to centrifugal filtration and the resulting material was combined. At each stage of the purification, samples were removed for analysis.

Immunoblot examination of the material confirmed the isolation of Claspin (Figure 3.5.2 A: lane 4). The purified material, post concentration, from both the empty vector control and Strep-Claspin cells, was then analysed by SDS-PAGE and silver staining. This demonstrated a differential banding pattern between samples (Figure 3.5.2 B), with minimal bands seen in the empty vector control. After combining the material from the Strep-Claspin and empty vector cells a small amount of the material was analysed by both Coomassie blue and silver staining (Figure 3.5.2 B). This demonstrated that a large quantity of material was available for proteomic studies.

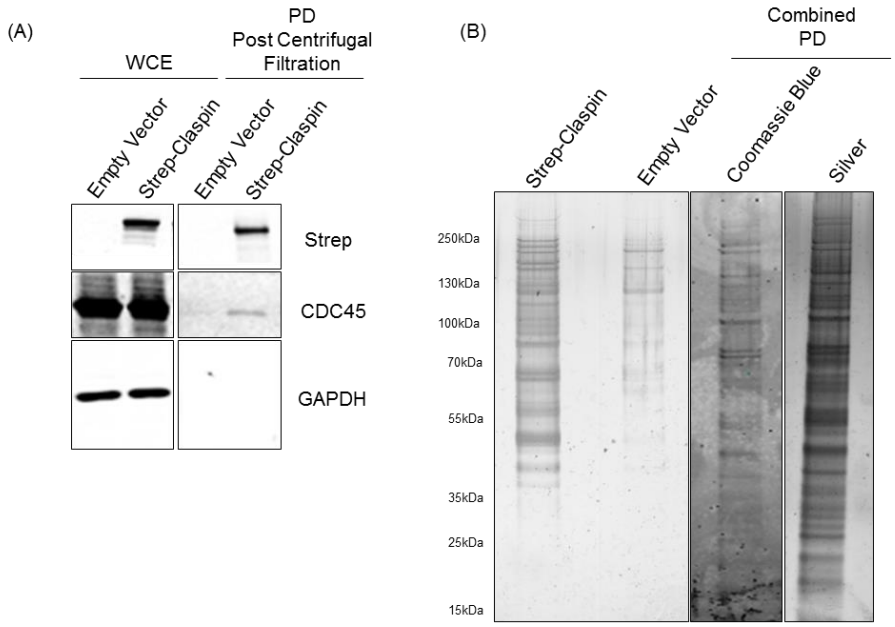

Figure 3.5.2. Preparation of protein material for SILAC analysis. (A) Strep-Claspin or empty vector cells were induced with Doxycycline and harvested 24 hr post induction and subjected to Strep purification before being subjected to centrifugal filtration. Proteins were analysed by immunoblotting. (B) Aliquots of the PD cleaned-up fractions from control and Strep-Claspin cells in (A) were subjected to silver staining, combined and stained again with Coomassie blue and silver.

3.6 - Analysis of SILAC data and selection of a candidate for further examination

To identify novel Claspin interacting proteins, a mixing after purification (MAP)-SILAC approach was applied. The purified material from 3.4.2, was subjected to SDS-PAGE and the gel was then stained with Coomassie blue (Figure 3.6 A), before being sliced up into 10 parts as described in Materials and Methods Section 2.5.1.

Briefly, each slice was digested with trypsin and subjected to mass spectrometry analysis. The peptides and proteins were identified with MaxQuant and only proteins with at least 2 peptides were identified (Cox and Mann, 2008). The list of identified proteins contained the protein Uniprot identification, gene name, protein name and the SILAC ratio, (expressed as Log2 of the ratio of empty vector over the Strep-Claspin) (Appendix I). Following the removal of reverse hits, 332 proteins were identified and quantified.

As expected, Claspin displayed the highest ratio, with a value of -5.8. This demonstrated an enrichment of the bait protein over the control. All the ratios showed a distribution markedly skewed towards the bait (Figure 3.6 B). Several known Claspin interactors were also detected, including the MCM 2-3-6 subunits of the MCM complex, with ratios of >-2.7 (Rainey et al., 2013). The detection of these interactors confirmed the effectiveness of the protein identification strategy used in this study.

To select candidates for further investigation, an arbitrary cut-off, which eliminated proteins with <3 fold enrichment was applied to the data, that is proteins with a SILAC ratio of <-1.5. This narrowed the list to 280 candidate proteins (Appendix II).

To further focus candidate assessment, the protein list was analysed using the contaminant repository for affinity purification, termed the CRAPome (Mellacheruvu et al., 2013). Again, an arbitrary cut off value was employed, with proteins present in > 30% of the CRAPome control lists eliminated from the investigation.

This indiscriminate data analysis generated a list of 176 proteins and putative Claspin interactors (Appendix III). Importantly, after the application of a stringent filtration

criteria, known Claspin interactors of the MCM complex were still retained within the final data set.

This filtered protein list was then subjected to examination using bioinformatics tools EnrichR (Chen et al., 2013) and Panther (Mi et al., 2013) and categorised by protein pathways and enriched molecular function.

EnrichR analysis identified several protein networks amongst the data set, including pathways in which a role for Claspin has been implicated, such as the cell cycle, apoptosis and proteasomal regulation (Figure 3.6 C) (Mailand et al., 2006; Petermann et al., 2008; Semple et al., 2007).

Panther analysis then revealed that proteins associated with the ubiquitin proteasome pathway, were the most enriched protein network, with subunits of the 26S proteasome, proteasomal ubiquitin recruiters, ubiquitin-activating enzymes, deubiquitinases and E3 ubiquitin protein ligases identified amongst the data (Figure 3.6 D).

Owing to this enrichment, it was amongst this network a candidate for functional analysis was selected with USP9X identified as the candidate protein of interest.

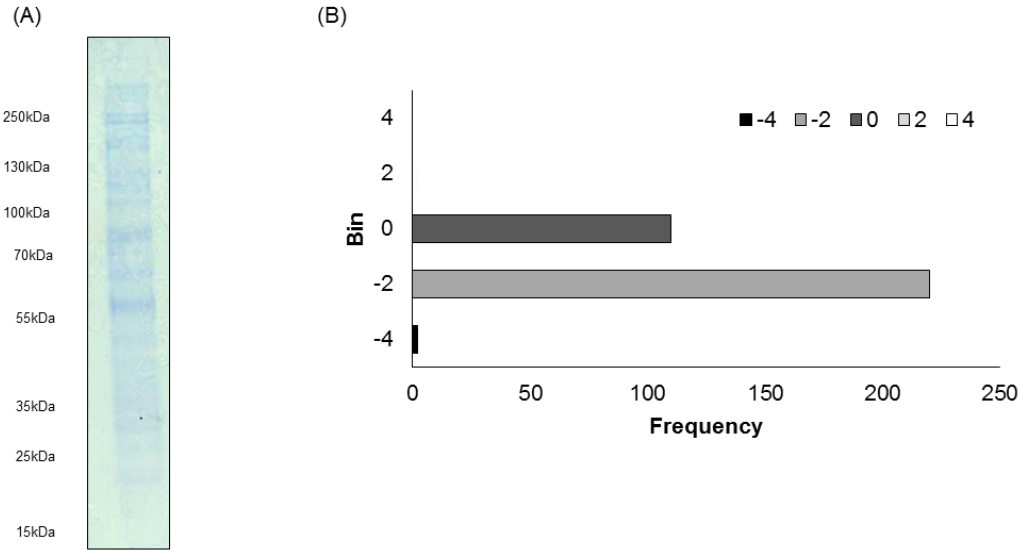

(C)

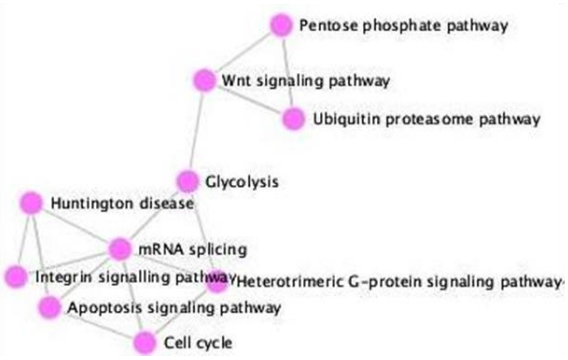

(D)

Rank	Name	P-value
1	Ubiquitin proteasome pathway	0.000008520
2	mRNA splicing	0.03977
3	Cell cycle	0.09670
4	Glycolysis	0.2013
5	Apoptosis signalling pathway	0.5108

Figure 3.6. Analysis of SILAC data. (A) The purification material obtained, as described in 3.4.2, was combined and subjected to SDS-PAGE and Coomassie staining. (B) The frequency distribution histogram of SILAC ratios. On the x-axis is the frequency of proteins binned according to their SILAC ratio. On the y-axis is the bins used ranging from -4 to 4. (C) EnrichR network analysis of the filtered data set. (D) Panther analysis of the protein pathways enriched in the data set.

3.7 – Discussion

The aim of this work was to gain further mechanistic insight into the regulation and function of Claspin, through the identification of novel interacting partners.

To this end, a method of Claspin protein purification was required, however purification of proteins of a large size, such as Claspin, can often be problematic, due to protein instability (Uno and Masai, 2011). Added to that, commercially available antibodies for Claspin are not very specific. Further still, commercial antibodies have limited experimental uses, with only a handful of papers reporting immunofluorescence studies with such antibodies (Bennett and Clarke, 2006; Chini and Chen, 2003).

This lead to the generation of an in-house affinity purified Claspin antibody, that has been well characterised (Rainey et al., 2013). However whilst this antibody offered more specificity in immunoblot detection, it failed to specifically detect Claspin by immunofluorescence. Further still, its use for immunoprecipitation experiments was associated with a high level of non-specific binding (data not shown).

Considering all these factors and in view of Claspin being a relatively low abundance protein (Wang et al., 2015b), the Flp-In TREx HEK-293 cellular system, in which Claspin over expression could be regulated by Doxycycline addition, was generated.

The Flp-In TREx system involves the generation of stable, tetracycline-inducible mammalian cell lines, by taking advantage of a yeast DNA recombination system that uses Flp recombinase and site-specific recombination to allow integration of the gene of interest (GOI) into the genome (Ward et al., 2011). To generate the cell line two plasmids were integrated into the genome. The first plasmid contained an Flp Recombination Target (FRT) site and the second a gene which could express the tetracycline repressor (tet repressor).

The established cell line contained a single copy per cell of the inducibly expressed GOI, Claspin. To facilitate purification and detection of induced Claspin, the gene was tagged with two routinely used affinity tags on the C-terminus; Strep and Flag.

The advancement of this cell-based system, that allows the integration of a GOI into a specific site on the genome, has made the generation of mammalian cell lines able to express proteins relatively easy and efficiently. This approach has been well utilised in the literature for a wide variety of proteins (Al-Mulla et al., 2011; Aslanoglou et al., 2015; Longo et al., 2013), although this study presents the first reported use of this system for inducible Claspin expression.

This system offered many advantages over the use of transiently transfected cells, which is a frequently used method to quickly produce proteins of interest (Kuhn et al., 2012). Transient transfections are characterised by large differences in protein expression levels amongst a cellular population and between experiments (Colosimo et al., 2000). The stable expression of Claspin, in an inducible manner, afforded by the Flp-In TREx system eliminates differences in expression patterns.

Further still, the system has advantages over stable cells lines which continually overexpress a GOI. Owing to the inducible nature of this system, cells can be maintained in culture without the expression of Claspin until such a time as it is required. This helps avoid potentially detrimental effects upon cell growth, associated with continuous overexpression of protein. Finally, the Flp-In TREx system minimizes the prospect of expression being lost due to non-expressing cells outgrowing those which are still expressing.

Importantly, this study demonstrated that the inducible expression of Claspin was not associated with any aberrant effects, as examined by cell growth, viability and DNA content (Figure 3.2). Further still, this system also facilitated immunofluorescence detection of tagged Claspin and confirmed that its cellular location was strictly nuclear, as described in the literature (Chini and Chen, 2003).

The optimised Claspin purification protocol, described in this study, led to the generation of a highly robust and efficient method of protein isolation (Figure 3.3.3) and offered a method of protein purification which could be utilised to effectively identify novel Claspin interacting proteins.

Protein-protein interactions are essential for all biological processes. It has been well documented that aberrant interactions contribute to human disease and cancer (Carneiro et al., 2015). Every essential biological process, including DNA replication, protein degradation and cell cycle control are carried out by an assembly of protein complexes. These complexes facilitate normal cellular homeostasis (Kaake et al., 2010; Vellucci et al., 2010). Modulation of protein-protein interactions represents an emerging therapeutic strategy with protein interaction interfaces providing a novel class of targets for drug development. In particular disruption of the MDM2/MDM4-p53 interaction by small molecule inhibition, which can prevent the excessive degradation of p53 shows potential as a therapeutic target in cancer (Bieging et al., 2014; Khoo et al., 2014). The isolation, identification and characterisation of protein-protein interactions can be either straightforward or complex depending on the dynamics of the interaction itself. Numerous methodologies including yeast two-hybrid system, protein microarray, fluorescence imaging and affinity purification coupled with mass spectrometry (AP-MA) have been successfully utilised for the study of protein-protein interactions (Chen et al., 2015; Trinkle-Mulcahy et al., 2008; Wang and Huang, 2014). The later strategy has emerged as one of the most effective methods. In combination with quantitative mass spectrometry, specific protein interactions can be efficiently identified from non-specific background proteins (Carneiro et al., 2015; Kaake et al., 2010).

Appropriate sample preparation is essential for obtaining reliable results in mass spectrometry analysis. Protein samples should be free of salt and other contaminating factors such as detergents to ensure the purified material was compatible with the choice of down-stream proteomic analysis (Jiang et al., 2004). To find the most effective method of sample preparation, four widely applied approaches were examined; namely dialysis, acetone precipitation, desalting columns and centrifugal filtration.

Dialysis, is a separation technique that allows the removal of small, unwanted compounds from proteins in solution by selective and passive diffusion through a semi-permeable membrane and is a commonly employed method of sample preparation for mass spectrometry (Mann et al., 2001; Manza et al., 2005; Thornalley and Rabbani, 2014). The

sample and the dialysis buffer are placed on opposite sides of the membrane. Proteins present in the sample that are larger than the membrane-pores are retained on the sample side of the membrane, but buffer salts pass freely through the membrane, reducing the concentration of those molecules in the sample. Using this approach, an attempt to dialyse Claspin from a sample environment of high salt to a mass spectrometry compatible bicarbonate solution was performed. However immunoblot examination of the sample pre and post dialysis demonstrated significant loss of the bait protein (Figure 3.5.1 A). One concern, is the length of time dialysis must occur for, typically 24 hr (Aebersold, 2003; Aebersold and Mann, 2003). Whilst the buffer exchange occurred at 4 °C, larger proteins such as Claspin are reported to be highly unstable (Uno and Masai, 2011) and it is plausible that the length of time in dialysis contributed protein instability and loss.

Protein precipitation methods such as TCA, acetone and methanol provide commonly a used and simple approach of sample clean-up for proteomic analysis (Jiang et al., 2004). Precipitation can also be used to concentrate dilute samples. Both TCA and acetone precipitation methods have been described to be comparably efficient at sample clean-up, without significant loss of sample, compared to methanol which lead to ineffective sample recovery (Jiang et al., 2004). However subsequent studies reported that acetone precipitation is the more efficient method (Hirano et al., 2006). Therefore acetone precipitation was attempted in this study. However, this method appeared inefficient for the sample clean-up of the purified Claspin. Whilst these precipitation methods offer a cheap and simple solution with reported success (Hirano et al., 2006), in this study they lead to complete loss of protein (Figure 3.5.1 A).

The third method employed, desalting, as the name alludes to, refers to the removal of salts from a sample. This is facilitated by size exclusion chromatography, in which the solution containing the purified protein is passed through a porous resin that has been packed into a column (Aebersold and Mann, 2003; Manza et al., 2005). The proteins will be too large to enter the porous resin and thus pass through the column. In contrast, salts and detergents will have a slower rate of migration as they are able to enter the resin bed. This difference in flow rate allows the effective separation of solutions. As separation is

aided by centrifugation, this method is quick and therefore lessens the time for the purified material to be degraded, however this method also led to significant protein loss (Figure 3.5.1 A).

The final method tested, centrifugal filtration is similar to dialysis, using a semi-permeable membrane to separate proteins from low molecular-weight contaminants (Merrell et al., 2004). However, dialysis involves passive diffusion whilst centrifugal filtration comprises using pressure to force solutions diffusion, therefore minimising sampling handling times. During centrifugal filtration low molecular-weight solutes and water are forced through the membrane and can be collected. Proteins remain on the sample side of the membrane and owing to the removal of water the sample is also concentrated (Manza et al., 2005). The centrifugal filtration appeared to be most efficient method of sample clean-up (Figure 3.5.1 A). Whilst a faint band for our bait protein was detectable in all the methods tested, with the exclusion of acetone precipitation, the high recovery obtained by the centrifugal filtration was striking. Centrifugal filtration was selected as the method for mass spectrometry sample preparation (Figure 3.4.1 A).

As mentioned the use of AP-MS has become the principal method for the study of protein interactions *in vivo* (Aebersold, 2003; Aebersold and Mann, 2003; Mann et al., 2001). Since mass spectrometry is intrinsically non-quantitative, its renders it impossible to quantify relative abundance changes, between various experimental, samples in the same mass spectrometry analysis (Kaake et al., 2010).

The introduction of stable isotopes into proteins can overcome this problem, by facilitating relative quantification of these molecules form various samples within a single analysis (Chen et al., 2015; Griffin et al., 2003; Wang and Huang, 2014). The use of a quantitative approach reduces variability from sample injection between different sample runs. In recent years, owing to technological advancement, quantitative mass spectrometry coupled with affinity purification has become the method of choice for studying protein-protein interactions. The sensitivity, specificity and accuracy of the

quantitative AP-MS approach generates highly reliable interaction data (Chen et al., 2015; Ong and Mann, 2005).

Quantitative mass spectrometry approaches can be divided into three categories, namely metabolic labelling, chemical labelling and label free. Briefly, chemical labelling such as ICAT, ICPL or iTRAQ involves adding mass tags to proteins (Chen et al., 2015; Kaake et al., 2010). Metabolic labelling such as stable isotope labelling of amino acids in cell culture (SILAC) and ^{15}N labelling consists of biological incorporation of stable isotope labels into the proteins of mammalian cells in cell culture. Finally, the relatively new label-free approach, allows quantification without any labelling by measuring ion intensity changes in chromatography or by spectrum counting (Chen et al., 2015)

Ultimately the success of quantitative mass spectrometry analysis is defined by ability to distinguish specific from non-specific interactions and the generation of high confidence data that is easy to interpret. Each of the aforementioned approaches have particular advantages and disadvantages, but all have successfully been applied to identify novel protein-protein interactions, however the metabolic strategy SILAC, first described in 2002, is reported to be the most accurate of all (Carneiro et al., 2015; Ong et al., 2002).

SILAC involves adding stable isotope labelled amino acids to the growth media of cells. These isotopes can then get incorporated into the proteome during metabolism. Only specific amino acid, typically ^{13}C or ^{15}N labelled arginine or lysine, are labelled. This enables the relative comparison of the cellular proteome of different samples in a single experiment (Ong et al., 2002; Ong and Mann, 2005). This is advantageous when compared to other metabolic quantitative approaches such as ^{15}N labelling, which involves replacing all the nitrogen atoms of the proteome and complicated data quantification based on the number of nitrogen atoms (Chen et al., 2015).

With SILAC, the relative intensities of the differentially labelled peptides, indicates the relative expression of the protein, when the cell cultures are compared in the same analysis. Implicit in the SILAC approach is that the labelling is complete (Wang and

Huang, 2014). Thus, an assumption with SILAC experiments is the completeness of labelling of the culture, typically >95% isotope incorporation. If any unlabelled proteins remain, their peptides will add to the peak intensity of the peptides representing protein from the unlabelled culture. Therefore peak ratios will not indicate true biological protein abundance ratios (Carneiro et al., 2015; Chen et al., 2015; Ong et al., 2002). Incomplete labelling as a consequence of sampling cells before they are fully labelled, can compromise a SILAC experiment if not detected or complicate the data analysis if known.

The application of purification after mixing- (PAM) SILAC, the most described SILAC strategy, can be associated with loss of detection of dynamic interactors (Vermeulen et al., 2008). Only protein interactions with high affinity are preserved during AP-MS. Although the mixing of differentially labelled cell lysates prior to purification should not affect stable interactions, it may interfere with dynamic interactions. This can result in some of the labelled dynamic interactors initially bound to the bait protein becoming replaced with the unlabelled light forms from the control cell lysate and manifest in decreased SILAC ratios. This could severely hamper the identification of real interactors (Kaake et al., 2010). A prolonged purification time, involving long incubation periods of mixed lysate can also add to the loss of dynamic interactors.

Whilst the use of the Strep-column facilitated a robust and reproducible purification protocol, the process of gravity flow involved a substantial purification time and therefore prolonged incubation of mixed lysate. Therefore use of PAM-SILAC in this study could have contributed to decreased SILAC ratios of potential true interactors, close to those of background proteins. As it has been proposed that the PAM-SILAC method may not be ideal for the identification of dynamic interactors or prolonged purification protocols (Wang and Huang, 2008), the PAM strategy was not applied in this study.

A simpler method to quantitatively identify both stable and dynamic interactors, is termed mixing after purification- (MAP) SILAC (Kaake et al., 2010). MAP-SILAC eliminates the incubation of the differentially labelled lysates during purification, therefore

minimising loss of dynamic interactions and was the strategy applied in this study. With MAP-SILAC protein purifications are carried out separately, from matched amounts of the differentially labelled cell lysates, after which the purified protein complexes are mixed before being digested and subject to mass spectrometry analysis. This approach has facilitated the identification of previously unidentifiable protein interactions and in particular has been used to identify dynamic interactors of the proteasome (Wang and Huang, 2008).

In this study 332 proteins, excluding reverse hits, were identified and quantified using MAP–SILAC. Importantly, several known interactors of Claspin were identified including members of the MCM complex. The proteins showed a distribution of SILAC ratio markedly skewed towards the Strep-Claspin labelled lysate (Figure 3.6 B). This could reflect the large enrichment of the bait Claspin (SILAC ratio -5.82) and the relatively clean negative empty vector control as observed by silver staining (Figure 3.5.2). However this skew may also reveal the major pitfall associated with MAP-SILAC.

When using the MAP-SILAC approach, purifications of the differentially labelled cell lysates occur independently, prior to mixing. Therefore differences between purifications can occur, due to differences in binding efficacy of columns used or human error. This can introduce experimental variability that can be mistaken as biological variation. Ideally, the application of MAP-SILAC should involve the use of multiple purifications replicates, to eliminate such discrepancies (Wang and Huang, 2008).

Another consideration was the labelling strategy used in this study, with the Strep-Claspin cells cultured in the light media containing unlabelled arginine and lysine amino acids and the control cells metabolically incorporating ^{13}C labelled arginine. Therefore protein contamination which occurred after labelling, during sample purification and handling, might have been identified and quantified as ‘light’ and mistaken as biologically relevant.

Preferably repetitive SILAC experiments should include a reversal of metabolic labels between the Strep-Claspin and empty vector cells to identify post labelling containments. However, owing to limitation of access to high quality mass spectrometry equipment, further proteomic analysis, including reverse labelling, was not possible during this study.

In lieu of this, to generate higher confidence data sets, a strategy to systematically select a candidate for functional studies, through the use of online bioinformatics tools was applied. Such tools facilitate the elimination of common containments associated with AP-MS and can identify enriched protein pathways amongst the users data.

The CRAPome offers an online resource that stores and interprets negative controls from AP-MS experiments that have been submitted by the proteomics research community (Mellacheruvu et al., 2013). The negative controls are generated from proteomic screens that have employed commonly used affinity tags, cell lines and affinity supports. The inclusion of HEK-293 cells and the Strep affinity tag amongst these controls made this online resource valuable for this study. By amassing a large number of negative control data lists, currently 411, from independent laboratories, the CRAPome generates lists of probable containments from which any user can compare their data to help identify *bona fide* interaction partners.

Whilst the CRAPome may aid in the prediction of purification ‘containments’, proteins which may be common experimental ‘containments’ could also be potential interactors. For example members of dead box family of proteins, 3 of which were quantified in this SILAC analysis, are identified in over half of all CRAPome control studies. As such, they were removed from further analysis, having surpassed the > 30% cut-off used in this study. However, the dead box family of proteins have been identified in a screen of ATM and ATR substrate analysis of protein networks responsive to DNA damage (Matsuoka et al., 2007). Owing to the well described role of Claspin in the ATR mediated damage response, it is possible the dead box proteins may be *bona fide* Claspin interactors (Allera-Moreau et al., 2012; Izawa et al., 2011; Petermann et al., 2008). Therefore it is important

to urge caution when using the CRAPome and even more imperative to accompany its use with literature searches.

EnrichR and Panther analysis revealed an enrichment of proteasomal associated proteins (Figure 3.6 C and D). The identification of multiple components involved in the dynamic process of ubquitylation was likely facilitated by the MAP-SILAC approach used in this study. As discussed, this strategy had been successfully employed for the detection of previously unidentifiable dynamic protein complexes of the proteasome (Wang and Huang, 2008).

Owing to this enrichment, is was from this dynamic network, a candidate for further functional analysis was selected. Within in this network, 3 subunits of the proteasome were identified including PSMD1, PSMD2 and PMSD4, all of which contribute to the regulation of proteolysis in eukaryotic cells (Hamazaki et al., 2006).

Other candidates included a poly-ubiquitin receptor located on the proteasome, ADRM1. ADRM1 can capture polyubiquitylated substrates by covalently recognising ubiquitin chains. ADRM1 can then recruit and activate UCH37 (Yao et al., 2006). UCH37 is a member of the UCH-family of DUBs and the only member of this family to associate with the proteasome (Eletr and Wilkinson, 2014). Following its activation UCH37 can disassemble ubiquitin from proteins by hydrolysing the distal ubiquitin (Eletr and Wilkinson, 2014) (Yao et al., 2006). ADRM1 is upregulated in many cancers including ovarian, breast and liver and this is linked to increased NF-κB activity (Shenoy, 2015). Of particular intrigue, two DUBs, USP9X and USP5 were identified with SILAC ratios comparable to known Claspin interactors MCM 2-3-6.

USP5 has been shown to regulate poly- ubiquitin chains, p53 transcriptional activity and double-strand DNA repair (Dayal et al., 2009). Knockdown and overexpression studies have demonstrated that USP5 regulates p53 levels and alters cell growth and cell cycle distribution in melanoma cells. USP5 also regulates the intrinsic apoptotic pathway by modulating p53-dependent FAS expression (Potu et al., 2014). As such USP5 inhibition

could provide an alternate strategy in recovery of diminished p53 function in certain carcinomas (Potu et al., 2014).

Following a comprehensive literature search, USP9X was selected as the candidate protein of interest because, as extensively discussed in the introduction, USP9X is an emerging oncology target, however little molecular mechanism of this DUB is understood (Boise, 2015; Murtaza et al., 2015). The identification of USP9X as a potential Claspin interactor offered the opportunity to investigate whether one mechanism of USP9X action may be related to DNA replication. Considering the well documented role of DUB mediated regulation of Claspin, the identification of USP9X was of particular intrigue as a fifth putative DUB involved in Claspin regulation. Added to this, an E3 ligase identified in the SILAC study, MULE, has been reported to bind USP9X by immunoprecipitation experiments (Gomez-Bougie et al., 2011; Mojsa et al., 2014). As discussed in the Introduction, MULE and USP9X compete for binding to MCL-1, to impose opposite effects of degradation and stabilisation. In the future, it would be interesting to understand why another known MCL-1 regulator was identified amongst our Claspin SILAC data. It would also be fascinating to examine whether USP5 is another DUB which can influence Claspin regulation.

Overall, the development of the Flp-In TREx system for the inducible expression of Claspin, coupled with a SILAC mass spectrometry based approach helped generated a list of putative interaction partners. Using bioinformatics tools, proteins associated with the proteasomal were highlighted as particularly abundant in the data set. As Claspin is heavily regulated by the process of ubquitylation and deubiquitylation the identification of the DUB USP9X was particular intriguing. Although extensively described in the literature as contributing to a multitude of cancers, with this context little mechanism is understood. As such, the study of a putative relationship between a cell cycle mediator protein, Claspin, and an emerging therapeutic target, USP9X, was particularly tantalising.

CHAPTER 4

USP9X CONTROLS DNA REPLICATION FORK STABILITY AND THE REPLICATION STRESS CHECKPOINT THROUGH CLASPIN

4. 1 – Introduction: The putative interaction between Claspin and USP9X

The identification of USP9X as a putative Claspin interacting protein was particularly intriguing as several DUBs have recently been shown to be involved in regulating Claspin stability, including USP28, USP7, USP20 and USP29 (Faustrup et al., 2009; Martin et al., 2015; Yuan et al., 2014; Zhang et al., 2006; Zhu et al., 2014).

Added to that, as extensively discussed in the introduction, USP9X is an emerging therapeutic target in oncology. However, with conflicting reports suggesting both tumour suppressor and tumour promoting activity, the necessity to understand complete USP9X molecular function is imperative (Perez-Mancera et al., 2012; Schwickart et al., 2010).

Finally, whilst SILAC analysis indicated a putative interaction between Claspin and USP9X, a comprehensive assessment of binding followed by extensive examination of the molecular relationship is essential to reveal the significance of an interaction between Claspin and USP9X.

4.2 – USP9X protein levels are consistently expressed in the cell cycle

To begin biochemical studies of USP9X, a preliminary experiment examining whether the lysate conditions of buffer A, used to extract the majority of Claspin from the chromatin (Figure 3.3), was compatible with USP9X protein extraction was performed.

U2OS cells were lysed in buffer A, and after centrifugation the soluble fraction was removed and quantified, following which a sample was prepared for immunoblotting. The remaining insoluble pellet was subjected to sonication and a sample prepared for immunoblotting. Conditions where total protein is extracted from cells, namely Laemmli extraction and TCA, were also examined. These methods were performed as described in Materials and Methods Section 2.4.1.

From immunoblot analysis (Figure 4.2 A), it appeared that the majority of USP9X was detected in the soluble fraction, when buffer A lysate conditions were used. There was little detectable USP9X remaining in the insoluble fraction. The soluble extraction method appeared to solubilise the majority of USP9X, when compared to the total protein extraction methods of TCA and Laemmli buffer (Figure 4.2 A). Therefore, in all remaining experiments USP9X protein manipulation was conducted in buffer A.

The levels of Claspin protein expression are heavily regulated in the cell cycle, down regulated in G1 and G2/M, as discussed in Introduction Section 1.6 (Faustrup et al., 2009). To examine whether USP9X protein levels were subject to a similar oscillation cycle, a preliminary trap and release experiment was conducted. U2OS cells were trapped in mitosis, using Nocodazole, for 18 hr. The drug was then removed and the cells were subsequently released in to fresh media. Samples were harvested at various time points, up to 14 hr post-release and prepared for immunoblotting in buffer A.

From the immunoblot analysis (Figure 4.2.B), using Cyclin B1 as a marker of synchronization (Bassermann et al., 2008), with Cyclin B1 levels low in G1 and gradually increasing towards late S and entry into mitosis, it appeared that the levels of USP9X do not oscillate throughout the cell cycle.

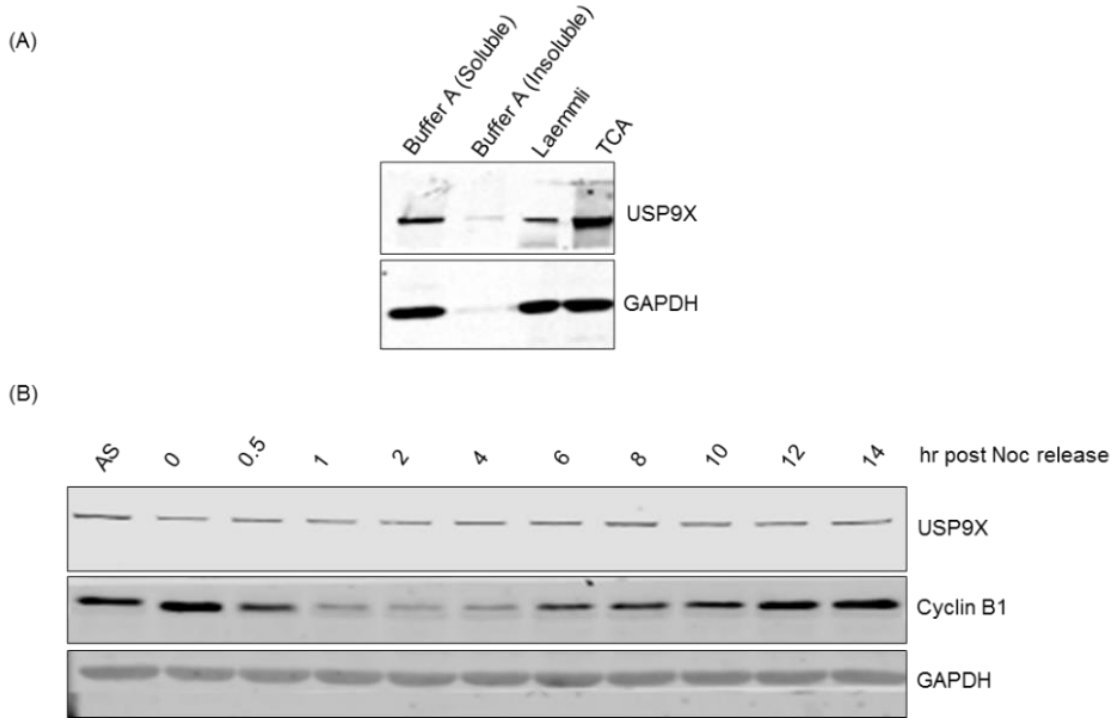

Figure 4.2. USP9X protein levels are consistently expressed in the cell cycle. (A) U2OS cells were harvested lysed in buffer A. Proteins were separated into soluble and chromatin enriched fractions by centrifugation and analysed by immunoblotting. Total cell was lysates were also prepared in Laemmli buffer or extracted by TCA. GAPDH was used as control of loading and fractionation. (B) U2OS cells were subjected to 18 hr Nocodazole treatment and released with samples collected up to 14 hr post released and analysed by immunoblotting. Cyclin B1 served as a marker of cell synchronization and GAPDH as a loading control.

4.3 USP9X interacts with both ectopically expressed and endogenous Claspin

To verify whether the candidate protein USP9X, as identified by mass spectrometry analysis, interacted with Claspin, a small scale Strep-Claspin pulldown experiment was performed as described in Materials and Methods Section 2.4.3.3.

Briefly, cells conditionally expressing Strep-Claspin and empty vector cells were harvested. The cells were then prepared for Strep-Claspin pulldown experiment and the recovered material was examined by immunoblotting (Figure 4.3 A). This immunoblot demonstrated the successful isolation of the bait Strep-Claspin. Importantly, USP9X is

detected in the Strep-Claspin pull down sample. Therefore, Claspin appeared to interact with USP9X.

To verify this interaction, a reciprocal immunoprecipitation was performed. To this end, an antibody to USP9X was used to purify USP9X from cells conditionally expressing Strep-Claspin, as described in Materials and Methods Section 2.4.3.4. In this experiment, Strep Claspin cells were also subjected to immunoprecipitation using rabbit IgG bound to beads in place of the antibody, as a control.

Immunoblot examination of the precipitated fractions demonstrated that USP9X could be efficiently immunoprecipitated (Figure 4.3 B). USP9X appeared to specifically interact with Strep-Claspin, when compared with the control, with no evidence of binding in the IgG lane (Figure 4.3 B).

Whilst these two experiments indicated and interaction between USP9X and Claspin, these experiments involved the use of ectopically expressed Claspin. To examine whether this interaction could be captured at the level of endogenous protein and owing to the high efficacy of the USP9X antibody for immunoprecipitation, USP9X was immunoprecipitated from U2OS extracts. Rabbit IgG bound to beads in place of the antibody, to provide a control (Figure 4.3 C).

Immunoblot analysis demonstrated that endogenous Claspin could interact with USP9X (Figure 4.3 C). This use of U2OS cells also demonstrated that the interaction between USP9X and Claspin was not restricted to one cell line, as it was detectable in both U2OS and HEK-293 cells. Taken altogether these experiments confirmed an interaction between Claspin and USP9X.

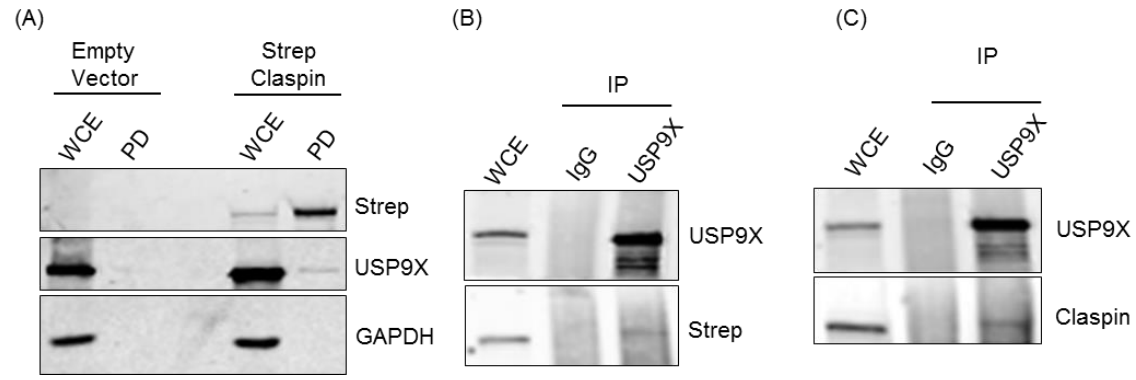

Figure 4.3. USP9X interacts with both ectopically expressed and endogenous Claspin. (A) Proteins were pulled down using Strep-Tactin resin from extracts prepared from empty vector cells or cells expressing Strep-Claspin. Whole cell extracts (WCE) and pulled down material (PD) were probed with either, anti-Strep antibody or with anti-USP9X antibodies. (B) Immunoprecipitated proteins with anti-USP9X antibodies or control IgG from extracts prepared from cells expressing Strep-Claspin were analysed by immunoblotting. Tagged Claspin interacting with USP9X was detected with an anti-Strep antibody. (C) As in (B), but extracts were prepared from U2OS cells and endogenous Claspin interacting with USP9X was detected using an anti-Claspin antibody.

4.4 – USP9X can be shuttled in and out of the nucleus

Multiple cellular localisations of USP9X has been described in the literature (Murtaza et al., 2015), although the protein is predominantly detected in the cytoplasm. To examine this variable localisation, USP9X in U2OS cells was visualised using immunofluorescence, as described in Materials and Methods Section 2.7.1. Recapitulating what has already been reported in the literature, USP9X majority localised to the cytoplasm (Figure 4.4 A), however a small amount of nuclear spots were also detected (Trinkle-Mulcahy et al., 2008).

The localisation of USP9X differs from that of Claspin, which is reported to be a nuclear protein, (Bennett and Clarke, 2006; Chini and Chen, 2003). This was confirmed in this study with use of the Strep-Claspin system. Using detection of the Strep tag, Claspin was found to be confined to PML bodies (Figure 3.2 D).

Considering this small USP9X nuclear pool, it seemed possible that USP9X may by shuttled in and out of the nucleus, which may facilitate an interaction with nuclear Claspin. To examine this, U2OS cells were treated with Leptomycin B (LMB), which can inhibit nuclear export factor CRM1 (Kudo et al., 1998), for a time course of up to 8 hr of treatment.

USP9X localisation was then examined by immunofluorescence. With increasing time in the presence of LMB, an increase in nuclear staining of USP9X was observed (Figure 4.4 A), peaking at 8 hr. A time point after 8 hr was not conducted, as such treatment is associated with high levels of toxicity.

The 8 hr time point immunofluorescence slides were then imaged and quantified using the Operetta Automated Imaging system and compared to untreated cells (Figure 4.4 B). Each dot in Figure 4.4 C represents a single nucleus, with the signal of nuclear intensity normalised to total intensity of USP9X staining in the whole cell. This quantification demonstrated a significant increase in nuclear staining upon export inhibition (Figure 4.4 B). This analysis establishes that a small fraction of USP9X is located in the nucleus at any time, which may facilitate the interaction between Claspin and USP9X.

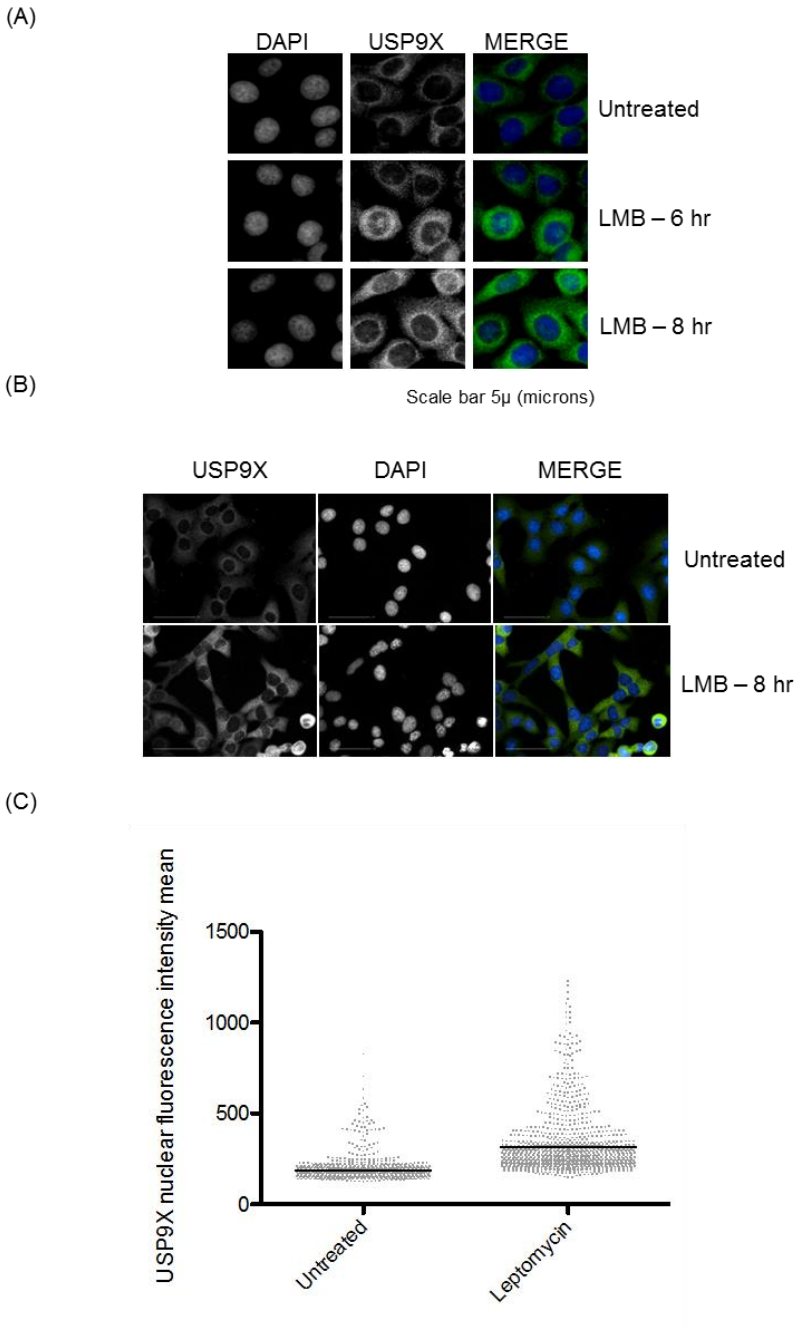

Figure 4.4. Treatment with LMB induces accumulation of USP9X in the nucleus in a time dependent manner. (A) U2OS cells were fixed before and at indicated time points after treatment with Leptomycin B (LMB) and stained with anti-USP9X antibodies and imaged on an IX71 Olympus microscope under 100X magnification. (B) As (A) but imaged on an Operetta high content microscope (Perkin Elemer) under 40X magnification. (C) The intensity of USP9X nuclear signal was quantified with Operetta high content microscopy (Perkin Elemer). Each dot represents a single nucleus.

4.5 – siRNA mediated depletion of USP9X causes a down regulation of Claspin

Due to the well documented role of DUBs in Claspin stability with USP28, USP7, USP29 and USP20 (Faustrup et al., 2009; Martin et al., 2015; Yuan et al., 2014; Zhang et al., 2006; Zhu et al., 2014), all contributing to Claspin regulation and having confirmed an interaction between USP9X and Claspin, studies to examine whether Claspin levels could also be affected by depletion of USP9X were conducted.

For this small interfering RNA mediated depletion of USP9X was utilised to examine effects on Claspin protein levels. Since the first description of RNA interference in 1998 and the subsequent experiments that demonstrated that synthetic small interfering RNA siRNA could perform sequence specific gene depletion in mammalian cell lines, the use of siRNA has revolutionised biochemical studies of protein function (Whitehead et al., 2009).

The Strep-Claspin cells were transfected with a USP9X siRNA candidate sequence well validated in the literature (Dupont et al., 2009). JetPrime, a molecule based on a polymer formulation, was utilised for cellular transfection. To preliminarily characterise the siRNA mediated depletion of USP9X, varying concentrations of the siRNA (ranging from 25 nM to 100nM) were tested. As a control, Strep-Claspin cells were transfected with siCTRL (Ambion) at 100nM. 24 hr after siRNA transfection, Doxycycline was added to induce cells. 24 hr post induction, cells were harvested and samples prepared for immunoblotting.

From immunoblot analysis, 100 nM of USP9X siRNA provided the most efficient concentration for the depletion of USP9X, at the 48 hr time point (Figure 4.5.1 A). Intriguingly, increased efficacy of USP9X depletion correlated with increased depletion of Strep-Claspin (Figure 4.5.1 A).

To eliminate possible off-target effects associated with the use of a single siRNA sequence, a second USP9X siRNA sequence, extensively described in the literature, was selected for this study (Schwickart et al., 2010). BLAST analysis revealed that the two sequences, referred to as USP9X (A) and USP9X (B), (Dupont et al., 2009; Schwickart

et al., 2010), were specific to USP9X and importantly, were not complementary to the sequences of any of the DUBs implicated in Claspin regulation (data not shown).

Having determined an optimal siRNA concentration (100 nM), that depleted USP9X with USP9X (A) siRNA, an investigation of whether extending siRNA treatment time would further enhance USP9X depletion was conducted in HEK-293 cells, using both siRNA. HEK-293 cells were transfected with 100nM USP9X (A) or (B) or CTRL and following 48 and 72 hr transfection, samples were harvested and prepared for immunoblotting.

The resulting immunoblot demonstrated that increasing the length of siRNA treatment time did not improve protein depletion and may have hindered the reduction of USP9X using siRNA USP9X (A) (Figure 4.5.1 B). Therefore in all subsequent siRNA experiments a 100 nM concentration of either USP9X siRNA (A) or (B) and a 48 hr timeframe was implemented. Unless otherwise specified, the use of the USP9X (A) siRNA was predominantly utilised in studies involving siRNA mediated depletion of the protein.

Using the optimised siRNA protocol, an experiment to confirm the effect of USP9X depletion on Claspin levels was performed (Figure 4.5.1 C). Empty vector and Strep-Claspin cells were transfected with USP9X (A) or CTRL siRNA. 24 hr after transfection Doxycycline was added to the Strep-Claspin cells. 24 hr post induction the cells were harvested and samples prepared for immunoblot. This immunoblot confirmed the depletion of both endogenous Claspin, as seen in the empty vector cells, as well as ectopically expressed Claspin, in the Strep-Claspin cells (Figure 4.5.1 C).

To further confirm the specificity of the effect of USP9X depletion on Claspin at an endogenous level of protein, HEK-293 cells were transfected with the 2 USP9X siRNA, as well as CTRL siRNA. The inclusion of a siRNA targeting Claspin, served as a positive control in this experiment. Following 48 hr of transfection, cells were harvested and prepared for immunoblot examination. The downregulation of Claspin associated with USP9X depletion was evident with 2 independent siRNA targeting USP9X (Figure 4.5.1 D).

Further still the effects of USP9X depletion on Claspin was not limited to a single cell line, but evident in both U2OS and HEK-293 cells, which had been transfected with siCTRL or siUSP9X (A), for 48 hr, prior to immunoblot analysis (Fig 4.5.1 E). All these results indicate that USP9X may regulate Claspin stability.

To examine whether USP9X depletion was efficient in each cell, an immunofluorescence experiment was conducted. U2OS were transfected with CTRL, USP9X (A) or USP9X (B) and 48 hr after transfection, cells were prepared for immunofluorescence.

Comparison of USP9X staining in cells treated with siCTRL or either USP9X targeting siRNA sequences, demonstrated that depletion of USP9X was evident across the cellular population (Figure 4.5.1 F). This confirmed the effectiveness of the siRNA used in this study.

As discussed in the Introduction Section 1.6, the levels of Claspin oscillate in the cell cycle. As such it is possible that the effect of USP9X depletion on Claspin levels was mediated by arresting the cells in a stage of the cell cycle where Claspin levels have been demonstrated to be down regulated (Faustrup et al., 2009; Peschiaroli et al., 2006). To examine this possibility HEK-293 and U2OS cells were transfected with CTRL or USP9X (A) siRNA sequences. 48 hr post transfection the cells were fixed and stained with propidium iodide (PI). Flow cytometry analysis examining DNA content in the two cell lines, demonstrated no obvious difference when compared to the control cells (Figure 4.5.2).

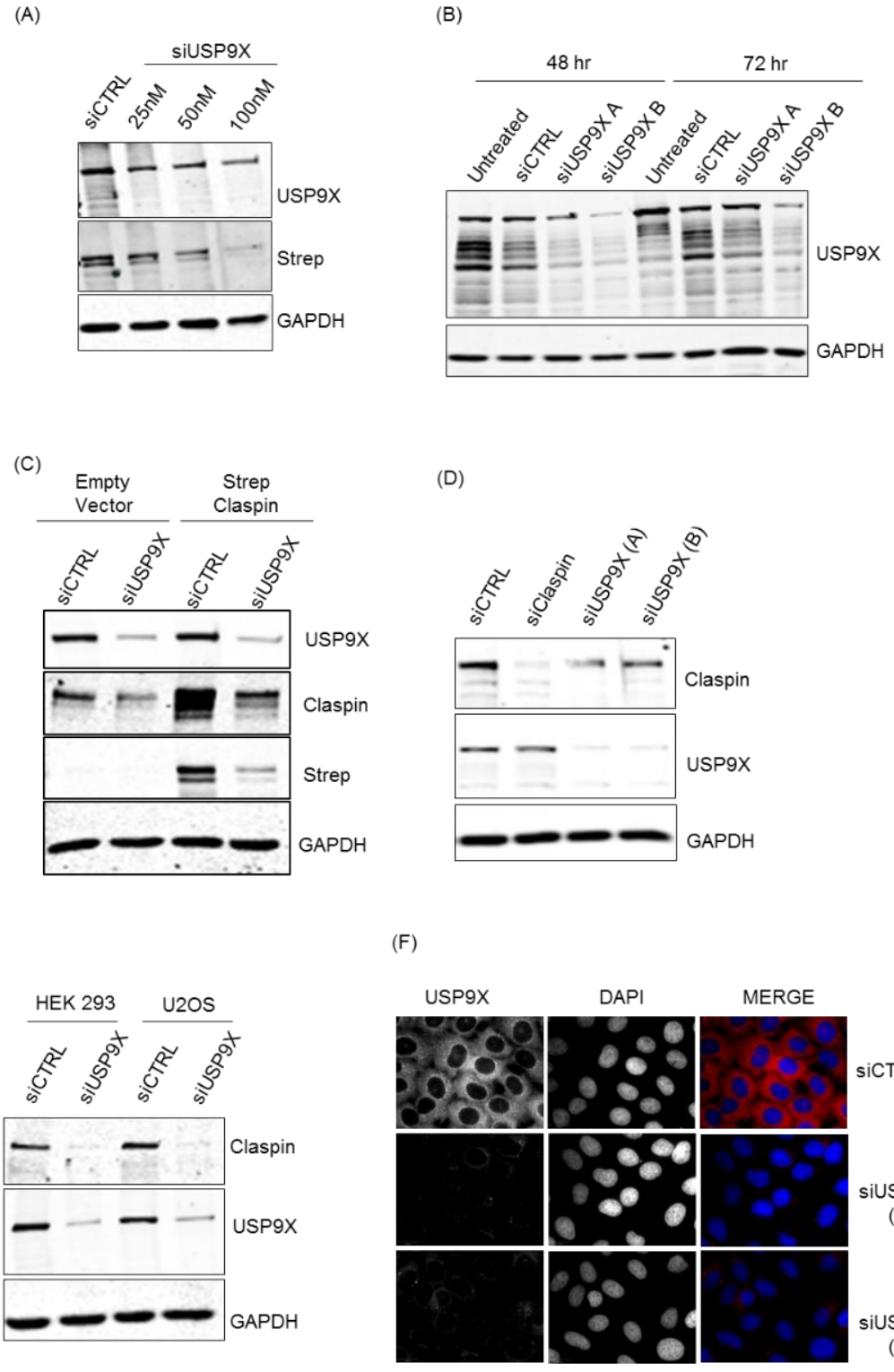
(A)
siUSP9X
siCTRL
25nM
50nM
100nM
USP9X
Strep
GAPDH
(B)
48 hr
72 hr
Untreated
siCTRL
siUSP9X A
siUSP9X B
Untreated
siCTRL
siUSP9X A
siUSP9X B
USP9X
GAPDH
(C)
Empty Vector
Strep Claspin
siCTRL
siUSP9X
siCTRL
siUSP9X
USP9X
Claspin
Strep
GAPDH
(D)
siCTRL
siClaspin
siUSP9X (A)
siUSP9X (B)
Claspin
USP9X
GAPDH
(E)
HEK 293
U2OS
siCTRL
siUSP9X
siCTRL
siUSP9X
Claspin
USP9X
GAPDH
(F)
USP9X
DAPI
MERGE
siCTRL
siUSP9X (A)
siUSP9X (B)

Figure 4.5.1. siRNA targeting USP9X leads to efficient protein depletion and a reduction of Claspin protein levels. (A) HEK-293 with induced Strep-Claspin expression were transfected with varying concentrations of a siRNA targeting USP9X (25 nM, 50 nM or 100 nM) or a control siRNA (100 nM). After 48 hr, cells were harvested and proteins analysed by immunoblotting. (B) HEK-293 were transfected with USP9X or control siRNA (100 nM). Proteins were then analysed after 48 and 72 hr. (C) Both empty vector and Strep-Claspin HEK-293 cells were treated with USP9X or control siRNA (100 nM). Proteins were then analysed after 48 hr. (D) Empty vector cells were treated with 2 independent USP9X or control siRNA (100 nM). Proteins were then analysed after 48 hr. (E) Both HEK-293 and U2OS cells were treated with USP9X or control siRNA (100 nM). Proteins were then analysed after 48 hr. (F) U2OS cells were treated with 2 independent USP9X or control siRNA (100 nM). Proteins were then analysed by immunofluorescence after 48 hr.

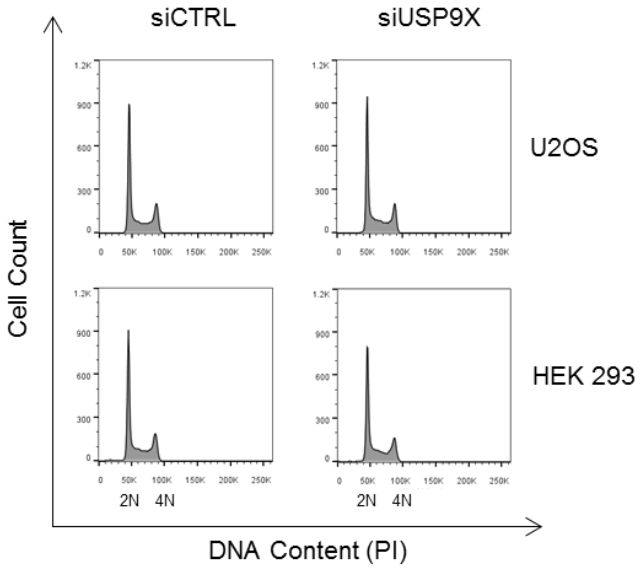

Figure 4.5.2. USP9X depletion has no effect on DNA content. HEK-293 cells or U2OS were transfected with either a siRNA targeting USP9X or siCTRL (100 nM). After 48 hr, cells were fixed and DNA stained with PI. DNA content was determined by flow cytometry analysis.

4.6 - USP9X prevents proteasomal mediated degradation of Claspin in S-phase

The roles of USP9X is multifaceted, with the DUB reversing both mono- and poly-ubiquitylation (Murtaza et al., 2015). Of the possible lysine chains bonds, ubiquitin K48 linkages, which become poly-ubiquitylated, are targeted for degradation by the proteasome (Sahtoe and Sixma, 2015). USP9X has been shown to stablise substrates,

such as MCL-1, by cleaving such bonds and preventing degradation (Schwickart et al., 2010). While all the other DUBs described to regulate Claspin can protect the protein from proteasomal mediated degradation (Yuan et al., 2014).

To examine whether USP9X contributed to the protection of proteasomal mediated Claspin degradation, U2OS cells were transfected with siRNA targeting USP9X or CTRL for 48 hr and subsequently treated with the proteasome inhibitor, MG132, for 3 hr prior to harvesting. The samples were then examined by immunoblotting (Figure 4.6 A). Treatment with MG132 in control cells, caused an increase in the levels of Claspin, as has been reported (Peschiaroli et al., 2006) and USP9X.

Importantly, treatment with MG132 was able to rescue the level of Claspin in the presence of USP9X depletion. This indicates that USP9X protects Claspin from the proteasome.

Several ubiquitylation mechanisms have been reported to control Claspin degradation, in different phases of the cell cycle, as discussed in Introduction Section 1.6. In order to understand which phase of the cell cycle USP9X contributed to Claspin protection, the rate of Claspin degradation was assessed, in different stages of the cell cycle, following treatment with the USP9X inhibitor WP1130. Strep-Claspin cells were arrested in either S-phase or mitosis, using Hydroxyurea or Nocodazole respectively for 18 hr. Following drug induced arrest, cells were treated with Cycloheximide to prevent protein synthesis and cells were collected at 2 hr intervals, up to 6 hr post Cycloheximide treatment. Samples were analysed by immunoblotting (Figure 4.6 B and Figure 4.6 C).

As previously reported, the levels of Claspin were stabilised in S-phase compared to mitosis (Bennett and Clarke, 2006). However in cells treated with WP1330, Claspin stability was impaired, indicating that USP9X contributes to Claspin stability in S-phase cells (Figure 4.6 B). USP9X inhibition did not affect Claspin regulation in cells arrested in mitosis (Figure 4.6 C).

These studied indicated that USP9X contributes to stabilisation of Claspin in S-phase and can counteract proteasome mediated degradation of Claspin. To confirm that USP9X

contributed to ubiquitylation levels of Claspin, an ubiquitylation assay was conducted using the Strep-Claspin cellular system.

Strep-Claspin cells were transfected with a construct expressing HA-tagged ubiquitin, arrested in S-phase with Hydroxyurea for 18 hr and treated with WP1130 in the presence of MG132. Following Strep-affinity pulldown, ubiquitylation was assessed by immunoblotting using anti-HA antibodies. Figure 4.6 D shows that in untreated cells, the levels of Claspin ubiquitylation are barely detectable above background. Following the addition of MG132, an increase Clapsin ubiquitylation was observed, as previously reported (Mamely et al., 2006). However, the addition of the USP9X inhibitor WP1130 leads to an enhanced accumulation of ubiquitylated Claspin. This further demonstrates that USP9X contributes to the removal of ubiquitin chains from Claspin, in S-phase, and indicates that Claspin is a substrate of USP9X (Figure 4.6 D).

While the use of WP1130 is commonly reported in the literature (Cox et al., 2014; Liu et al., 2015; Paemka et al., 2015; Peterson et al., 2015), upon drug treatment in this study, cells became detached from adherent surfaces. The cells rounded up, a feature indicative of apoptosis (Taylor et al., 2008), within minutes of drug treatment.

To examine whether apoptosis was being induced, a time course of WP1130 treatment was conducted in HEK-293 cells. The samples were then examined by immunoblotting for total and cleaved Caspase-3, a commonly used marker of apoptosis (Clarke et al., 2005). Caspase-3 is an essential regulator of apoptosis and normally exists in an inactive form. Following proteolytic cleavage, two subunits are produced which then dimerize to form an active enzyme. The activated enzyme, cleaved Caspase-3, initiates activation of other caspases in a collection of events leading up to apoptosis (Brentnall et al., 2013).

Immunoblot examination (Figure 4.6 E) demonstrated cleavage of Caspase-3 upon increasing WP1130 treatment time, confirming the cells had begun to undergo apoptosis. This was in contrast to how cells behaved with USP9X siRNA treatment, with no sub G1 cell population, another indication of an apoptotic phenotype, seen in DNA content profiles upon USP9X depletion (Figure 4.5.2).

Whilst WP1130 has been extensively used in the literature, none of these papers have reported the cell detachment observed in this study. Owing to the juxtaposition in cell morphology between drug and siRNA treatment, and the specificity afforded by siRNA sequence, the use of WP1130 was eliminated from further use in this study.

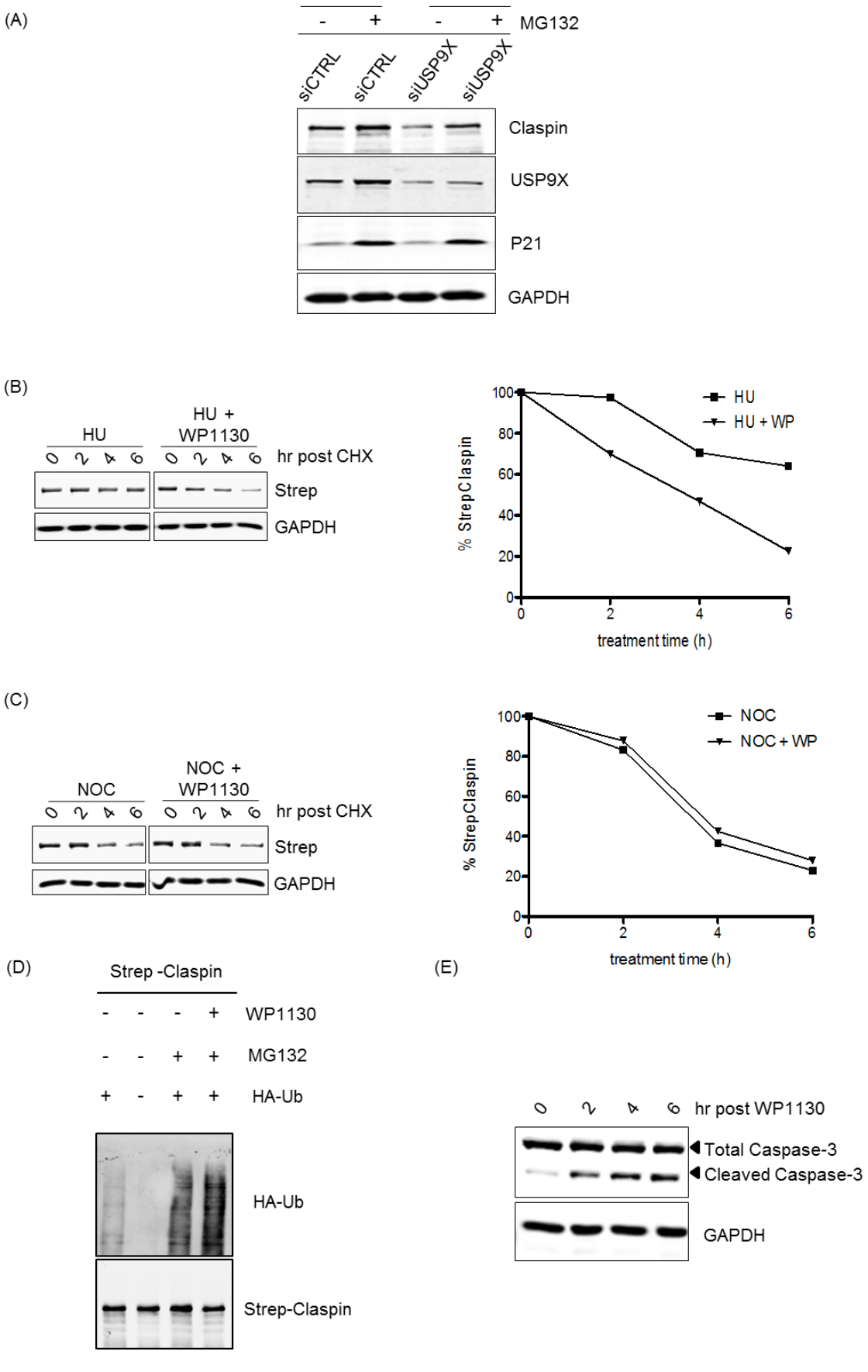
(A)
- + - + MG132
siCTRL siCTRL siUSP9X siUSP9X
Claspin
USP9X
P21
GAPDH
(B)
HU
HU + WP1130
0 2 4 6 0 2 4 6 hr post CHX
Strep
GAPDH
% StrepClaspin
HU
HU + WP
treatment time (h)
(C)
NOC
NOC + WP1130
0 2 4 6 0 2 4 6 hr post CHX
Strep
GAPDH
% StrepClaspin
NOC
NOC + WP
treatment time (h)
(D)
Strep -Claspin
- - - + WP1130
- - + + MG132
+ - + + HA-Ub
HA-Ub
Strep-Claspin
(E)
0 2 4 6 hr post WP1130
Total Caspase-3
Cleaved Caspase-3
GAPDH

Figure 4.6. USP9X controls Claspin levels in S-phase by reversing proteasomal degradation. (A) U2OS cells were transfected with either USP9X or control siRNA; 45 hr post transfection MG132 was added as indicated, cells were then collected 3 hr later and protein analysed. (B) HEK-293 cells expressing Strep-Claspin were first arrested in S-phase with Hydroxyurea or (C) in mitosis with Nocodazole. Cycloheximide was then added to prevent further protein synthesis in the presence or absence of the USP9X inhibitor WP1130 and samples harvested at the indicated times and analysed. The intensities of the Strep-Claspin bands shown in the immunoblots of (B) and (C) were quantified on the Li-Cor imaging system, normalized to the GAPDH loading control and graphed against the time in cell treatment with Cycloheximide. (D) Empty vector or Strep-Claspin expressing cells were transfected with a plasmid expressing HA-tagged ubiquitin and arrested in S-phase with Hydroxyurea. Pull downs were performed with Strep-Tactin resin and samples were analysed with anti-Strep antibody and anti-HA antibody to detect ubiquitylated protein. (E) U2OS cells were treated with WP1130 for the times indicated and samples were then analysed for cleavage of Caspase-3 by immunoblot.

4.7 The catalytic activity of USP9X is required to protect Claspin

The results indicated that USP9X regulation of Claspin is mediated by cleaving ubiquitin linked chains, which prevents proteasomal degradation of Claspin. Cleavage of such isopeptide linkages depend on the catalytic activity of USP9X (Al-Hakim et al., 2008). To confirm that the stabilisation of Claspin by USP9X, was dependent on this catalytic activity, experiments were performed using a HA-tagged full length wild type USP9X (termed WT hereafter) construct, as well as a catalytically inactive mutant (C1556) construct (termed CI hereafter), which contains a mutation in the catalytic domain rendering its ability to deconjugate ubiquitin, as reported in the literature (Al-Hakim et al., 2008).

Preliminary characterisation of transfection of these constructs, into U2OS cells, was conducted using JetPrime with a titration of DNA concentrations, ranging from 0.5 μg – 2 μg. 24 hr post transfection, cells were examined for both expression USP9X and the HA tag by immunofluorescence, to examine expression at a single cell level. Evident from the images was that whilst increasing concentrations of DNA led to more intense staining of USP9X and the HA-tag, it was at the expense of cellular toxicity (data not

shown). Therefore a DNA concentration of 1.25 µg was selected for further studies, as balanced between moderate levels of USP9X overexpression and cellular toxicity.

To examine expression of WT and CI USP9X U2OS were transfected with 1.25 µg of DNA. As a control, cells were also treated with the transfection reagents alone, that is non transfected (NT). 24 hr post transfection, the cells were examined by immunofluorescence (Figure 4.7 A). From the images, it appeared that the number of cells transfected with either WT or CI USP9X were comparable, with similar number of cells counted as high or low expressing, in both samples (Figure 4.7 A).

These constructs and transfection conditions were then utilised to examine whether the catalytic domain of USP9X contributes to Claspin stability. U2OS were transfected with 1.25 µg of WT or CI USP9X, or NT as a control. 24 hr post transfection cells, were treated with Cycloheximide for 6 hr, to inhibit protein synthesis. Following drug treatment cells were harvested and samples prepared for immunoblotting.

From immunoblot analysis it appeared that the overexpression of WT or CI USP9X did not lead to increased Claspin levels at a steady state (Figure 4.7 B). However, following Cycloheximide treatment, the overexpression of WT USP9X could prevent Claspin degradation (Figure 4.7 B). The inactive mutant failed to offer such protection to Claspin, demonstrating further evidence that USP9X contributes to Claspin stability through the cleavage of ubiquitin chains.

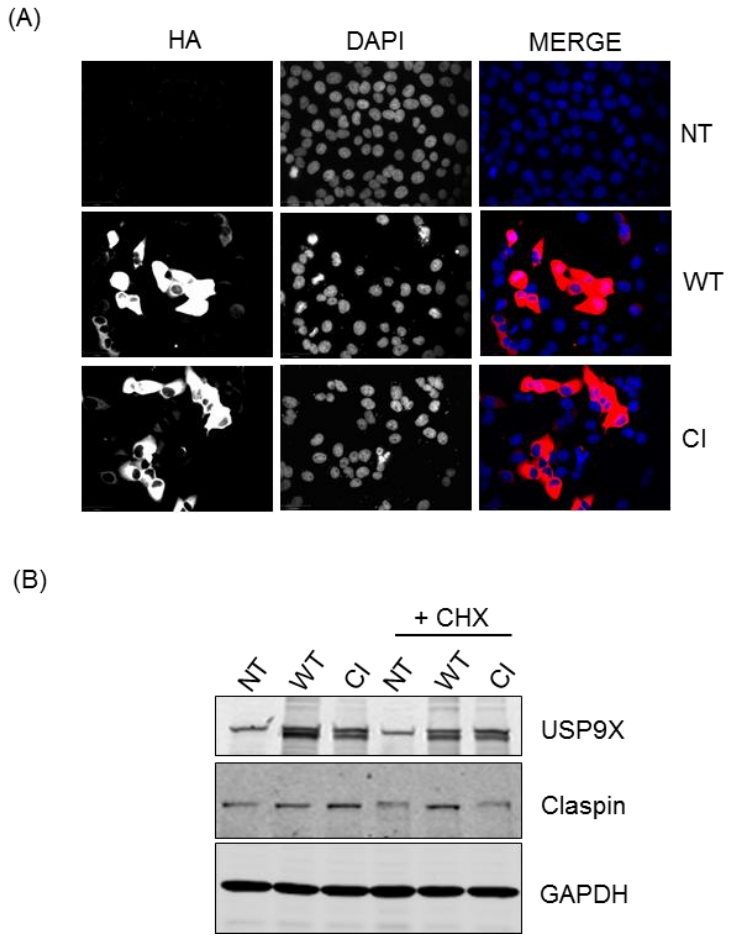

Figure 4.7. Overexpression of WT but not CI USP9X can stabilise Claspin degradation. (A) WT and CI USP9X DNA were transfected into U2OS cells and 24 hr later the cells were examined by immunofluorescence. (B) U2OS were transfected with constructs expressing either functional WT or CI USP9X. After 24 hr cells were either collected (lanes 1-3) or treated with Cycloheximide (CHX) for a further 6 hr (lanes 4-6). Protein extracts were then prepared and analysed by immunoblotting.

4.8 - USP9X depletion does not influence the protein levels of the DUBs involved in S-phase Claspin regulation and their depletion has no effect on USP9X protein levels

In order to understand the role of USP9X in the context of the other DUBs, namely USP7, USP29 and USP20 (Faustrup et al., 2009; Martin et al., 2015; Yuan et al., 2014; Zhu et al., 2014), shown to regulate Claspin in S-phase, examination of whether USP9X depletion affected their protein levels was conducted.

U2OS cells were transfected with siRNA targeting USP9X for 48 hr, after which cells were harvested and samples prepared for immunoblotting. Form immunoblot analysis (Figure 4.8 A) it appeared that the depletion of USP9X did not affect the protein levels of any of these DUBs.

Asking the reciprocal question, whether the depletion of USP7or USP20 would affect USP9X abundance, U2OS cell were transfected with siRNA targeting these DUBs and protein levels assessed by immunoblotting 48 hr post transfection (Figure 4.8.1 A). As USP20 has been reported to be continually degraded by the HERC2 E3 ubiquitin ligase in the absence of DNA damage, as discussed in the Introduction Section 1.6.5.4, examination of the effect of HERC2 depletion on USP9X protein levels was also conducted (Figure 4.8.1 A). Following immunoblot analysis it was observed that neither USP7 nor USP20 affected USP9X protein levels (Figure 4.8.1 A). Similarly HERC2 depletion did not affect USP9X levels, but as previously reported HERC2 depletion did promote USP20 stabilisation. In an independent experiment, siRNA mediated depletion of USP29, as analysed by immunoblotting, did not affect USP9X levels (Figure 4.8.1 B).

Altogether these data suggest that USP9X may act in an independent manner from the previously reported USPs that control Claspin stability in S-phase. Interestingly, in these experiments USP20 depletion correlated with a decrease in USP29, suggesting functional cross-talk between the two DUBs.

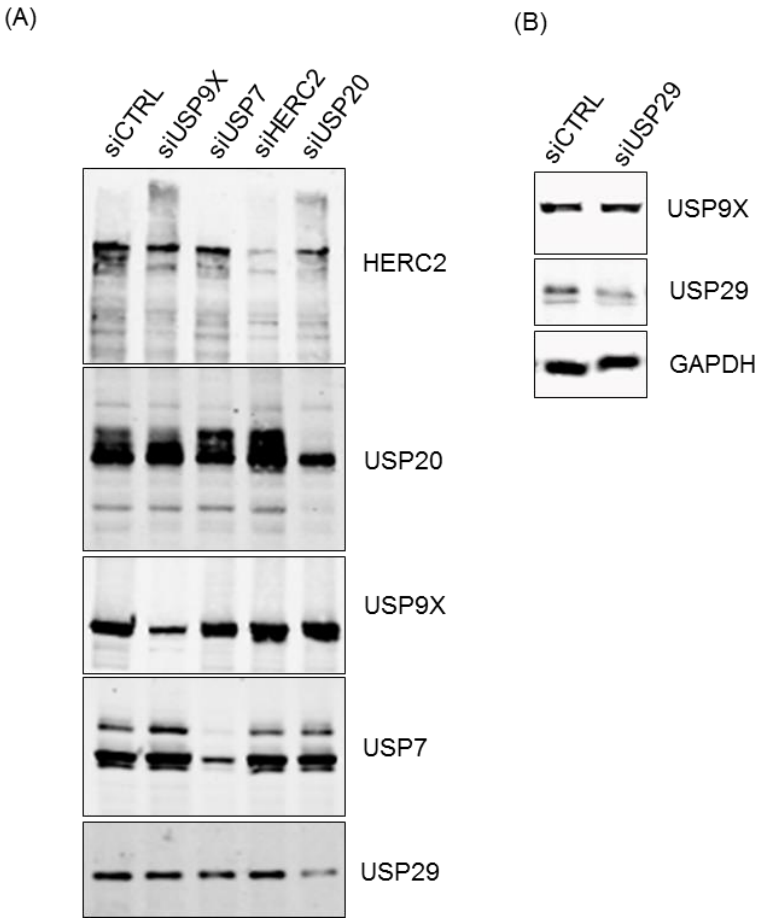

Figure 4.8.1. USP9X depletion does not influence the protein levels of the DUBs involved in S-phase Claspin regulation and their depletion has no effect on USP9X protein levels. (A) U2OS were transfected with siRNA targeting the indicted transcripts. After 48 hr cells were collected and protein extracts analysed by immunoblotting. (B) As in (A) but including siRNA targeting USP29.

Even more intriguingly, the depletion of USP9X and USP20, but not USP7, led to a differential banding pattern for HERC2 as observed by immunoblotting (Figure 4.8.1). This is indicative of USP9X and USP7 contributing to a PTM modification of HERC2 (Figure 4.8.1 A: lane 2 and lane 5).

To further examine the relationship between HERC2 and two DUBs, USP9X and USP7, that appeared to differentially affect HERC2, U2OS cells were transfected with siRNA targeting HERC2, USP7, USP9X or CTRL. 48 hr post transfection, HERC2 abundance was examined, at a single cell level, by immunofluorescence.

The figures show that (Figure 4.8.2. A), HERC2 staining in cells depleted of USP9X became brighter and this was not observed in cells depleted of USP7. This increase in HERC2 staining only occurred in siRNA conditions, where a modification was observed by immunoblot. The inclusion of siRNA targeting HERC2 and subsequent immunofluorescence confirmed the specificity of the HERC2 antibody for immunofluorescence studies as no staining was detected (Figure 4.8.2 A).

To determine whether USP9X and HERC2 could interact immunoprecipitation experiments were conducted. Antibodies for both USP9X and HERC2 were used to immunoprecipitate their respective proteins from U2OS cells. As a positive control of HERC2 interaction, a USP20 antibody was also used for immunoprecipitation experiments. Following immunoblot analysis, an interaction between USP9X and HERC2 was observed, using immunoprecipitation with the USP9X antibody (Figure 4.8.2 B) indicating that the 2 proteins may bind. The reciprocal experiment conducted with the HERC2 antibody could not confirm the interaction, however the efficacy of this antibody for immunoprecipitation was low.

To examine whether the differential HERC2 banding pattern associated with USP9X and USP20 depletion, as observed by immunoblotting, was due to HERC2 ubiquitylation, both USPs were depleted independently and HERC2 was immunoprecipitated from these U2OS cells. The immunoprecipitated HERC2 was than immunoblotted with a ubiquitin antibody, however no increase in HERC2 ubiquitylation was observed in the USP9X or USP20 depleted samples compared to the control, indicating that the modification is not likely to be ubiquitylation (Figure 4.8.2 C).

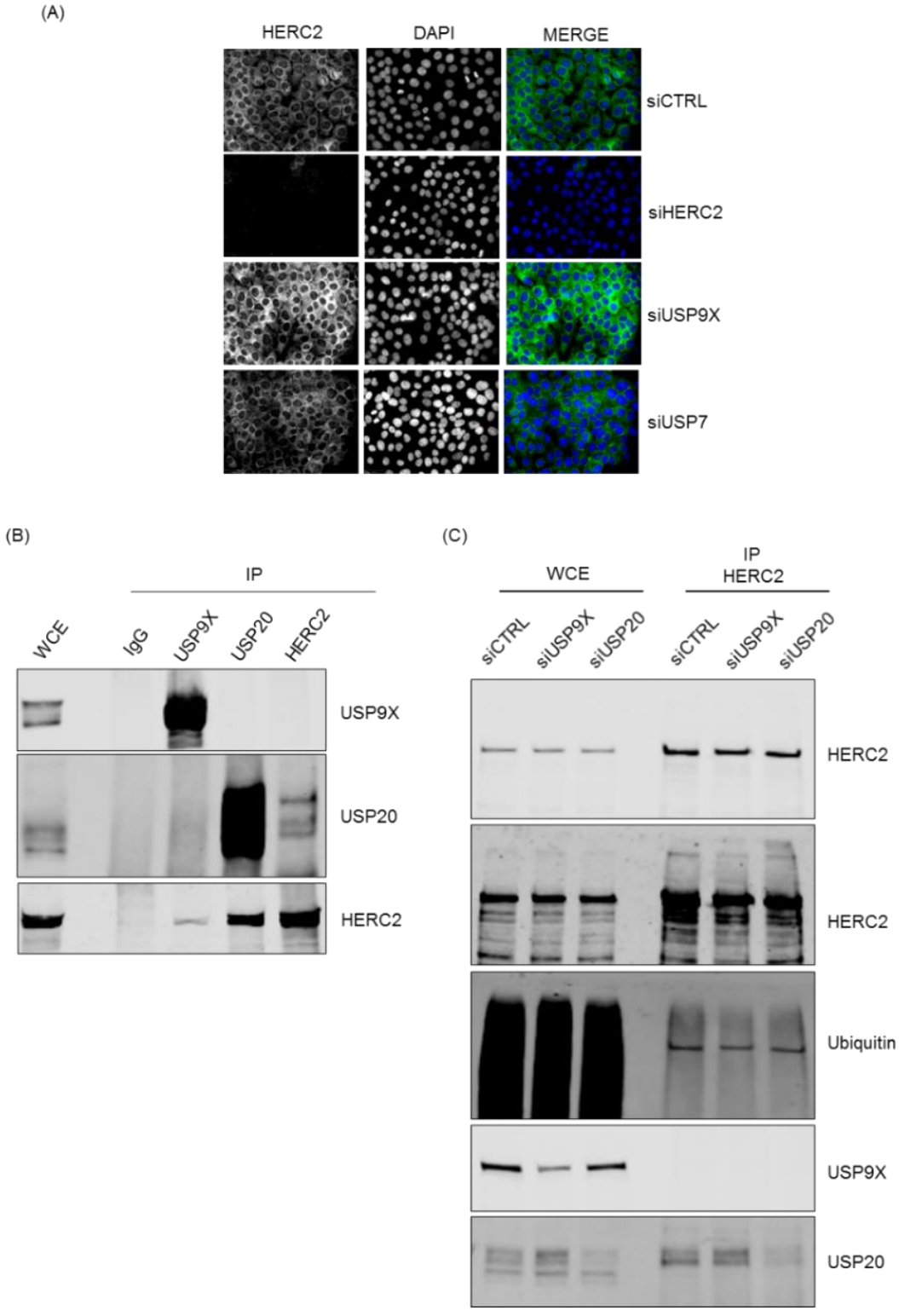
(A)
HERC2
DAPI
MERGE
siCTRL
siHERC2
siUSP9X
siUSP7
(B)
IP
WCE
IgG
USP9X
USP20
HERC2
USP9X
USP20
HERC2
(C)
WCE
IP
HERC2
siCTRL
siUSP9X
siUSP20
siCTRL
siUSP9X
siUSP20
HERC2
HERC2
Ubiquitin
USP9X
USP20

Figure 4.8.2. USP9X and USP20 can interact with HERC2 and likely affect an ubiquitin independent modification of the protein. (A) U2OS were treated with the indicated siRNA for 48 hr and then analysed by immunofluorescence (B) UPSP9X, USP20, HERC2 were immunoprecipitated from U2OS and the isolated material was examined by immunoblot (C) U2OS were treated with siRNA to USP9X, USP20 or CTRL for 48 hr after which HERC2 were immunoprecipitated and the isolated material was examined by immunoblot. *Figure 4.8.2 (B) and (C) was performed in collaboration with Kevin Wu.*

4.9 - USP9X, through its regulation of Claspin, contributes to genome stability

4.9.1- USP9X depletion impairs DNA replication fork stability

Previous experiments in this study demonstrated that USP9X controls Claspin levels in S-phase. Owing to the well documented role of Claspin, in DNA replication, (Petermann et al., 2008) the hypothesis that DNA replication dynamics could be influenced by USP9X was tested.

To investigate the effect of USP9X depletion on on-going replication forks, the fiber labelling technique was utilised. A similar approach was used to demonstrate the role of Claspin in replication (Petermann et al., 2008).

U2OS cells were transfected with CTRL or USP9X targeting siRNA and after 48 hr of transfection, nascent DNA was sequentially labelled with the nucleotide analogue iodo-deoxyuridine (IdU) for 30 min, this was then washed off and a second nucleotide analogue cloro-deoxyuridine (CldU) was added for a further 30 min. As a control siRNA targeting Claspin was also included in this experiment. DNA fibers were then prepared as described in Materials and Methods Section 2.8. Nascent DNA was visualised by fluorescence microscopy, with IdU labelled DNA visualised with TRITC conjugated antibodies (red tracks) and the CldU labelled DNA with FITC conjugated antibodies (green tracks).

To analyse whether USP9X depletion affected replication, replication fork tracks arising from each treatment were counted. A minimum of 150 of these structures were counted per sample, per experiment and 3 independent replicates were performed. The structures included red and green labelled tracks, which represent on-going replication forks, labelled with both IdU and CldU, red only tracks representing stalled forks or

terminations events, labelled only with IdU or finally green only tracks, indicative of newly-fired origins, labelled only with CldU.

In the USP9X depleted cells, a striking increase in the amount of termination events or stalled forks was observed. These were scored as red only tracks, with these forks labelled only in the first labelling period and subsequently stalled or terminated before the beginning of the second labelling period (Figure 4.9.1). The number of red only tracks was significantly increased compared to the siRNA CTRL transfected cells and was comparable to the number of red only tracks observed in Claspin depleted cells (Figure 4.9.1).

Interestingly, the amount of DNA synthesized during the second labelling period was severely reduced, as observed by short green tracks, in the USP9X depleted cells. This was comparable to what has been reported in Claspin depleted cells (Petermann et al., 2008) (Figure 4.9.1). Whilst such structures were counted as on-going replication forks, by virtue of the fact they were labelled with both labelling strategies, the shorten tracks associated with CldU labelling could be indicative that the USP9X depleted cells were sensitive to the stress of media changing and washing.

These results indicate that USP9X contributes to replication, as downregulation of the protein can impair replication fork stability.

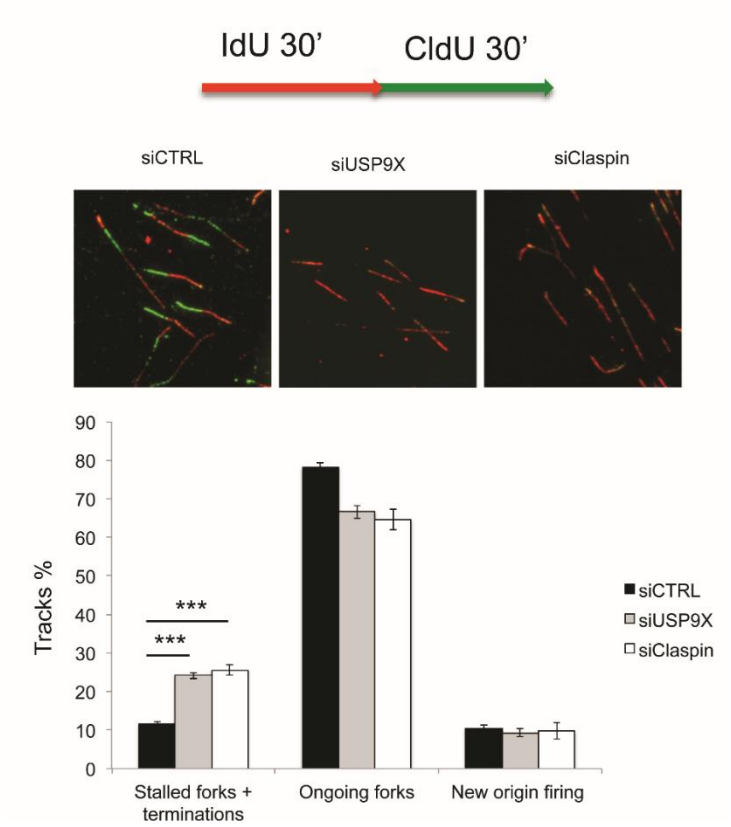

Figure 4.9.1. USP9X depletion impairs DNA replication fork stability. U2OS cells were transfected with either control (black bars), USP9X (grey bars) or Claspin (white bars) targeting siRNA. After 48 hr, cells were labelled with consecutive pulses of IdU and CldU. Replication intermediates were detected by fiber labelling technique and fluorescence microscopy. The figure shows the labelling strategy, representative examples of tracks observed in each sample and quantification of red only tracks representing termination/stalling events occurring during first labelling period, red/green tracks representing ongoing forks and green only tracks representing initiation events occurring during the second labelling period .Error bars are standard deviation, p is <0.001 and n=3.

4.9.2 - USP9X contributes to DNA replication checkpoint signalling and recovery

As discussed in the Introduction Section 1.5.2, Claspin mediates the ATR-dependent phosphorylation of CHK1, in response to replication blockade. (Jeong et al., 2003; Lee et al., 2003a). Due to the downregulation of Claspin in cells depleted of USP9X, the examination of whether replication stress induced CHK1 signalling was impacted upon depletion of USP9X, was considered.

U2OS cells were transfected with either control or two individual USP9X targeting siRNA and treated with Hydroxyurea for 30 min before cells were harvested and protein analysed by immunoblotting. As a control, siRNA targeting Claspin was also included in this experiment, as depletion of Claspin leads to inefficient checkpoint signalling (Chini and Chen, 2003).

Immunoblot examination (Figure 4.9.2 A) demonstrated inefficient phosphorylation of CHK1 at Serine 317, upon Hydroxyurea treatment, with both USP9X siRNA. The attenuated signal seen in the USP9X depleted cells was similar to that of the Claspin depleted shows (Figure 4.9.2 A). This demonstrates that USP9X contributes to an appropriate replication stress response, which is required to maintain genome integrity.

To expand this observation, a time course experiment, during which samples were collected throughout a 2 hr time period post Hydroxyurea treatment, in both USP9X depleted and control cells, was conducted. Immunoblot analysis of USP9X depleted cells compared to control cells demonstrated a marked reduction in CHK1 phosphorylation signal, at all time points tested, implicating a role for USP9X in both establishment and/or maintenance of the checkpoint (Figure 4.9.2 B).

In response to damage some proteins can relocalise from one cellular location to another (Tkach et al., 2012). Having demonstrated that USP9X can be shuttled in and out of the nucleus (Figure 4.4), examination of whether USP9X relocalised to the nucleus in cells treated with Hydroxyurea was performed. However replication blockade did not affect USP9X cellular location (Figure 4.9.2 C).

Considering the effects of USP9X depletion on replication fork stability and checkpoint activation, it was plausible that the protein contributes to replication fork recovery after stress. To examine this, the fiber labelling strategy, discussed in 4.9.1, was again used.

Using a different labelling strategy, the effect of USP9X and Claspin depletion on replication fork restart, after forks had been blocked by treatment with Hydroxyurea, was assessed. In these experiments the double labelling strategy was intercepted with

Hydroxyurea treatment for 30 min after IdU addition, before being washed and proceeding with CldU labelling, as described.

Again compared to controls, in both USP9X and Claspin depleted cells a significant increase in the number of red only tracks was observed (Figure 4.9.2 D). This was indicative of replication forks that collapsed or were unable to restart after Hydroxyurea removal.

These results indicate that USP9X contributes to replication checkpoint signalling, as well as fork recovery, following replication blockade.

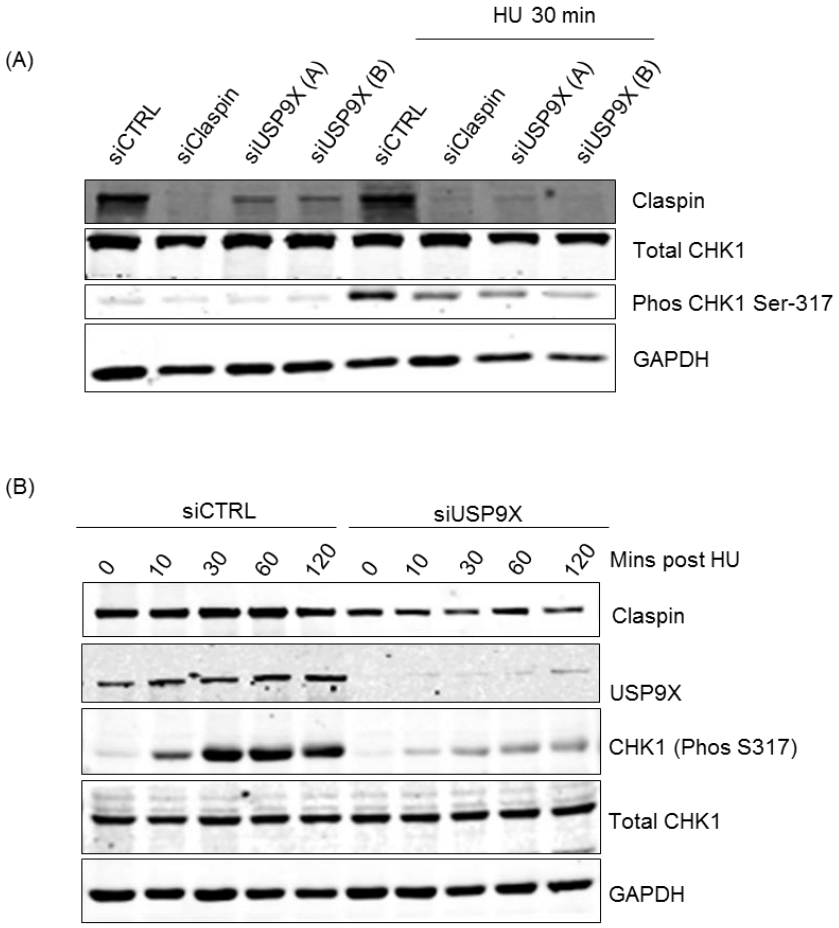

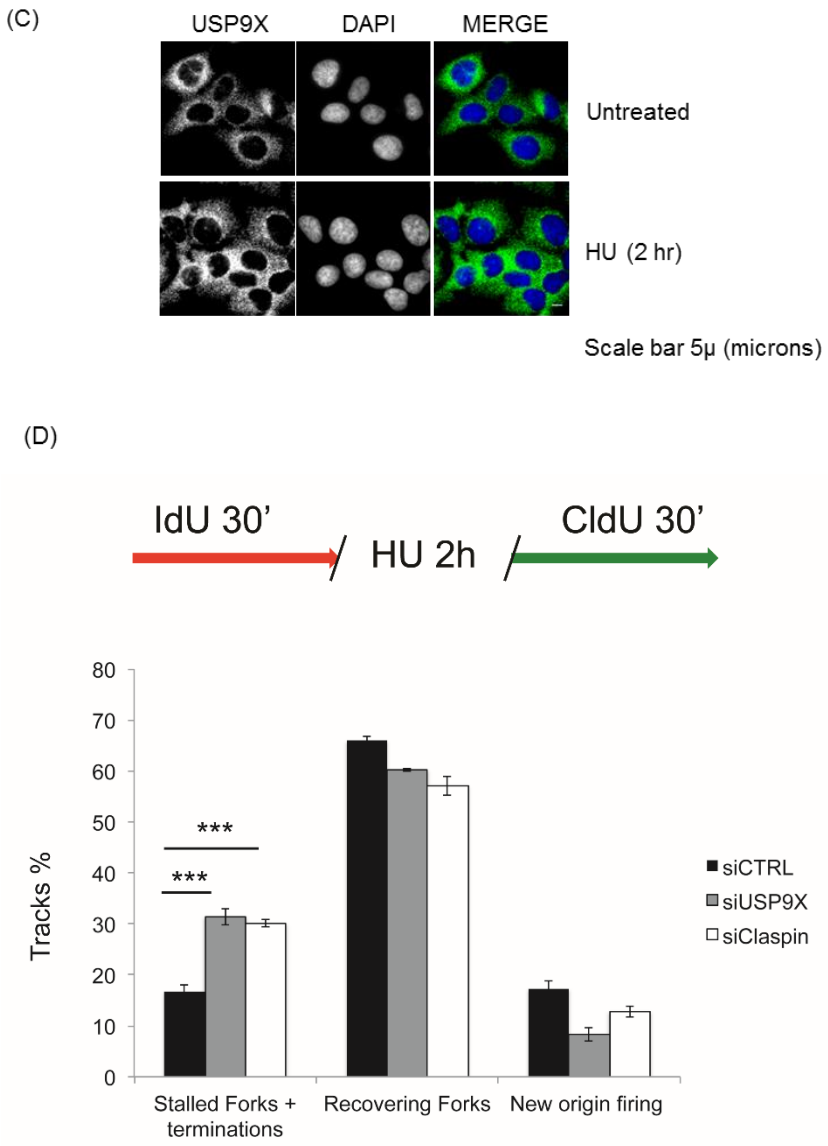

Figure 4.9.2. USP9X promotes checkpoint signalling and fork recovery. (A) U2OS cells were transfected with control or 2 different siRNA targeting USP9X or a siRNA targeting Claspin. After 48 hr Hydroxyurea was added and samples taken 30 min later. Phosphorylation of CHK1 at Ser317 as a marker of checkpoint activation was monitored by immunoblotting. (B) As in (A) U2OS cells were transfected with control or USP9X targeting siRNA. After 48 hr Hydroxyurea was added and samples taken at the indicated times. (C) Control U2OS cells or cells treated with HU for 2 hr were examined by immunofluorescence. (D) U2OS cells were transfected with either control (black bars), USP9X (grey bars) or Claspin (white bars) targeting siRNA. After 48 hr,

cells were labelled with pulses of with IdU for 30 min, cells were then treated for 2 hr with HU, before the second labelling period with CldU for 30 min. Replication intermediates were detected by fiber labelling technique and fluorescence microscopy. The figure shows the labelling strategy, and quantification of red only tracks representing termination events occurring during first labelling period and fork collapse events, red/green tracks representing forks able to restart after HU treatment, and green only tracks representing initiation events occurring during the second labelling period. Error bars are standard deviation, p is <0.001 and n=3.

4.9.3 - USP9X promotes survival in response to replication stress

Whilst all experiments thus far demonstrate a role for USP9X in replication and replication stress, all these experiments had short end points. To assess the effects of prolonged replication stress on cell viability in USP9X depleted cells, a colony formation assay was performed, as described in Materials and Methods Section 2.3.8.

U2OS were transfected with CTRL or USP9X targeting siRNA. 48 hr after transfection, cells were treated with varying concentrations of Hydroxyurea (up to 2 mM) for 18 hr. The cells were then removed from drug treatment and replated at a low density. The number of colonies formed, after 10 days incubation, was then scored.

A substantial decrease in plating efficacy was observed in USP9X depleted cells without, any replication stress (Figure 4.9.3 A). However, upon Hydroxyurea treatment, the decrease in colony formation was further enhanced in USP9X depleted cells compared to control cells at all doses tested (Figure 4.3 B).

The loss of clonogenic potential associated with USP9X depletion may indicate inherent problems with ongoing replication upon depletion of USP9X, in a normal cell cycle, or reflect problems with cell adhesion following USP9X depletion. However, the enhanced sensitivity to Hydroxyurea treatment further reveals that USP9X contributes an important role to a cells ability to cope with replication stress.

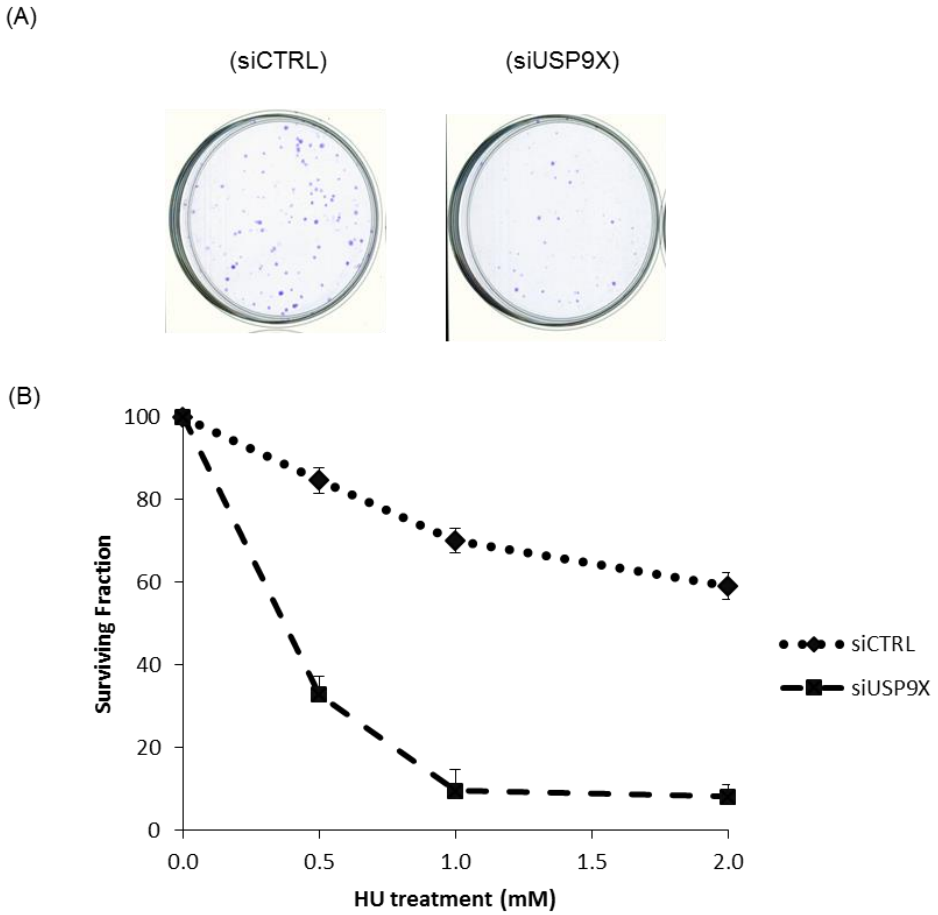

Figure 4.9.3. USP9X promotes survival in response to replication stress. (A) Example of the colonies formed from control cells, or siUSP9X depleted cells formed after 10 days of growth. (B) U2O2 cells were transfected with either control (diamonds) or USP9X targeting siRNA (squares). Cells were then incubated with the indicated concentrations of HU for 18 hr and then plated. In each case the percentage of colony forming units (CFU) scored after 10 days in the HU treated samples that have been normalized to the plating efficacy of siCTRL or siUSP9X is indicated.

4.9.4 - USP9X depletion results in the accumulation of DNA damage

This study has demonstrated that depletion of USP9X impairs replication fork stability and checkpoint signalling. It was plausible that such phenotype would lead to the accumulation of DNA damage. To examine whether USP9X depletion would result in such an insult, the examination of a marker of double stranded DNA breaks, that is the phosphorylation of H2AX at serine 139 (γ-H2AX), was visualised by immunofluorescence.

U2OS cells were transfected with 2 siRNA targeting USP9X, as well as a sequence targeting Claspin and CTRL. The inclusion of the Claspin siRNA served a positive control, as depletion of this protein leads to the generation of DSBs as marked by γ-H2AX (Freire et al., 2006). Following immunofluorescence examination, a large number of nuclei of USP9X depleted U2OS cells stained positive for this marker with the γ-H2AX staining pattern was very heterogeneous (Figure 4.9.4 A). These patterns were similar to the pattern observed upon depletion of Claspin (Figure 4.9.4 A) and recapitulated what has been reported the literature (Liu et al., 2006).

The effect on replication fork stability and the inefficient induction of the DNA replication checkpoint associated with the depletion of USP9X, strongly resemble Claspin depletion. To examine whether the downregulation of Claspin, associated with USP9X depletion, was among the primary factors contributing to DNA damage, the Strep-Claspin system was once again utilised to examine whether ectopic expression of Strep-Claspin could reduce the DNA damage.

Strep-Claspin or empty vector cells were transfected with siRNA targeting USP9X or CTRL. 24 hr later cells were induced with Doxycycline. 24 hr post induction the cells were examined by immunofluorescence (Figure 4.9.4 B). The presence of γ-H2AX was detectable in all cells depleted of USP9X including the cells which were conditionally expressing Claspin. However, on closer inspection of these images, the majority of cells expressing ectopic Claspin, were negative for γ-H2AX, indicating that the expression of Claspin could partially rescue the USP9X depletion phenotype (Figure 4.9.4 B).

To quantitatively assess the levels of damage in the cells, a flow cytometry based assay was utilised. Strep-Claspin or empty vector cells were transfected with siRNA targeting USP9X or CTRL. 24 hr later cells were either induced with Doxycycline. 24 hr post induction the cells were stained with a γ-H2AX antibody and examined by flow cytometry. Flow cytometry gating was based on the amount of γ-H2AX positive cells within a sample. 10,000 events were collected per sample, per experiment and 3 independent replicates were performed. Importantly, this assay demonstrated that the

ectopic expression of Claspin could significantly reduce damage in cells depleted of USP9X (Figure 4.9.4 C).

Altogether this data showed that the reduced levels of Claspin, as a result of USP9X depletion, are among the primary contributing factors to causing DNA damage.

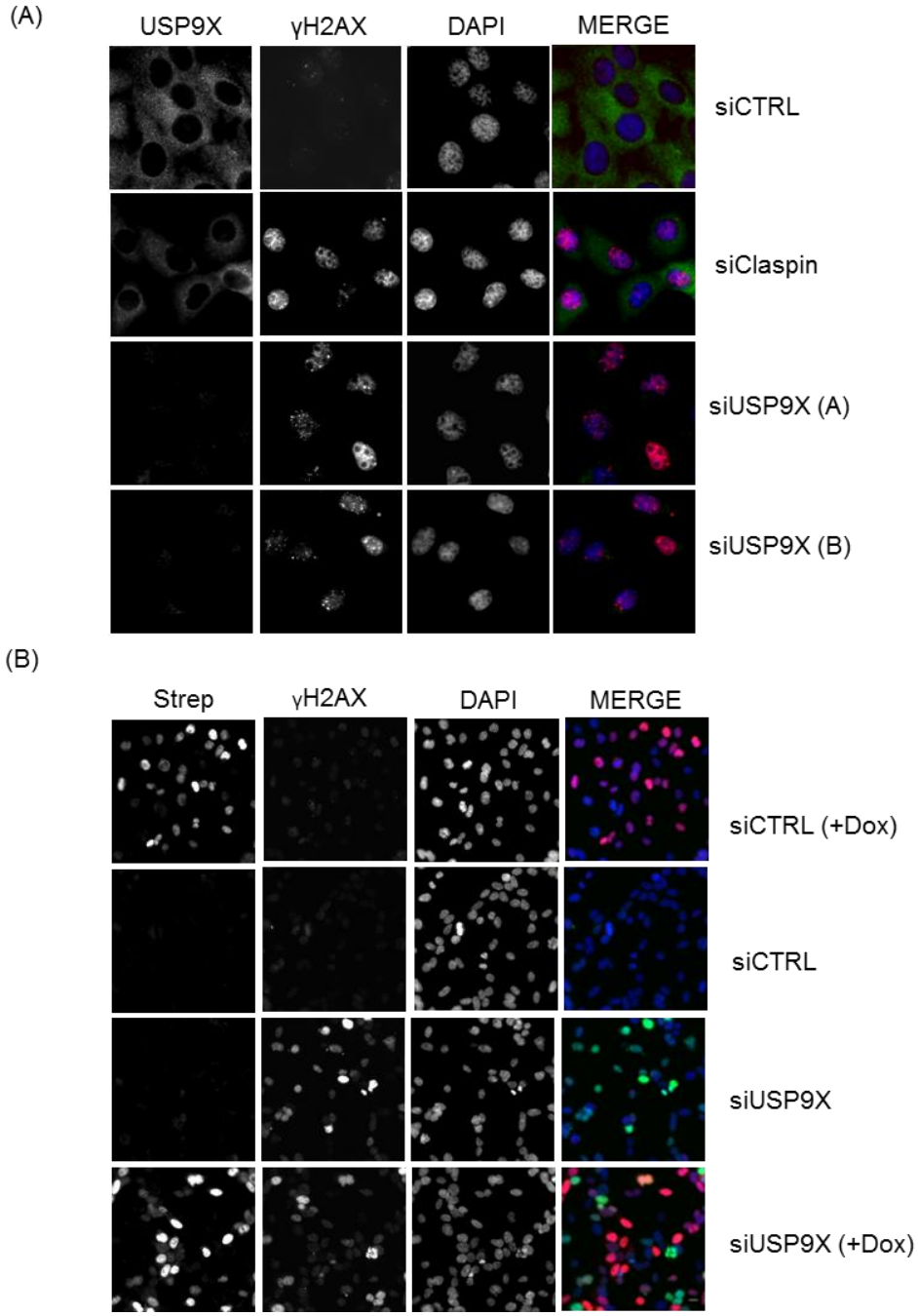

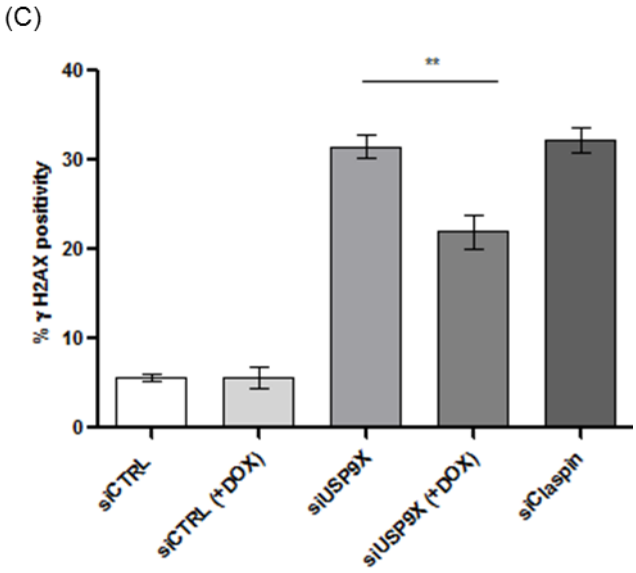

Figure 4.9.4. USP9X depletion results in the accumulation of DNA damage. (A) U2OS cells were transfected with control siRNA, Claspin siRNA or 2 different siRNA targeting USP9X. Cells were stained with anti- γ-H2AX antibody detecting H2AX phosphorylated on serine 139 and anti-USP9X antibody (B) Empty vector or Strep-Claspin expressing HEK-293 cells were transfected with USP9X or control siRNA. Cells were stained with anti- γ-H2AX antibody detecting H2AX phosphorylated on serine 139 and an anti-Strep antibody detecting the expression of Strep-Claspin protein in individual cells. (C) Analysis of γ-H2AX by flow cytometry. Bars indicate the average percentage of γ-H2AX positive cells in each sample in three independent experiments. Error bars represent standard deviation, p is<0.01 and n=3.

4.10 - Discussion and Future Perspectives

In this work, USP9X has been demonstrated to contribute to the stability of Claspin. Specifically, it appears that USP9X exerts its control on Claspin by counteracting its ubiquitylation, therefore stabilising Claspin levels in S-phase. Through its regulation of Claspin, USP9X can for the first time be implicated as important for efficient DNA replication. Depletion of USP9X causes spontaneous replication fork stalling. Further still, this study presents the novel observation that USP9X can impact on DNA replication checkpoint signalling. The effects of USP9X depletion on both replication and the replication checkpoint response resulted in replication fork collapse and the generation of DSBs. Importantly, exogenous expression of Claspin could rescue this damage phenotype indicating that Claspin is a direct substrate of USP9X.

In this study USP9X has been shown to co-immunoprecipitate with Claspin. siRNA mediated depletion of USP9X resulted in the downregulation of Claspin. As demonstrated in this study, USP9X is mostly cytoplasmic with a small nuclear fraction that can accumulate in nucleus when nuclear export is inhibited (Figure 4.4). It is tempting to speculate that some USP9X activity may play a direct role at replication forks. In agreement with this hypothesis, a proteomic study reported USP9X, similarly to Claspin, is preferentially found associated with nascent chromatin compared to mature replicative chromatin (Alabert et al., 2014). Further experiments demonstrated that USP9X protects the proteasomal mediated degradation of Claspin, specifically in S-phase. This work showed that the catalytic activity of USP9X is required for Claspin protection. An ubquitylation assay, using a USP9X inhibitor, demonstrated that Claspin ubquitylation is adversely affected by the depletion of USP9X. These studies strongly indicate that Claspin is a direct substrate of USP9X.

WP1130, the inhibitor used for this studies ubquitylation assay, is well described in the literature as an inhibitor of USP9X activity. Some of the seminal work examining a role for USP9X in oncology, utilised this drug (Schwickart et al., 2010). However, since its initial description many reports have proposed that it is in fact only partially selective for

USP9X and can target a multitude of other USPs including USP5, and USP14 as well as another DUB family member UCH37 (Peterson et al., 2015). The ability of WP1130 to affect multiple targets has some recognised clinical benefits, as it can target other USPs implicated in tumour progression (Boise, 2015). However, WP1130's clinical candidacy has been hindered by poor bioavailability (Peterson et al., 2015).

A recent paper has demonstrated that in the context of B-cell malignancies, inhibition of USP9X activity led to increased apoptosis. However short hairpin (shRNA) mediated USP9X knock down led to a compensatory upregulation of the closely related USP24 (Boise, 2015; Peterson et al., 2015). Reduction of both USP9X and USP24 in myeloma carcinoma could further enhance apoptotic induced death (Peterson et al., 2015). Using structural activity relationship experiments, Peterson and colleagues developed a novel compound, G9, which has superior metabolic stability and pharmacokinetics. This compound also showed enhanced USP9X inhibition activity compared to WP1130, but still targeted USP5 and USP24 (Peterson et al., 2015). The authors proclaim that the effectiveness of this compound is associated with the multi-target effects.

As such, whilst this studies ubquitylation assay indicates a role for USP9X in Claspin ubiquitylation, the off-target effects associated with drug treatment, hinders the use of WP1130 to confirm that Claspin is a direct substrate of USP9X, as one must consider the contribution of off-target upon Claspin ubiquitylation. Further still, as discussed in Chapter 3, USP5 was another DUB identified as a potential Claspin interactor. As USP5 is consistently described as an off-target effect, in the pursuit of the generation of USP9X selective inhibitors, it indicates a high degree of similarity between these two DUBs, at least in the drug binding domain of the these deubiquitinases (Peterson et al., 2015). Therefore the effects observed on Claspin regulation might be partially attributed to USP5, a putative Claspin interactor. It is also possible that the off-target effects associated with WP1130 treatment can also account for the stark difference between cellular detachment and apoptotic like phenotypes between USP9X siRNA depleted cells and USP9X chemical inhibition.

Instead of using small molecule compounds, the overexpression constructs for both WT and CI USP9X could be utilised to conduct an ubiquitylation assay to assess whether the overexpression of the WT or CI USP9X contributed to Claspin ubiquitylation in S-phase. The constructs would facilitate the confirmation that Claspin is a direct substrate of USP9X, as these constructs are specific for the overexpression of a sequence encoding USP9X alone. Efforts were endeavoured to perform this experiment, however these attempts were futile due to toxicity associated with transfection of large DNA concentrations. To circumvent this problem, in future studies, the use of a viral vector transfection system could perhaps be generated. Although a more labour intensive method, this method of transfection is associated with higher transfection efficacy, of large amounts of DNA, with less toxicity (Luo and Saltzman, 2000). Alternatively, the use of *in vitro* assays are commonly used in the literature to confirm a direct relationship between an enzyme and substrate (Alonso-de Vega et al., 2014; Izawa et al., 2011). Similar strategies helped to confirm a direct relationship between Claspin and various USPs (Yuan et al., 2014).

In this study the use of siRNA mediated protein depletion demonstrated that USP9X contributes to replication checkpoint signalling. Experiments demonstrated that up to 2 hr post Hydroxyurea treatment, CHK1 signalling was attenuated. This led to the conclusion that USP9X is required for the initiation of the replication checkpoint (Figure 4.9.2).

In future experiments it would be interesting to extend Hydroxyurea treatment (up to 24 hr), to determine whether USP9X contributes to both the establishment but also maintenance of the checkpoint response. Further still, employment of the Flp-In TREx system for the ectopic of Claspin could also be used, to examine whether overexpression of Claspin could alleviate the attenuated CHK1 signal associated with depletion of USP9X.

A colony formation assay examined the effects of USP9X depletion on prolonged replication stress and demonstrated that USP9X promotes survival in response to such conditions (Figure 4.9.3).

It would be interesting to again utilise the Strep-Claspin system to examine whether hypersensitivity to Hydroxyurea treatment, in USP9X depleted cells, could be attenuated by the overexpression of Claspin. Due to adherence problems HEK-293 cells are not routinely used in clonogenic survival assays, and extensive method optimisation would have to be conducted.

This study documented, through fiber labelling experiments, the novel observation that USP9X contributes to replication fork stability. The use of fiber labelling to examine contribution to genome stability has been well described in the literature with particular relevance to Claspin, by Dr Eva Peterman (Petermann et al., 2008; Petermann et al., 2010). However studies of Claspin regulation mediated by other DUBs, USP28, USP7, USP29 and USP20, failed to examine a role for these DUBs in normal replication (Faustrup et al., 2009; Martin et al., 2015; Yuan et al., 2014; Zhang et al., 2006; Zhu et al., 2014). It would be intriguing to assess the replication phenotype associated with the depletion of these DUBS, using a fiber labelling strategy.

The Strep-Claspin system could be employed to conduct fiber labelling experiments, to examine whether ectopic expression of Claspin could rescue the strong replication fork stalling phenotype observed upon USP9X depletion (Figure 4.9.1). To date, the use of HEK-293 cells in fiber labelling experiments in the literature has not been described. This is presumably due to difficulties associated with adherence of these cells. Therefore, the fiber labelling protocol, particularly the steps prior to fixation, would have to be optimised for compatibility with HEK-293 cells.

In this study siRNA mediated depletion of USP9X resulted DNA damage, as detected by immunofluorescence and flow cytometry. The effects of USP9X depletion on DNA replication strongly mirrors the direct down regulation of Claspin (Allera-Moreau et al., 2012; Peschiaroli et al., 2006; Petermann et al., 2008). Importantly the use of the Flp-In

TREx cellular system for Claspin overexpression was successfully employed to partially rescue the DNA damage phenotype associated with USP9X expression (Figure 4.9.4). This suggests that Claspin is the main target of USP9X in the process of DNA replication.

However, there was not complete rescue of DNA damage. This may be attributed to the inability of Claspin to be ectopically expressed in all cells, due to siRNA targeting USP9X decreasing the levels of ectopic as well as endogenous Claspin expression. However, it may also suggest that the depletion of USP9X causes damage unrelated to its regulation of Claspin. Considering the abundancy of cellular mechanisms USP9X has been implicated in, it seems plausible that USP9X may target another substrate during replication (Murtaza et al., 2015; Perez-Mancera et al., 2012; Schwickart et al., 2010). It would be interesting to examine how DNA damage originates in USP9X depleted conditions, aside from its regulation of Claspin.

Although depletion of UPS9X resulted in the accumulation of a marker of double DSBs, γ-H2AX (Mah et al., 2010) (Figure 4.9.4), only a single marker was assessed. In future studies it would be interesting to observe whether USP9X depletion affected other markers of damage such as the recruitment of DNA repair proteins 53BP1, RNF8, KU80 and RAD51 (Panier and Boulton, 2014) (Feng and Chen, 2012; Tarsounas et al., 2003).

Such proteins help to mediate the DNA repair process in response to DSBs. Immediate and efficient error correction, after DSB induction, is important to restore and preserve chromatin architecture and genome stability. The DDR pathways, including CHK1 signalling is responsible for the recognition, signalling and repair of DSBs in cells (Panier and Boulton, 2014). DSBs are largely overcome by two major mechanisms of repair, homologous recombination and non-homologous end joining, each with independent and overlapping roles in maintaining genomic integrity (Mah et al., 2010). Considering the detection of high levels of DNA damage, it would be intriguing to assess whether USP9X depletion impacted upon these DNA repair mechanisms. This knowledge would offer further insight into USP9X function.

It is interesting that four different deubiquitinases, USP7, USP29, USP20 and USP9X target the same protein in a non-redundant manner. To gain mechanistic insight into why 3 of these DUBs contribute to Claspin stability in replication, examination of depletion of the protein levels of all DUBs involved in Claspin stability, in S-phase was examined. For further knowledge, siRNA targeting the E3 ligase, HERC2, heavily implicated in Claspin regulation was also included (Izawa et al., 2011; Yuan et al., 2014; Zhu et al., 2014). Depletion of USP20, USP7 and USP29 did not affect USP9X nor did depletion of USP9X affect USP20, USP7 or USP29 protein level (Figure 4.8.1). Therefore, it is possible that each DUB may be involved in limiting Claspin ubiquitylation at different specific sites on the protein, thus allowing multiple layers of regulation to be independently imposed on Claspin.

Examination of HERC2 depletion was conducted in this study to establish if it was an E3 ligase involved in the ubiquitination of USP9X in S-phase, as a similar role for HERC2 has been reported for USP20 (Yuan et al., 2014; Zhu et al., 2014). However, depletion of HERC2 did not affect USP9X protein levels (Figure 4.8.1).

Intriguingly, depletion of USP9X appeared to modify HERC2, as observed by immunoblotting and immunofluorescence (Figure 4.8.2). Whilst not as well documented in the literature, the ability of a USP to exert control over an E3 ligase has been reported (de Bie and Ciechanover, 2011). USP16, a histone H2A deubiquitinase, has been shown to interact with HERC2 to negatively regulate DNA damage-induced ubiquitin foci and to terminate the ubiquitin signal (Zhang et al., 2014). Whilst USP20 downregulation seemed to exert a similar effect as USP9X depletion, although only demonstrated by the unique HERC2 immunoblotting pattern, the modification did not seem to relate to ubiquitylation (Figure 4.8.2 C). While outside the scope of this particular study, investigation of what modification on HERC2 can be influenced by USP9X and USP20 warrants further investigation. The process of ubiquitylation, tends to be a downstream PTM coming after other modifications such as phosphorylation (Berndsen and Wolberger, 2014), it would be important to unravel whether such a modification, or others

such as sumoylation, may contribute to the differences observed to HERC2 upon USP9X depletion.

While these effects may be independent of Claspin, it is interesting to speculate that USP9X may contribute to the relationship between HERC2 and Claspin. Claspin is a known target of BRCA1 E3 ligase activity (Sato et al., 2012). HERC2 can shuttle between the nucleus and cytoplasm, much like USP9X, to target BARD1-uncoupled BRCA1 for degradation (Wu et al., 2010). The HERC2-BRCA1 interaction is maximal during S-phase and rapidly diminishes as cells enter G2-M. In the presence of BRCA1, HERC2 interacts with Claspin. HERC2 depletion alleviates slow replication fork progression associated with Claspin deficient cells (Izawa et al., 2011). Perhaps a modification, such as the deconjugation of a mono-ubiquitin link, from HERC2, an event which would be difficult to capture from the assay used in this study, can be regulated by USP9X. This could permit its shuttling ability, which allows HERC2 to degrade BRCA1, preventing its degradation of Claspin. However this is just a speculative hypothesis which would require extensive investigation.

The E3 ligase involved in the regulation of USP9X in S-phase remains to be elucidated but intriguingly within the SILAC data the E3 ligase MULE was identified (Discussion Chapter 3). This protein has been previously shown to interact with USP9X and the relationship between these proteins can influence MCL-1 ubquitylation status (Gomez-Bougie et al., 2011). It would be interesting to examine whether MULE could influence the USP9X-Claspin interaction during replication.

This study primarily involved the use of siRNA to study USP9X depletion phenotypes, and although this offered a relatively simple and cheap strategy of protein depletion, well utilised in the literature, it is a method associated with slow kinetics and incomplete protein depletion. With the onslaught of genome editing tools (Nemudryi et al., 2014), in particular CRISPR/Cas9, which has already been applied to study USP9X (Chou et al., 2015), it would be worthy to study USP9X replication phenotypes using a genetic knockout of USP9X, to examine if the siRNA phenotype is recapitulated. Alternatively,

cells may adapt to genetic inhibition of USP9X, by using a closely related compensatory DUB like USP24, as has been eluded to in the literature when using shRNA mediated USP9X depletion (Peterson et al., 2015).

Consistent with the dual role of Claspin at replication forks and as a mediator of checkpoint signalling, USP9X depletion attenuates but does not abolish CHK1 activation in response to Hydroxyurea and leads to hypersensitivity to such treatment (Figure 4.9.2 and 4.9.3). Increased DNA damage and a diminished ability to promote efficient checkpoint signalling may account for the reported hypersensitivity to other genotoxic reagents such a 5-flourouracil in USP9X deficient colorectal cancer cells (Harris et al., 2012). The inhibition of USP9X as both a single agent and a combination strategy with other drugs has been heavily implicated as a therapeutic strategy for numerous carcinomas (Harris et al., 2012; Peterson et al., 2015; Schwickart et al., 2010). The majority of this work focused on the role of USP9X in the stabilisation of the anti-apoptotic protein MCL-1, and inhibition of USP9X enhanced the rate of apoptosis in these cells. In this study, while apoptosis was evident upon WP1130 treatment, siRNA mediated USP9X depletion did not lead to an increase in apoptotic cell death. The additive effects of USP9X depletion with Hydroxyurea was only revealed with the use of clonogenic assays that have long-term end points. This highlights the idea that excessive genome instability may be the main contributor to the lessened proliferative capability in our cellular model.

As extensively discussed, USP9X has been implicated in numerous cellular processes and multiple diseases, especially neurodegenerative disorders and cancer (Murtaza et al., 2015). While its role as a tumour suppressor in PDAC has been described, the exact mechanism requires deeper understanding (Cox et al., 2014). It is tempting to speculate that the observations of this study, which implicates USP9X in the protection of replication forks and defence from DNA damage, could be important attributes in the tumour suppressor role of USP9X.

This study also has important consequences for the development of USP9X inhibitors for clinical use. The potential therapeutic advantage of inhibiting USP9X has been well documented (Boise, 2015), however such inhibition may be associated with potential detrimental effects on the proliferation of non-cancerous cells. Such therapy could contribute to genome stability, which in itself, could ultimately lead to cancer. As such the indications from this study should be considered in future manipulation of USP9X in cancer.

In conclusion, this study, for the first time, implicates USP9X, through its regulation of Claspin, in the control of DNA replication and in preventing replication stress induced DNA damage. The experiments provide a conceptual framework to understand the mechanism by which USP9X can function as a tumour suppressor and raise a potential flag for the development of USP9X inhibitors. These results could strongly impact multiple research areas, related to cancer biology and therapeutics, and are of particular interest in the fields of genome stability and DNA replication.

Bibliography

Aebersold, R. (2003). A mass spectrometric journey into protein and proteome research. Journal of the American Society for Mass Spectrometry *14*, 685-695.

Aebersold, R., and Mann, M. (2003). Mass spectrometry-based proteomics. Nature *422*, 198-207.

Agrawal, P., Chen, Y.T., Schilling, B., Gibson, B.W., and Hughes, R.E. (2012). Ubiquitin-specific peptidase 9, X-linked (USP9X) modulates activity of mammalian target of rapamycin (mTOR). The Journal of biological chemistry *287*, 21164-21175.

Al-Hakim, A.K., Zagorska, A., Chapman, L., Deak, M., Peggie, M., and Alessi, D.R. (2008). Control of AMPK-related kinases by USP9X and atypical Lys(29)/Lys(33)-linked polyubiquitin chains. The Biochemical journal *411*, 249-260.

Al-Mulla, F., Bitar, M.S., Al-Maghrebi, M., Behbehani, A.I., Al-Ali, W., Rath, O., Doyle, B., Tan, K.Y., Pitt, A., and Kolch, W. (2011). Raf kinase inhibitor protein RKIP enhances signaling by glycogen synthase kinase-3beta. Cancer research *71*, 1334-1343.

Allera-Moreau, C., Rouquette, I., Lepage, B., Oumouhou, N., Walschaerts, M., Leconte, E., Schilling, V., Gordien, K., Brouchet, L., Delisle, M.B., *et al.* (2012). DNA replication stress response involving PLK1, CDC6, POLQ, RAD51 and CLASPIN upregulation prognoses the outcome of early/mid-stage non-small cell lung cancer patients. Oncogenesis *1*, e30.

Alonso-de Vega, I., Martin, Y., and Smits, V.A. (2014). USP7 controls Chk1 protein stability by direct deubiquitination. Cell Cycle *13*, 3921-3926.

Aslanoglou, D., Alvarez-Curto, E., Marsango, S., and Milligan, G. (2015). Distinct Agonist Regulation of Muscarinic Acetylcholine M2-M3 Heteromers and Their Corresponding Homomers. The Journal of biological chemistry *290*, 14785-14796.

Ayares, D., Ganea, D., Chekuri, L., Campbell, C.R., and Kucherlapati, R. (1987). Repair of single-stranded DNA nicks, gaps, and loops in mammalian cells. Molecular and cellular biology *7*, 1656-1662.

Aze, A., Zhou, J.C., Costa, A., and Costanzo, V. (2013). DNA replication and homologous recombination factors: acting together to maintain genome stability. Chromosoma *122*, 401-413.

Bassermann, F., Frescas, D., Guardavaccaro, D., Busino, L., Peschiaroli, A., and Pagano, M. (2008). The Cdc14B-Cdh1-Plk1 axis controls the G2 DNA-damage-response checkpoint. Cell *134*, 256-267.

Bennett, L.N., and Clarke, P.R. (2006). Regulation of Claspin degradation by the ubiquitin-proteosome pathway during the cell cycle and in response to ATR-dependent checkpoint activation. FEBS letters *580*, 4176-4181.

Bennett, L.N., Larkin, C., Gillespie, D.A., and Clarke, P.R. (2008). Claspin is phosphorylated in the Chk1-binding domain by a kinase distinct from Chk1. Biochemical and biophysical research communications *369*, 973-976.

Berndsen, C.E., and Wolberger, C. (2014). New insights into ubiquitin E3 ligase mechanism. Nature structural & molecular biology *21*, 301-307.

Besteiro, M.A.G., and Gottifredi, V. (2015). The fork and the kinase: A DNA replication tale from a CHK1 perspective. Mutat Res-Rev Mutat *763*, 168-180.

Bieging, K.T., Mello, S.S., and Attardi, L.D. (2014). Unravelling mechanisms of p53-mediated tumour suppression. Nature reviews Cancer *14*, 359-370.

Boise, L.H. (2015). DUB-ling down on B-cell malignancies. Blood *125*, 3522-3523.

Bradford, M.M. (1976). A rapid and sensitive method for the quantitation of microgram quantities of protein utilizing the principle of protein-dye binding. Analytical biochemistry *72*, 248-254.

Branzei, D., and Foiani, M. (2010). Maintaining genome stability at the replication fork. Nature reviews Molecular cell biology *11*, 208-219.

Brentnall, M., Rodriguez-Menocal, L., De Guevara, R.L., Cepero, E., and Boise, L.H. (2013). Caspase-9, caspase-3 and caspase-7 have distinct roles during intrinsic apoptosis. BMC cell biology *14*, 32.

Broderick, R., Rainey, M.D., Santocanale, C., and Nasheuer, H.P. (2013). Cell cycle-dependent formation of Cdc45-Claspin complexes in human cells is compromized by UV-mediated DNA damage. The FEBS journal *280*, 4888-4902.

Brown, G.M., Furlong, R.A., Sargent, C.A., Erickson, R.P., Longepied, G., Mitchell, M., Jones, M.H., Hargreave, T.B., Cooke, H.J., and Affara, N.A. (1998). Characterisation of the coding sequence and fine mapping of the human DFFRY gene and comparative expression analysis and mapping to the Sxrb interval of the mouse Y chromosome of the Dffry gene. Human molecular genetics *7*, 97-107.

Carmena, M., Wheelock, M., Funabiki, H., and Earnshaw, W.C. (2012). The chromosomal passenger complex (CPC): from easy rider to the godfather of mitosis. Nat Rev Mol Cell Bio *13*, 789-803.

Carneiro, D.G., Clarke, T., Davies, C.C., and Bailey, D. (2015). Identifying novel protein interactions: Proteomic methods, optimisation approaches and data analysis pipelines. Methods.

Cayrou, C., Coulombe, P., and Mechali, M. (2010). Programming DNA replication origins and chromosome organization. Chromosome research : an international journal on the molecular, supramolecular and evolutionary aspects of chromosome biology *18*, 137-145.

Cecchini, M.J., Amiri, M., and Dick, F.A. (2012). Analysis of cell cycle position in mammalian cells. Journal of visualized experiments : JoVE.

Chen, C.P., Chang, T.Y., Tzen, C.Y., Wang, W., Lee, C.C., Chen, L.F., Lee, M.S., and Lin, S.P. (2003). Second-trimester sonographic demonstration of retrognathia and bilateral pyelectasis in a fetus with a duplication of chromosome 10q24.1-->qter. Ultrasound in obstetrics & gynecology : the official journal of the International Society of Ultrasound in Obstetrics and Gynecology *21*, 516-518.

Chen, E.Y., Tan, C.M., Kou, Y., Duan, Q., Wang, Z., Meirelles, G.V., Clark, N.R., and Ma'ayan, A. (2013). Enrichr: interactive and collaborative HTML5 gene list enrichment analysis tool. BMC bioinformatics *14*, 128.

Chen, X., Overstreet, E., Wood, S.A., and Fischer, J.A. (2000). On the conservation of function of the Drosophila Fat facets deubiquitinating enzyme and Fam, its mouse homolog. Dev Genes Evol *210*, 603-610.

Chen, X., Wei, S., Ji, Y., Guo, X., and Yang, F. (2015). Quantitative proteomics using SILAC: Principles, applications, and developments. Proteomics *15*, 3175-3192.

Chevallet, M., Luche, S., and Rabilloud, T. (2006). Silver staining of proteins in polyacrylamide gels. Nature protocols *1*, 1852-1858.

Chini, C.C., and Chen, J. (2003). Human claspin is required for replication checkpoint control. The Journal of biological chemistry *278*, 30057-30062.

Chini, C.C., and Chen, J. (2004). Claspin, a regulator of Chk1 in DNA replication stress pathway. DNA repair *3*, 1033-1037.

Chini, C.C., and Chen, J. (2006). Repeated phosphopeptide motifs in human Claspin are phosphorylated by Chk1 and mediate Claspin function. The Journal of biological chemistry *281*, 33276-33282.

Chou, D.H., Vetere, A., Choudhary, A., Scully, S.S., Schenone, M., Tang, A., Gomez, R., Burns, S.M., Lundh, M., Vital, T., *et al.* (2015). Kinase-Independent Small-Molecule Inhibition of JAK-STAT Signaling. Journal of the American Chemical Society *137*, 7929-7934.

Cimprich, K.A., and Cortez, D. (2008). ATR: an essential regulator of genome integrity. Nature reviews Molecular cell biology *9*, 616-627.

Clarke, C.A., Bennett, L.N., and Clarke, P.R. (2005). Cleavage of claspin by caspase-7 during apoptosis inhibits the Chk1 pathway. The Journal of biological chemistry *280*, 35337-35345.

Clarke, C.A., and Clarke, P.R. (2005). DNA-dependent phosphorylation of Chk1 and Claspin in a human cell-free system. The Biochemical journal *388*, 705-712.

Colosimo, A., Goncz, K.K., Holmes, A.R., Kunzelmann, K., Novelli, G., Malone, R.W., Bennett, M.J., and Gruenert, D.C. (2000). Transfer and expression of foreign genes in mammalian cells. BioTechniques *29*, 314-318, 320-312, 324 passim.

Costa, A., Hood, I.V., and Berger, J.M. (2013). Mechanisms for initiating cellular DNA replication. Annual review of biochemistry *82*, 25-54.

Cox, J., and Mann, M. (2008). MaxQuant enables high peptide identification rates, individualized p.p.b.-range mass accuracies and proteome-wide protein quantification. Nature biotechnology *26*, 1367-1372.

Cox, J.L., Wilder, P.J., Gilmore, J.M., Wuebben, E.L., Washburn, M.P., and Rizzino, A. (2013). The SOX2-interactome in brain cancer cells identifies the requirement of MSI2 and USP9X for the growth of brain tumor cells. PloS one *8*, e62857.

Cox, J.L., Wilder, P.J., Wuebben, E.L., Ouellette, M.M., Hollingsworth, M.A., and Rizzino, A. (2014). Context-dependent function of the deubiquitinating enzyme USP9X in pancreatic ductal adenocarcinoma. Cancer biology & therapy *15*, 1042-1052.

Cui, J., Sun, W., Hao, X., Wei, M., Su, X., Zhang, Y., Su, L., and Liu, X. (2015). EHMT2 inhibitor BIX-01294 induces apoptosis through PMAIP1-USP9X-MCL1 axis in human bladder cancer cells. Cancer cell international *15*, 4.

Darzynkiewicz, Z., Juan, G., and Bedner, E. (2001). Determining cell cycle stages by flow cytometry. Current protocols in cell biology / editorial board, Juan S Bonifacino [et al] *Chapter 8*, Unit 8 4.

Dayal, S., Sparks, A., Jacob, J., Allende-Vega, N., Lane, D.P., and Saville, M.K. (2009). Suppression of the deubiquitinating enzyme USP5 causes the accumulation of unanchored polyubiquitin and the activation of p53. The Journal of biological chemistry *284*, 5030-5041.

de Bie, P., and Ciechanover, A. (2011). Ubiquitination of E3 ligases: self-regulation of the ubiquitin system via proteolytic and non-proteolytic mechanisms. Cell death and differentiation *18*, 1393-1402.

Devoy, A., Soane, T., Welchman, R., and Mayer, R.J. (2005). The ubiquitin-proteasome system and cancer. Essays in biochemistry *41*, 187-203.

Dewar, J.M., Budzowska, M., and Walter, J.C. (2015). The mechanism of DNA replication termination in vertebrates. Nature *525*, 345-350.

Dikic, I., Wakatsuki, S., and Walters, K.J. (2009). Ubiquitin-binding domains - from structures to functions. Nature reviews Molecular cell biology *10*, 659-671.

Duderstadt, K.E., Reyes-Lamothe, R., van Oijen, A.M., and Sherratt, D.J. (2014). Replication-fork dynamics. Cold Spring Harbor perspectives in biology *6*.

Dupont, S., Mamidi, A., Cordenonsi, M., Montagner, M., Zacchigna, L., Adorno, M., Martello, G., Stinchfield, M.J., Soligo, S., Morsut, L., *et al.* (2009). FAM/USP9x, a deubiquitinating enzyme essential for TGFbeta signaling, controls Smad4 monoubiquitination. Cell *136*, 123-135.

Eaton, S.L., Roche, S.L., Llavero Hurtado, M., Oldknow, K.J., Farquharson, C., Gillingwater, T.H., and Wishart, T.M. (2013). Total protein analysis as a reliable loading control for quantitative fluorescent Western blotting. PloS one *8*, e72457.

Eletr, Z.M., and Wilkinson, K.D. (2014). Regulation of proteolysis by human deubiquitinating enzymes. Biochimica et biophysica acta *1843*, 114-128.

Elgendy, M., Ciro, M., Abdel-Aziz, A.K., Belmonte, G., Dal Zuffo, R., Mercurio, C., Miracco, C., Lanfrancone, L., Foiani, M., and Minucci, S. (2014). Beclin 1 restrains tumorigenesis through Mcl-1 destabilization in an autophagy-independent reciprocal manner. Nature communications *5*, 5637.

Engelender, S. (2012). alpha-Synuclein fate: proteasome or autophagy? Autophagy *8*, 418-420.

Farshi, P., Deshmukh, R.R., Nwankwo, J.O., Arkwright, R.T., Cvek, B., Liu, J., and Dou, Q.P. (2015). Deubiquitinases (DUBs) and DUB inhibitors: a patent review. Expert opinion on therapeutic patents *25*, 1191-1208.

Faustrup, H., Bekker-Jensen, S., Bartek, J., Lukas, J., and Mailand, N. (2009). USP7 counteracts SCFbetaTrCP- but not APCCdh1-mediated proteolysis of Claspin. The Journal of cell biology *184*, 13-19.

Favaloro, B., Allocati, N., Graziano, V., Di Ilio, C., and De Laurenzi, V. (2012). Role of apoptosis in disease. Aging *4*, 330-349.

Feng, L., and Chen, J. (2012). The E3 ligase RNF8 regulates KU80 removal and NHEJ repair. Nature structural & molecular biology *19*, 201-206.

Fischervize, J.A., Rubin, G.M., and Lehmann, R. (1992). The Fat-Facets Gene Is Required for Drosophila Eye and Embryo Development. Development *116*, 985-&.

Flaggs, G., Plug, A.W., Dunks, K.M., Mundt, K.E., Ford, J.C., Quiggle, M.R., Taylor, E.M., Westphal, C.H., Ashley, T., Hoekstra, M.F., *et al.* (1997). Atm-dependent interactions of a mammalian chk1 homolog with meiotic chromosomes. Current biology : CB *7*, 977-986.

Focarelli, M.L., Soza, S., Mannini, L., Paulis, M., Montecucco, A., and Musio, A. (2009). Claspin inhibition leads to fragile site expression. Genes, chromosomes & cancer *48*, 1083-1090.

Foiani, M., Lucchini, G., and Plevani, P. (1997). The DNA polymerase alpha-primase complex couples DNA replication, cell-cycle progression and DNA-damage response. Trends Biochem Sci *22*, 424-427.

Foiani, M., Marini, F., Gamba, D., Lucchini, G., and Plevani, P. (1994). The B subunit of the DNA polymerase alpha-primase complex in Saccharomyces cerevisiae executes an essential function at the initial stage of DNA replication. Molecular and cellular biology *14*, 923-933.

Fragkos, M., Ganier, O., Coulombe, P., and Mechali, M. (2015). DNA replication origin activation in space and time. Nature reviews Molecular cell biology *16*, 360-374.

Freeman, A.K., and Monteiro, A.N. (2010). Phosphatases in the cellular response to DNA damage. Cell communication and signaling : CCS *8*, 27.

Freire, R., van Vugt, M.A., Mamely, I., and Medema, R.H. (2006). Claspin: timing the cell cycle arrest when the genome is damaged. Cell Cycle *5*, 2831-2834.

Gao, D., Inuzuka, H., Korenjak, M., Tseng, A., Wu, T., Wan, L., Kirschner, M., Dyson, N., and Wei, W. (2009). Cdh1 regulates cell cycle through modulating the claspin/Chk1 and the Rb/E2F1 pathways. Molecular biology of the cell *20*, 3305-3316.

Gewurz, B.E., and Harper, J.W. (2006). DNA-damage control: Claspin destruction turns off the checkpoint. Current biology : CB *16*, R932-934.

Gomez-Bougie, P., Menoret, E., Juin, P., Dousset, C., Pellat-Deceunynck, C., and Amiot, M. (2011). Noxa controls Mule-dependent Mcl-1 ubiquitination through the regulation of the Mcl-1/USP9X interaction. Biochemical and biophysical research communications *413*, 460-464.

Gorman, A.M. (2008). Neuronal cell death in neurodegenerative diseases: recurring themes around protein handling. Journal of cellular and molecular medicine *12*, 2263-2280.

Goyal, L., McCall, K., Agapite, J., Hartwieg, E., and Steller, H. (2000). Induction of apoptosis by Drosophila reaper, hid and grim through inhibition of IAP function. Embo J *19*, 589-597.

Griffin, T.J., Lock, C.M., Li, X.J., Patel, A., Chervetsova, I., Lee, H., Wright, M.E., Ranish, J.A., Chen, S.S., and Aebersold, R. (2003). Abundance ratio-dependent proteomic analysis by mass spectrometry. Analytical chemistry *75*, 867-874.

Grou, C.P., Pinto, M.P., Mendes, A.V., Domingues, P., and Azevedo, J.E. (2015). The de novo synthesis of ubiquitin: identification of deubiquitinases acting on ubiquitin precursors. Scientific reports *5*, 12836.

Hamazaki, J., Iemura, S., Natsume, T., Yashiroda, H., Tanaka, K., and Murata, S. (2006). A novel proteasome interacting protein recruits the deubiquitinating enzyme UCH37 to 26S proteasomes. Embo J *25*, 4524-4536.

Harris, D.R., Mims, A., and Bunz, F. (2012). Genetic disruption of USP9X sensitizes colorectal cancer cells to 5-fluorouracil. Cancer biology & therapy *13*, 1319-1324.

Heller, R.C., Kang, S., Lam, W.M., Chen, S., Chan, C.S., and Bell, S.P. (2011). Eukaryotic origin-dependent DNA replication in vitro reveals sequential action of DDK and S-CDK kinases. Cell *146*, 80-91.

Hirano, M., Rakwal, R., Shibato, J., Agrawal, G.K., Jwa, N.S., Iwahashi, H., and Masuo, Y. (2006). New protein extraction/solubilization protocol for gel-based proteomics of rat (female) whole brain and brain regions. Molecules and cells *22*, 119-125.

Homan, C.C., Kumar, R., Nguyen, L.S., Haan, E., Raymond, F.L., Abidi, F., Raynaud, M., Schwartz, C.E., Wood, S.A., Gecz, J., *et al.* (2014). Mutations in USP9X are associated with X-linked intellectual disability and disrupt neuronal cell migration and growth. American journal of human genetics *94*, 470-478.

Hutchins, A.P., Liu, S., Diez, D., and Miranda-Saavedra, D. (2013). The Repertoires of Ubiquitinating and Deubiquitinating Enzymes in Eukaryotic Genomes. Mol Biol Evol *30*, 1172-1187.

Izawa, N., Wu, W., Sato, K., Nishikawa, H., Kato, A., Boku, N., Itoh, F., and Ohta, T. (2011). HERC2 Interacts with Claspin and regulates DNA origin firing and replication fork progression. Cancer research *71*, 5621-5625.

Jackson, D.A., and Pombo, A. (1998). Replicon clusters are stable units of chromosome structure: evidence that nuclear organization contributes to the efficient activation and propagation of S phase in human cells. The Journal of cell biology *140*, 1285-1295.

Jeong, S.Y., Kumagai, A., Lee, J., and Dunphy, W.G. (2003). Phosphorylated claspin interacts with a phosphate-binding site in the kinase domain of Chk1 during ATR-mediated activation. The Journal of biological chemistry *278*, 46782-46788.

Jiang, L., He, L., and Fountoulakis, M. (2004). Comparison of protein precipitation methods for sample preparation prior to proteomic analysis. Journal of chromatography A *1023*, 317-320.

Jolly, L.A., Taylor, V., and Wood, S.A. (2009). USP9X enhances the polarity and self-renewal of embryonic stem cell-derived neural progenitors. Molecular biology of the cell *20*, 2015-2029.

Jones, R.M., and Petermann, E. (2012). Replication fork dynamics and the DNA damage response. The Biochemical journal *443*, 13-26.

Kaake, R.M., Wang, X., and Huang, L. (2010). Profiling of protein interaction networks of protein complexes using affinity purification and quantitative mass spectrometry. Molecular & cellular proteomics : MCP *9*, 1650-1665.

Karpel-Massler, G., Ba, M., Shu, C., Halatsch, M.E., Westhoff, M.A., Bruce, J.N., Canoll, P., and Siegelin, M.D. (2015a). TIC10/ONC201 synergizes with Bcl-2/Bcl-xL inhibition in glioblastoma by suppression of Mcl-1 and its binding partners in vitro and in vivo. Oncotarget.

Karpel-Massler, G., Shu, C., Chau, L., Banu, M., Halatsch, M.E., Westhoff, M.A., Ramirez, Y., Ross, A.H., Bruce, J.N., Canoll, P., *et al.* (2015b). Combined inhibition of Bcl-2/Bcl-xL and Usp9X/Bag3 overcomes apoptotic resistance in glioblastoma in vitro and in vivo. Oncotarget *6*, 14507-14521.

Kharitidi, D., Apaja, P.M., Manteghi, S., Suzuki, K., Malitskaya, E., Roldan, A., Gingras, M.C., Takagi, J., Lukacs, G.L., and Pause, A. (2015). Interplay of Endosomal pH and Ligand Occupancy in Integrin alpha5beta1 Ubiquitination, Endocytic Sorting, and Cell Migration. Cell reports.

Khoo, K.H., Verma, C.S., and Lane, D.P. (2014). Drugging the p53 pathway: understanding the route to clinical efficacy. Nature reviews Drug discovery *13*, 217-236.

Khoronenkova, S.V., Dianova, II, Parsons, J.L., and Dianov, G.L. (2011). USP7/HAUSP stimulates repair of oxidative DNA lesions. Nucleic acids research *39*, 2604-2609.

Khut, P.Y., Tucker, B., Lardelli, M., and Wood, S.A. (2007). Evolutionary and expression analysis of the zebrafish deubiquitylating enzyme, usp9. Zebrafish *4*, 95-101.

Kim, J.M., Kakusho, N., Yamada, M., Kanoh, Y., Takemoto, N., and Masai, H. (2008). Cdc7 kinase mediates Claspin phosphorylation in DNA replication checkpoint. Oncogene *27*, 3475-3482.

Kireeva, N., Lakonishok, M., Kireev, I., Hirano, T., and Belmont, A.S. (2004). Visualization of early chromosome condensation: a hierarchical folding, axial glue model of chromosome structure. The Journal of cell biology *166*, 775-785.

Komander, D., Clague, M.J., and Urbe, S. (2009). Breaking the chains: structure and function of the deubiquitinases. Nature reviews Molecular cell biology *10*, 550-563.

Kudo, N., Wolff, B., Sekimoto, T., Schreiner, E.P., Yoneda, Y., Yanagida, M., Horinouchi, S., and Yoshida, M. (1998). Leptomycin B inhibition of signal-mediated nuclear export by direct binding to CRM1. Experimental cell research *242*, 540-547.

Kuhn, A.N., Beibetaert, T., Simon, P., Vallazza, B., Buck, J., Davies, B.P., Tureci, O., and Sahin, U. (2012). mRNA as a versatile tool for exogenous protein expression. Current gene therapy *12*, 347-361.

Kumagai, A., and Dunphy, W.G. (2000). Claspin, a novel protein required for the activation of Chk1 during a DNA replication checkpoint response in Xenopus egg extracts. Molecular cell *6*, 839-849.

Kumagai, A., and Dunphy, W.G. (2003). Repeated phosphopeptide motifs in Claspin mediate the regulated binding of Chk1. Nature cell biology *5*, 161-165.

Kumagai, A., Kim, S.M., and Dunphy, W.G. (2004). Claspin and the activated form of ATR-ATRIP collaborate in the activation of Chk1. The Journal of biological chemistry *279*, 49599-49608.

Laemmli, U.K. (1970). Cleavage of structural proteins during the assembly of the head of bacteriophage T4. Nature *227*, 680-685.

Lallemand-Breitenbach, V., and de The, H. (2010). PML nuclear bodies. Cold Spring Harbor perspectives in biology *2*, a000661.

Langston, L.D., Indiani, C., and O'Donnell, M. (2009). Whither the replisome: emerging perspectives on the dynamic nature of the DNA replication machinery. Cell Cycle *8*, 2686-2691.

Lee, J., Kumagai, A., and Dunphy, W.G. (2003a). Claspin, a Chk1-regulatory protein, monitors DNA replication on chromatin independently of RPA, ATR, and Rad17. Molecular cell *11*, 329-340.

Lee, K.H., Song, G.J., Kang, I.S., Kim, S.W., Paick, J.S., Chung, C.H., and Rhee, K. (2003b). Ubiquitin-specific protease activity of USP9Y, a male infertility gene on the Y chromosome. Reproduction, fertility, and development *15*, 129-133.

Leung-Pineda, V., Ryan, C.E., and Piwnica-Worms, H. (2006). Phosphorylation of Chk1 by ATR is antagonized by a Chk1-regulated protein phosphatase 2A circuit. Molecular and cellular biology *26*, 7529-7538.

Lindsey-Boltz, L.A., Sercin, O., Choi, J.H., and Sancar, A. (2009). Reconstitution of human claspin-mediated phosphorylation of Chk1 by the ATR (ataxia telangiectasia-mutated and rad3-related) checkpoint kinase. The Journal of biological chemistry *284*, 33107-33114.

Liu, H., Chen, W., Liang, C., Chen, B.W., Zhi, X., Zhang, S., Zheng, X., Bai, X., and Liang, T. (2015). WP1130 increases doxorubicin sensitivity in hepatocellular carcinoma cells through usp9x-dependent p53 degradation. Cancer letters *361*, 218-225.

Liu, J., Chung, H.J., Vogt, M., Jin, Y., Malide, D., He, L., Dundr, M., and Levens, D. (2011). JTV1 co-activates FBP to induce USP29 transcription and stabilize p53 in response to oxidative stress. Embo J *30*, 846-858.

Liu, S., Bekker-Jensen, S., Mailand, N., Lukas, C., Bartek, J., and Lukas, J. (2006). Claspin operates downstream of TopBP1 to direct ATR signaling towards Chk1 activation. Molecular and cellular biology *26*, 6056-6064.

Liu, S., Song, N., and Zou, L. (2012). The conserved C terminus of Claspin interacts with Rad9 and promotes rapid activation of Chk1. Cell Cycle *11*, 2711-2716.

Longo, P.A., Kavran, J.M., Kim, M.S., and Leahy, D.J. (2013). Transient mammalian cell transfection with polyethylenimine (PEI). Methods in enzymology *529*, 227-240.

Lu, X., Nannenga, B., and Donehower, L.A. (2005). PPM1D dephosphorylates Chk1 and p53 and abrogates cell cycle checkpoints. Genes & development *19*, 1162-1174.

Luo, D., and Saltzman, W.M. (2000). Synthetic DNA delivery systems. Nature biotechnology *18*, 33-37.

Macheret, M., and Halazonetis, T.D. (2015). DNA replication stress as a hallmark of cancer. Annual review of pathology *10*, 425-448.

Mah, L.J., El-Osta, A., and Karagiannis, T.C. (2010). gammaH2AX: a sensitive molecular marker of DNA damage and repair. Leukemia *24*, 679-686.

Mailand, N., Bekker-Jensen, S., Bartek, J., and Lukas, J. (2006). Destruction of Claspin by SCFbetaTrCP restrains Chk1 activation and facilitates recovery from genotoxic stress. Molecular cell *23*, 307-318.

Mamely, I., van Vugt, M.A., Smits, V.A., Semple, J.I., Lemmens, B., Perrakis, A., Medema, R.H., and Freire, R. (2006). Polo-like kinase-1 controls proteasome-dependent degradation of Claspin during checkpoint recovery. Current biology : CB *16*, 1950-1955.

Mann, M., Hendrickson, R.C., and Pandey, A. (2001). Analysis of proteins and proteomes by mass spectrometry. Annual review of biochemistry *70*, 437-473.

Manza, L.L., Stamer, S.L., Ham, A.J., Codreanu, S.G., and Liebler, D.C. (2005). Sample preparation and digestion for proteomic analyses using spin filters. Proteomics *5*, 1742-1745.

Marechal, A., and Zou, L. (2013). DNA damage sensing by the ATM and ATR kinases. Cold Spring Harbor perspectives in biology *5*.

Marheineke, K., Hyrien, O., and Krude, T. (2005). Visualization of bidirectional initiation of chromosomal DNA replication in a human cell free system. Nucleic acids research *33*, 6931-6941.

Marini, F., Pellicioli, A., Paciotti, V., Lucchini, G., Plevani, P., Stern, D.F., and Foiani, M. (1997). A role for DNA primase in coupling DNA replication to DNA damage response. Embo J *16*, 639-650.

Martin, Y., Cabrera, E., Amoedo, H., Hernandez-Perez, S., Dominguez-Kelly, R., and Freire, R. (2015). USP29 controls the stability of checkpoint adaptor Claspin by deubiquitination. Oncogene *34*, 1058-1063.

Matsuoka, S., Ballif, B.A., Smogorzewska, A., McDonald, E.R., 3rd, Hurov, K.E., Luo, J., Bakalarski, C.E., Zhao, Z., Solimini, N., Lerenthal, Y., *et al.* (2007). ATM and ATR substrate analysis reveals extensive protein networks responsive to DNA damage. Science *316*, 1160-1166.

Maxfield, F.R. (2014). Role of endosomes and lysosomes in human disease. Cold Spring Harbor perspectives in biology *6*, a016931.

McClurg, U.L., and Robson, C.N. (2015). Deubiquitinating enzymes as oncotargets. Oncotarget *6*, 9657-9668.

McMurray, C.T. (2010). Mechanisms of trinucleotide repeat instability during human development. Nature reviews Genetics *11*, 786-799.

Mechali, M. (2010). Eukaryotic DNA replication origins: many choices for appropriate answers. Nature reviews Molecular cell biology *11*, 728-738.

Mellacheruvu, D., Wright, Z., Couzens, A.L., Lambert, J.P., St-Denis, N.A., Li, T., Miteva, Y.V., Hauri, S., Sardiu, M.E., Low, T.Y., *et al.* (2013). The CRAPome: a contaminant repository for affinity purification-mass spectrometry data. Nature methods *10*, 730-736.

Meng, Z., Capalbo, L., Glover, D.M., and Dunphy, W.G. (2011). Role for casein kinase 1 in the phosphorylation of Claspin on critical residues necessary for the activation of Chk1. Molecular biology of the cell *22*, 2834-2847.

Merrell, K., Southwick, K., Graves, S.W., Esplin, M.S., Lewis, N.E., and Thulin, C.D. (2004). Analysis of low-abundance, low-molecular-weight serum proteins using mass spectrometry. Journal of biomolecular techniques : JBT *15*, 238-248.

Merrick, C.J., Jackson, D., and Diffley, J.F. (2004). Visualization of altered replication dynamics after DNA damage in human cells. The Journal of biological chemistry *279*, 20067-20075.

Mi, H., Muruganujan, A., and Thomas, P.D. (2013). PANTHER in 2013: modeling the evolution of gene function, and other gene attributes, in the context of phylogenetic trees. Nucleic acids research *41*, D377-386.

Mojsa, B., Lassot, I., and Desagher, S. (2014). Mcl-1 ubiquitination: unique regulation of an essential survival protein. Cells *3*, 418-437.

Montagnoli, A., Valsasina, B., Brotherton, D., Troiani, S., Rainoldi, S., Tenca, P., Molinari, A., and Santocanale, C. (2006). Identification of Mcm2 phosphorylation sites by S-phase-regulating kinases. The Journal of biological chemistry *281*, 10281-10290.

Montagnoli, A., Valsasina, B., Croci, V., Menichincheri, M., Rainoldi, S., Marchesi, V., Tibolla, M., Tenca, P., Brotherton, D., Albanese, C., *et al.* (2008). A Cdc7 kinase inhibitor restricts initiation of DNA replication and has antitumor activity. Nature chemical biology *4*, 357-365.

Mouchantaf, R., Azakir, B.A., McPherson, P.S., Millard, S.M., Wood, S.A., and Angers, A. (2006). The ubiquitin ligase itch is auto-ubiquitylated in vivo and in vitro but is protected from degradation by interacting with the deubiquitylating enzyme FAM/USP9X. Journal of Biological Chemistry *281*, 38738-38747.

Murtaza, M., Jolly, L.A., Gecz, J., and Wood, S.A. (2015). La FAM fatale: USP9X in development and disease. Cellular and molecular life sciences : CMLS *72*, 2075-2089.

Nagai, H., Noguchi, T., Homma, K., Katagiri, K., Takeda, K., Matsuzawa, A., and Ichijo, H. (2009). Ubiquitin-like sequence in ASK1 plays critical roles in the recognition and stabilization by USP9X and oxidative stress-induced cell death. Molecular cell *36*, 805-818.

Nakamura, K., Tanaka, T., Kuwahara, A., and Takeo, K. (1985). Microassay for proteins on nitrocellulose filter using protein dye-staining procedure. Analytical biochemistry *148*, 311-319.

Nemudryi, A.A., Valetdinova, K.R., Medvedev, S.P., and Zakian, S.M. (2014). TALEN and CRISPR/Cas Genome Editing Systems: Tools of Discovery. Acta naturae *6*, 19-40.

Nijman, S.M., Luna-Vargas, M.P., Velds, A., Brummelkamp, T.R., Dirac, A.M., Sixma, T.K., and Bernards, R. (2005). A genomic and functional inventory of deubiquitinating enzymes. Cell *123*, 773-786.

Nishi, R., Wijnhoven, P., le Sage, C., Tjeertes, J., Galanty, Y., Forment, J.V., Clague, M.J., Urbe, S., and Jackson, S.P. (2014). Systematic characterization of deubiquitylating enzymes for roles in maintaining genome integrity. Nature cell biology *16*, 1016-1026, 1011-1018.

O'Shea, J.J., Schwartz, D.M., Villarino, A.V., Gadina, M., McInnes, I.B., and Laurence, A. (2015). The JAK-STAT pathway: impact on human disease and therapeutic intervention. Annual review of medicine *66*, 311-328.

Ogi, T., Walker, S., Stiff, T., Hobson, E., Limsirichaikul, S., Carpenter, G., Prescott, K., Suri, M., Byrd, P.J., Matsuse, M., *et al.* (2012). Identification of the first ATRIP-deficient patient and novel mutations in ATR define a clinical spectrum for ATR-ATRIP Seckel Syndrome. Plos Genet *8*, e1002945.

Okazaki, R., Okazaki, T., Sakabe, K., and Sugimoto, K. (1967). Mechanism of DNA replication possible discontinuity of DNA chain growth. Japanese journal of medical science & biology *20*, 255-260.

Ong, S.E., Blagoev, B., Kratchmarova, I., Kristensen, D.B., Steen, H., Pandey, A., and Mann, M. (2002). Stable isotope labeling by amino acids in cell culture, SILAC, as a simple and accurate approach to expression proteomics. Molecular & cellular proteomics : MCP *1*, 376-386.

Ong, S.E., and Mann, M. (2005). Mass spectrometry-based proteomics turns quantitative. Nature chemical biology *1*, 252-262.

Oosterkamp, H.M., Hijmans, E.M., Brummelkamp, T.R., Canisius, S., Wessels, L.F., Zwart, W., and Bernards, R. (2014). USP9X downregulation renders breast cancer cells resistant to tamoxifen. Cancer research *74*, 3810-3820.

Osborn, A.J., and Elledge, S.J. (2003). Mrc1 is a replication fork component whose phosphorylation in response to DNA replication stress activates Rad53. Genes & development *17*, 1755-1767.

Paemka, L., Mahajan, V.B., Ehaideb, S.N., Skeie, J.M., Tan, M.C., Wu, S., Cox, A.J., Sowers, L.P., Gecz, J., Jolly, L., *et al.* (2015). Seizures are regulated by ubiquitin-specific peptidase 9 X-linked (USP9X), a de-ubiquitinase. Plos Genet *11*, e1005022.

Panier, S., and Boulton, S.J. (2014). Double-strand break repair: 53BP1 comes into focus. Nature reviews Molecular cell biology *15*, 7-18.

Pearl, L.H., Schierz, A.C., Ward, S.E., Al-Lazikani, B., and Pearl, F.M. (2015). Therapeutic opportunities within the DNA damage response. Nature reviews Cancer *15*, 166-180.

Perez-Mancera, P.A., Rust, A.G., van der Weyden, L., Kristiansen, G., Li, A., Sarver, A.L., Silverstein, K.A., Grutzmann, R., Aust, D., Rummele, P., *et al.* (2012). The deubiquitinase USP9X suppresses pancreatic ductal adenocarcinoma. Nature *486*, 266-270.

Peschiaroli, A., Dorrello, N.V., Guardavaccaro, D., Venere, M., Halazonetis, T., Sherman, N.E., and Pagano, M. (2006). SCFbetaTrCP-mediated degradation of Claspin regulates recovery from the DNA replication checkpoint response. Molecular cell *23*, 319-329.

Petermann, E., Helleday, T., and Caldecott, K.W. (2008). Claspin promotes normal replication fork rates in human cells. Molecular biology of the cell *19*, 2373-2378.

Petermann, E., Maya-Mendoza, A., Zachos, G., Gillespie, D.A., Jackson, D.A., and Caldecott, K.W. (2006). Chk1 requirement for high global rates of replication fork progression during normal vertebrate S phase. Molecular and cellular biology *26*, 3319-3326.

Petermann, E., Orta, M.L., Issaeva, N., Schultz, N., and Helleday, T. (2010). Hydroxyurea-stalled replication forks become progressively inactivated and require two different RAD51-mediated pathways for restart and repair. Molecular cell *37*, 492-502.

Peterson, L.F., Sun, H., Liu, Y., Potu, H., Kandarpa, M., Ermann, M., Courtney, S.M., Young, M., Showalter, H.D., Sun, D., *et al.* (2015). Targeting deubiquitinase activity with a novel small-molecule inhibitor as therapy for B-cell malignancies. Blood *125*, 3588-3597.

Polo, S.E., and Jackson, S.P. (2011). Dynamics of DNA damage response proteins at DNA breaks: a focus on protein modifications. Genes & development *25*, 409-433.

Potenski, C.J., and Klein, H.L. (2014). How the misincorporation of ribonucleotides into genomic DNA can be both harmful and helpful to cells. Nucleic acids research *42*, 10226-10234.

Potu, H., Peterson, L.F., Pal, A., Verhaegen, M., Cao, J., Talpaz, M., and Donato, N.J. (2014). Usp5 links suppression of p53 and FAS levels in melanoma to the BRAF pathway. Oncotarget *5*, 5559-5569.

Pursell, Z.F., Isoz, I., Lundstrom, E.B., Johansson, E., and Kunkel, T.A. (2007). Yeast DNA polymerase epsilon participates in leading-strand DNA replication. Science *317*, 127-130.

Rainey, M.D., Harhen, B., Wang, G.N., Murphy, P.V., and Santocanale, C. (2013). Cdc7-dependent and -independent phosphorylation of Claspin in the induction of the DNA replication checkpoint. Cell Cycle *12*, 1560-1568.

Rebecca, V.W., and Amaravadi, R.K. (2015). Emerging strategies to effectively target autophagy in cancer. Oncogene.

Renard-Guillet, C., Kanoh, Y., Shirahige, K., and Masai, H. (2014). Temporal and spatial regulation of eukaryotic DNA replication: from regulated initiation to genome-scale timing program. Seminars in cell & developmental biology *30*, 110-120.

Restuccia, U., Boschetti, E., Fasoli, E., Fortis, F., Guerrier, L., Bachi, A., Kravchuk, A.V., and Righetti, P.G. (2009). pI-based fractionation of serum proteomes versus anion exchange after enhancement of low-abundance proteins by means of peptide libraries. Journal of proteomics *72*, 1061-1070.

Rott, R., Szargel, R., Haskin, J., Bandopadhyay, R., Lees, A.J., Shani, V., and Engelender, S. (2011). alpha-Synuclein fate is determined by USP9X-regulated monoubiquitination. Proceedings of the National Academy of Sciences of the United States of America *108*, 18666-18671.

Sahtoe, D.D., and Sixma, T.K. (2015). Layers of DUB regulation. Trends Biochem Sci *40*, 456-467.

Sanchez, Y., Wong, C., Thoma, R.S., Richman, R., Wu, Z., Piwnica-Worms, H., and Elledge, S.J. (1997). Conservation of the Chk1 checkpoint pathway in mammals: linkage of DNA damage to Cdk regulation through Cdc25. Science *277*, 1497-1501.

Sar, F., Lindsey-Boltz, L.A., Subramanian, D., Croteau, D.L., Hutsell, S.Q., Griffith, J.D., and Sancar, A. (2004). Human claspin is a ring-shaped DNA-binding protein with high affinity to branched DNA structures. The Journal of biological chemistry *279*, 39289-39295.

Sato, K., Sundaramoorthy, E., Rajendra, E., Hattori, H., Jeyasekharan, A.D., Ayoub, N., Schiess, R., Aebersold, R., Nishikawa, H., Sedukhina, A.S., *et al.* (2012). A DNA-damage selective role for BRCA1 E3 ligase in claspin ubiquitylation, CHK1 activation, and DNA repair. Current biology : CB *22*, 1659-1666.

Schwickart, M., Huang, X., Lill, J.R., Liu, J., Ferrando, R., French, D.M., Maecker, H., O'Rourke, K., Bazan, F., Eastham-Anderson, J., *et al.* (2010). Deubiquitinase USP9X stabilizes MCL1 and promotes tumour cell survival. Nature *463*, 103-107.

Scorah, J., and McGowan, C.H. (2009). Claspin and Chk1 regulate replication fork stability by different mechanisms. Cell Cycle *8*, 1036-1043.

Semple, J.I., Smits, V.A., Fernaud, J.R., Mamely, I., and Freire, R. (2007). Cleavage and degradation of Claspin during apoptosis by caspases and the proteasome. Cell death and differentiation *14*, 1433-1442.

Shenoy, N. (2015). Is ADRM1 a Good Target for Cancer Therapy? Acta haematologica *134*, 86-87.

Sherstyuk, V.V., Shevchenko, A.I., and Zakian, S.M. (2014). Epigenetic landscape for initiation of DNA replication. Chromosoma *123*, 183-199.

Siddiqui, K., On, K.F., and Diffley, J.F. (2013). Regulating DNA replication in eukarya. Cold Spring Harbor perspectives in biology *5*.

Silkworth, W.T., Nardi, I.K., Scholl, L.M., and Cimini, D. (2009). Multipolar spindle pole coalescence is a major source of kinetochore mis-attachment and chromosome mis-segregation in cancer cells. PloS one *4*, e6564.

Smith, D.J., and Whitehouse, I. (2012). Intrinsic coupling of lagging-strand synthesis to chromatin assembly. Nature *483*, 434-438.

Sowa, M.E., Bennett, E.J., Gygi, S.P., and Harper, J.W. (2009). Defining the human deubiquitinating enzyme interaction landscape. Cell *138*, 389-403.

Stark, G.R., and Darnell, J.E., Jr. (2012). The JAK-STAT pathway at twenty. Immunity *36*, 503-514.

Stegeman, S., Jolly, L.A., Premarathne, S., Gecz, J., Richards, L.J., Mackay-Sim, A., and Wood, S.A. (2013). Loss of Usp9x disrupts cortical architecture, hippocampal development and TGFbeta-mediated axonogenesis. PloS one *8*, e68287.

Stiff, T., Walker, S.A., Cerosaletti, K., Goodarzi, A.A., Petermann, E., Concannon, P., O'Driscoll, M., and Jeggo, P.A. (2006). ATR-dependent phosphorylation and activation of ATM in response to UV treatment or replication fork stalling. Embo J *25*, 5775-5782.

Sun, J., Fernandez-Cid, A., Riera, A., Tognetti, S., Yuan, Z., Stillman, B., Speck, C., and Li, H. (2014). Structural and mechanistic insights into Mcm2-7 double-hexamer assembly and function. Genes & development *28*, 2291-2303.

Sun, J., Shi, Y., Georgescu, R.E., Yuan, Z., Chait, B.T., Li, H., and O'Donnell, M.E. (2015). The architecture of a eukaryotic replisome. Nature structural & molecular biology.

Tanaka, K. (2010). Multiple functions of the S-phase checkpoint mediator. Bioscience, biotechnology, and biochemistry *74*, 2367-2373.

Tanaka, K., and Russell, P. (2001). Mrc1 channels the DNA replication arrest signal to checkpoint kinase Cds1. Nature cell biology *3*, 966-972.

Tao, H., Manak, J.R., Sowers, L., Mei, X., Kiyonari, H., Abe, T., Dahdaleh, N.S., Yang, T., Wu, S., Chen, S., *et al.* (2011). Mutations in prickle orthologs cause seizures in flies, mice, and humans. American journal of human genetics *88*, 138-149.

Tarsounas, M., Davies, D., and West, S.C. (2003). BRCA2-dependent and independent formation of RAD51 nuclear foci. Oncogene *22*, 1115-1123.

Taylor, R.C., Cullen, S.P., and Martin, S.J. (2008). Apoptosis: controlled demolition at the cellular level. Nature reviews Molecular cell biology *9*, 231-241.

Theard, D., Labarrade, F., Partisani, M., Milanini, J., Sakagami, H., Fon, E.A., Wood, S.A., Franco, M., and Luton, F. (2010). USP9x-mediated deubiquitination of EFA6 regulates de novo tight junction assembly. Embo J *29*, 1499-1509.

Thornalley, P.J., and Rabbani, N. (2014). Detection of oxidized and glycated proteins in clinical samples using mass spectrometry--a user's perspective. Biochimica et biophysica acta *1840*, 818-829.

Tkach, J.M., Yimit, A., Lee, A.Y., Riffle, M., Costanzo, M., Jaschob, D., Hendry, J.A., Ou, J., Moffat, J., Boone, C., *et al.* (2012). Dissecting DNA damage response pathways by analysing protein localization and abundance changes during DNA replication stress. Nature cell biology *14*, 966-976.

Trenz, K., Smith, E., Smith, S., and Costanzo, V. (2006). ATM and ATR promote Mre11 dependent restart of collapsed replication forks and prevent accumulation of DNA breaks. Embo J *25*, 1764-1774.

Trinkle-Mulcahy, L., Boulon, S., Lam, Y.W., Urcia, R., Boisvert, F.M., Vandermoere, F., Morrice, N.A., Swift, S., Rothbauer, U., Leonhardt, H., *et al.* (2008). Identifying specific protein interaction partners using quantitative mass spectrometry and bead proteomes. Journal of Cell Biology *183*, 223-239.

Uno, S., and Masai, H. (2011). Efficient expression and purification of human replication fork-stabilizing factor, Claspin, from mammalian cells: DNA-binding activity and novel protein interactions. Genes to cells : devoted to molecular & cellular mechanisms *16*, 842-856.

Urbe, S., Liu, H., Hayes, S.D., Heride, C., Rigden, D.J., and Clague, M.J. (2012). Systematic survey of deubiquitinase localization identifies USP21 as a regulator of centrosome- and microtubule-associated functions. Molecular biology of the cell *23*, 1095-1103.

Vellucci, D., Kao, A., Kaake, R.M., Rychnovsky, S.D., and Huang, L. (2010). Selective enrichment and identification of azide-tagged cross-linked peptides using chemical ligation and mass spectrometry. Journal of the American Society for Mass Spectrometry *21*, 1432-1445.

Vermeulen, M., Hubner, N.C., and Mann, M. (2008). High confidence determination of specific protein-protein interactions using quantitative mass spectrometry. Current opinion in biotechnology *19*, 331-337.

Vieweg, M., Dvorakova-Hortova, K., Dudkova, B., Waliszewski, P., Otte, M., Oels, B., Hajimohammad, A., Turley, H., Schorsch, M., Schuppe, H.C., *et al.* (2015). Methylation analysis of histone H4K12ac-associated promoters in sperm of healthy donors and subfertile patients. Clinical epigenetics *7*, 31.

Vong, Q.P., Cao, K., Li, H.Y., Iglesias, P.A., and Zheng, Y.X. (2005). Chromosome alignment and segregation regulated by ubiquitination of survivin. Science *310*, 1499-1504.

Vucic, D., Dixit, V.M., and Wertz, I.E. (2011). Ubiquitylation in apoptosis: a post-translational modification at the edge of life and death. Nature reviews Molecular cell biology *12*, 439-452.

Walker, M., Black, E.J., Oehler, V., Gillespie, D.A., and Scott, M.T. (2009). Chk1 C-terminal regulatory phosphorylation mediates checkpoint activation by de-repression of Chk1 catalytic activity. Oncogene *28*, 2314-2323.

Walworth, N., Davey, S., and Beach, D. (1993). Fission yeast chk1 protein kinase links the rad checkpoint pathway to cdc2. Nature *363*, 368-371.

Walworth, N.C., and Bernards, R. (1996). rad-dependent response of the chk1-encoded protein kinase at the DNA damage checkpoint. Science *271*, 353-356.

Wang, H., Zhang, X., Teng, L., and Legerski, R.J. (2015a). DNA damage checkpoint recovery and cancer development. Experimental cell research *334*, 350-358.

Wang, M., Herrmann, C.J., Simonovic, M., Szklarczyk, D., and von Mering, C. (2015b). Version 4.0 of PaxDb: Protein abundance data, integrated across model organisms, tissues, and cell-lines. Proteomics *15*, 3163-3168.

Wang, X., and Huang, L. (2008). Identifying dynamic interactors of protein complexes by quantitative mass spectrometry. Molecular & cellular proteomics : MCP *7*, 46-57.

Wang, X., and Huang, L. (2014). Defining dynamic protein interactions using SILAC-based quantitative mass spectrometry. Methods Mol Biol *1188*, 191-205.

Wang, Y., Liu, Y., Yang, B., Cao, H., Yang, C.X., Ouyang, W., Zhang, S.M., Yang, G.F., Zhou, F.X., Zhou, Y.F., *et al.* (2015c). Elevated expression of USP9X correlates with poor prognosis in human non-small cell lung cancer. Journal of thoracic disease *7*, 672-679.

Ward, R.J., Alvarez-Curto, E., and Milligan, G. (2011). Using the Flp-In T-Rex system to regulate GPCR expression. Methods Mol Biol *746*, 21-37.

Whitehead, K.A., Langer, R., and Anderson, D.G. (2009). Knocking down barriers: advances in siRNA delivery. Nature reviews Drug discovery *8*, 129-138.

Williams, J.S., Smith, D.J., Marjavaara, L., Lujan, S.A., Chabes, A., and Kunkel, T.A. (2013). Topoisomerase 1-mediated removal of ribonucleotides from nascent leading-strand DNA. Molecular cell *49*, 1010-1015.

Wing, J.P., Schreader, B.A., Yokokura, T., Wang, Y., Andrews, P.S., Huseinovic, N., Dong, C.K., Ogdahl, J.L., Schwartz, L.M., White, K., *et al.* (2002). Drosophila Morgue is an F box/ubiquitin conjugase domain protein important for grim-reaper mediated apoptosis. Nature cell biology *4*, 451-456.

Wood, S.A., Pascoe, W.S., Ru, K., Yamada, T., Hirchenhain, J., Kemler, R., and Mattick, J.S. (1997). Cloning and expression analysis of a novel mouse gene with sequence similarity to the Drosophila fat facets gene. Mechanisms of development *63*, 29-38.

Wu, W., Sato, K., Koike, A., Nishikawa, H., Koizumi, H., Venkitaraman, A.R., and Ohta, T. (2010). HERC2 is an E3 ligase that targets BRCA1 for degradation. Cancer research *70*, 6384-6392.

Xie, Y., Avello, M., Schirle, M., McWhinnie, E., Feng, Y., Bric-Furlong, E., Wilson, C., Nathans, R., Zhang, J., Kirschner, M.W., *et al.* (2013). Deubiquitinase FAM/USP9X interacts with the E3 ubiquitin ligase SMURF1 protein and protects it from ligase activity-dependent self-degradation. The Journal of biological chemistry *288*, 2976-2985.

Yamazaki, S., Hayano, M., and Masai, H. (2013). Replication timing regulation of eukaryotic replicons: Rif1 as a global regulator of replication timing. Trends in genetics : TIG *29*, 449-460.

Yao, N.Y., Georgescu, R.E., Finkelstein, J., and O'Donnell, M.E. (2009). Single-molecule analysis reveals that the lagging strand increases replisome processivity but slows replication fork progression. Proceedings of the National Academy of Sciences of the United States of America *106*, 13236-13241.

Yao, N.Y., and O'Donnell, M. (2009). Replisome structure and conformational dynamics underlie fork progression past obstacles. Current opinion in cell biology *21*, 336-343.

Yao, T., Song, L., Xu, W., DeMartino, G.N., Florens, L., Swanson, S.K., Washburn, M.P., Conaway, R.C., Conaway, J.W., and Cohen, R.E. (2006). Proteasome recruitment and activation of the Uch37 deubiquitinating enzyme by Adrm1. Nature cell biology *8*, 994-1002.

Yekezare, M., Gomez-Gonzalez, B., and Diffley, J.F. (2013). Controlling DNA replication origins in response to DNA damage - inhibit globally, activate locally. Journal of cell science *126*, 1297-1306.

Yu, H., Lim, H.H., Tjokro, N.O., Sathiyanathan, P., Natarajan, S., Chew, T.W., Klonisch, T., Goodman, S.D., Surana, U., and Droge, P. (2014). Chaperoning HMGA2 protein protects stalled replication forks in stem and cancer cells. Cell reports *6*, 684-697.

Yuan, J., Luo, K., Deng, M., Li, Y., Yin, P., Gao, B., Fang, Y., Wu, P., Liu, T., and Lou, Z. (2014). HERC2-USP20 axis regulates DNA damage checkpoint through Claspin. Nucleic acids research *42*, 13110-13121.

Zeman, M.K., and Cimprich, K.A. (2014). Causes and consequences of replication stress. Nature cell biology *16*, 2-9.

Zhang, D., Zaugg, K., Mak, T.W., and Elledge, S.J. (2006). A role for the deubiquitinating enzyme USP28 in control of the DNA-damage response. Cell *126*, 529-542.

Zhang, Y., and Hunter, T. (2014). Roles of Chk1 in cell biology and cancer therapy. International journal of cancer Journal international du cancer *134*, 1013-1023.

Zhang, Z., Yang, H., and Wang, H. (2014). The histone H2A deubiquitinase USP16 interacts with HERC2 and fine-tunes cellular response to DNA damage. The Journal of biological chemistry *289*, 32883-32894.

Zhou, M., Wang, T., Lai, H., Zhao, X., Yu, Q., Zhou, J., and Yang, Y. (2015). Targeting of the deubiquitinase USP9X attenuates B-cell acute lymphoblastic leukemia cell survival and overcomes glucocorticoid resistance. Biochemical and biophysical research communications *459*, 333-339.

Zhu, M., Zhao, H., Liao, J., and Xu, X. (2014). HERC2/USP20 coordinates CHK1 activation by modulating CLASPIN stability. Nucleic acids research *42*, 13074-13081.

APPENDIX I

List of putative Claspin interacting proteins identified by MAP-SILAC mass spectrometry analysis. Column 1 contains the Uniprot accession code, column 2 the gene name, column 3 the protein name and column 4 the SILAC ratio expressed as the Log2 SILAC ratio of empty vector/Claspin. The data is listed by SILAC ratio from smallest to largest, with the most negative SILAC ratio representing the most enriched protein compared to the control. Proteins displaying a < 3 fold enrichment in SILAC ratios (< -1.5) are displayed in italics, were eliminated from further analysis.

Protein ID	Gene Name	Protein name	SILAC ratio Log2 (EV/CLSPN)
Q9HAW4	CLSPN	Claspin	-5.82
P15924	DESP	Desmoplakin	-5.00
Q92598	HS105	Heat shock protein 105 kDa	-3.92
Q9UGI8	TES	Testin	-3.35
O95433	AHSA1	Activator of 90 kDa heat shock protein ATPase homolog 1	-3.19
Q04637	IF4G1	Eukaryotic translation initiation factor 4 gamma 1	-3.18
P49588	SYAC	Alanine--tRNA ligase, cytoplasmic	-3.07
Q96AE4	FUBP1	Far upstream element-binding protein 1	-2.93
P58107	EPIPL	Epiplakin	-2.90
Q9UBE0	SAE1	SUMO-activating enzyme subunit 1	-2.90
P63151	2ABA	Serine/threonine-protein phosphatase 2A 55 kDa regulatory subunit B alpha isoform	-2.90
O75534	CSDE1	Cold shock domain-containing protein E1	-2.89
Q93008	USP9X	Probable ubiquitin carboxyl-terminal hydrolase FAF-X	-2.84
Q9Y490	TLN1	Talin-1	-2.82
P25205	MCM3	DNA replication licensing factor MCM3	-2.81
P53041	PPP5	Serine/threonine-protein phosphatase 5	-2.80
Q00796	DHSO	Sorbitol dehydrogenase	-2.76
Q10567	AP1B1	AP-1 complex subunit beta-1	-2.76
Q13011	ECH1	Delta(3,5)-Delta(2,4)-dienoyl-CoA isomerase, mitochondrial	-2.75
P51858	HDGF	Hepatoma-derived growth factor	-2.74
P06737	PYGL	Glycogen phosphorylase, liver form	-2.74
Q9BXJ9	NAA15	N-alpha-acetyltransferase 15, NatA auxiliary subunit	-2.74
P11586	C1TC	C-1-tetrahydrofolate synthase, cytoplasmic	-2.73
P45974	USP5	Ubiquitin carboxyl-terminal hydrolase 5	-2.72

Q14566	MCM6	DNA replication licensing factor MCM6	-2.72
P49736	MCM2	DNA replication licensing factor MCM2	-2.71
O43491	E41L2	Band 4.1-like protein 2	-2.67
Q13263	TIF1B	Transcription intermediary factor 1-beta	-2.65
P38117	ETFB	Electron transfer flavoprotein subunit beta	-2.65
Q9UHD1	CHRD1	Cysteine and histidine-rich domain-containing protein 1	-2.64
Q6IN85	P4R3A	Serine/threonine-protein phosphatase 4 regulatory subunit 3A	-2.63
P17858	PFKAL	ATP-dependent 6-phosphofructokinase, liver type	-2.62
P09651	ROA1	Heterogeneous nuclear ribonucleoprotein A1	-2.60
O95757	HS74L	Heat shock 70 kDa protein 4L	-2.60
P62495	ERF1	Eukaryotic peptide chain release factor subunit 1	-2.60
P18206	VINC	Vinculin	-2.59
P46940	IQGA1	Ras GTPase-activating-like protein IQGAP1	-2.58
Q2VIR3	IF2GL	Putative eukaryotic translation initiation factor 2 subunit 3-like protein	-2.58
P50502	F10A1	Hsc70-interacting protein	-2.58
O00299	CLIC1	Chloride intracellular channel protein 1	-2.58
P62191	PRS4	26S protease regulatory subunit 4	-2.57
Q9Y266	NUDC	Nuclear migration protein nudC	-2.57
P14618	KPYM	Pyruvate kinase PKM	-2.57
Q9UBT2	SAE2	SUMO-activating enzyme subunit 2	-2.57
P30153	2AAA	Serine/threonine-protein phosphatase 2A 65 kDa regulatory subunit A alpha isoform	-2.56
P28482	MK01	Mitogen-activated protein kinase 1	-2.54
Q16543	CDC37	Hsp90 co-chaperone Cdc37	-2.54
P31948	STIP1	Stress-induced-phosphoprotein 1	-2.54
Q12931	TRAP1	Heat shock protein 75 kDa, mitochondrial	-2.53
P22314	UBA1	Ubiquitin-like modifier-activating enzyme 1	-2.53
Q01581	HMCS1	Hydroxymethylglutaryl-CoA synthase, cytoplasmic	-2.53

P49327	FAS	Fatty acid synthase	-2.52
P37837	TALDO	Transaldolase	-2.52
Q14697	GANAB	Neutral alpha-glucosidase AB	-2.52
Q14978	NOLC1	Nucleolar and coiled-body phosphoprotein 1	-2.51
P63244	GBLP	Guanine nucleotide-binding protein subunit beta-2-like 1	-2.50
P62987	RL40	Ubiquitin-60S ribosomal protein L40	-2.50
P22234	PUR6	Multifunctional protein ADE2	-2.50
Q99832	TCPH	T-complex protein 1 subunit eta	-2.49
P06744	G6PI	Glucose-6-phosphate isomerase	-2.49
Q15365	PCBP1	Poly(rC)-binding protein 1	-2.48
Q9Y617	SERC	Phosphoserine aminotransferase	-2.48
P30566	PUR8	Adenylosuccinate lyase	-2.47
Q99615	DNJC7	DnaJ homolog subfamily C member 7	-2.47
B4DJ98	B4DJ98	highly similar to Protein disulfide-isomerase A3	-2.47
P34932	HSP74	Heat shock 70 kDa protein 4	-2.47
Q15366	PCBP2	Poly(rC)-binding protein 2	-2.46
P12081	SYHC	Histidine--tRNA ligase, cytoplasmic	-2.46
P07900	HS90A	Heat shock protein HSP 90-alpha	-2.45
Q86VP6	CAND1	Cullin-associated NEDD8-dissociated protein 1	-2.45
P00558	PGK1	Phosphoglycerate kinase 1	-2.45
Q01518	CAP1	Adenylyl cyclase-associated protein 1	-2.45
P13639	EF2	Elongation factor 2	-2.44
O43175	SERA	D-3-phosphoglycerate dehydrogenase	-2.42
O60256	KPRB	Phosphoribosyl pyrophosphate synthase-associated protein 2	-2.42
P49321	NASP	Nuclear autoantigenic sperm protein	-2.41
Q8NC51	PAIRB	Plasminogen activator inhibitor 1 RNA-binding protein	-2.41
P04406	G3P	Glyceraldehyde-3-phosphate dehydrogenase	-2.41

P13667	PDIA4	Protein disulfide-isomerase A4	-2.40
Q13838	DX39B	Spliceosome RNA helicase DDX39B	-2.40
P63010	AP2B1	AP-2 complex subunit beta	-2.40
P34897	GLYM	Serine hydroxymethyltransferase, mitochondrial	-2.39
P30101	PDIA3	Protein disulfide-isomerase A3	-2.39
P15121	ALDR	Aldose reductase	-2.38
P11142	HSP7C	Heat shock cognate 71 kDa protein	-2.38
Q9BT78	CSN4	COP9 signalosome complex subunit 4	-2.38
P60842	IF4A1	Eukaryotic initiation factor 4A-I	-2.38
Q16181	SEPT7	Septin-7	-2.37
P07355	ANXA2	Annexin A2	-2.35
P78371	TCPB	T-complex protein 1 subunit beta	-2.35
Q92945	FUBP2	Far upstream element-binding protein 2	-2.35
P55060	XPO2	Exportin-2	-2.35
P48643	TCPE	T-complex protein 1 subunit epsilon	-2.35
P26640	SYVC	Valine--tRNA ligase	-2.34
P08238	HS90B	Heat shock protein HSP 90-beta	-2.34
O43684	BUB3	Mitotic checkpoint protein BUB3	-2.34
P35221	CTNA1	Catenin alpha-1	-2.33
P50995	ANX11	Annexin A11	-2.33
P08107	HSP71	Heat shock 70 kDa protein 1A/1B	-2.33
Q02790	FKBP4	Peptidyl-prolyl cis-trans isomerase FKBP4	-2.32
P26639	SYTC	Threonine--tRNA ligase, cytoplasmic	-2.31
Q5VTE0	EF1A3	Putative elongation factor 1-alpha-like 3	-2.31
P11413	G6PD	Glucose-6-phosphate 1-dehydrogenase	-2.31
Q13347	EIF3I	Eukaryotic translation initiation factor 3 subunit I	-2.31
P55809	SCOT1	Succinyl-CoA:3-ketoacid coenzyme A transferase 1, mitochondrial	-2.30

P25789	PSA4	Proteasome subunit alpha type-4	-2.30
P07437	TBB5	Tubulin beta chain	-2.30
Q13867	BLMH	Bleomycin hydrolase	-2.30
P06733	ENOA	Alpha-enolase	-2.30
P60228	EIF3E	Eukaryotic translation initiation factor 3 subunit E	-2.30
P55072	TERA	Transitional endoplasmic reticulum ATPase	-2.30
Q8WUM4	PDC6I	Programmed cell death 6-interacting protein	-2.30
P22626	ROA2	Heterogeneous nuclear ribonucleoproteins A2/B1	-2.30
P46821	MAP1B	Microtubule-associated protein 1B	-2.30
P29401	TKT	Transketolase	-2.30
O14744	ANM5	Protein arginine N-methyltransferase 5	-2.30
P25786	PSA1	Proteasome subunit alpha type-1	-2.30
P50990	TCPQ	T-complex protein 1 subunit theta	-2.29
P53396	ACLY	ATP-citrate synthase	-2.29
P17987	TCPA	T-complex protein 1 subunit alpha	-2.29
Q7Z6Z7	MULE	E3 ubiquitin-protein ligase MULE	-2.29
P49368	TCPG	T-complex protein 1 subunit gamma	-2.28
P31946	1433B	14-3-3 protein beta/alpha	-2.28
P33176	KINH	Kinesin-1 heavy chain	-2.28
Q8N1F7	NUP93	Nuclear pore complex protein Nup93	-2.28
Q9Y230	RUVB2	RuvB-like 2	-2.27
P49189	AL9A1	4-trimethylaminobutyraldehyde dehydrogenase	-2.27
P27348	1433T	14-3-3 protein theta	-2.26
P40227	TCPZ	T-complex protein 1 subunit zeta	-2.25
P08865	RSSA	40S ribosomal protein SA	-2.25
Q15084	PDIA6	Protein disulfide-isomerase A6	-2.25
P04075	ALDOA	Fructose-bisphosphate aldolase A	-2.24

P55036	PSMD4	26S proteasome non-ATPase regulatory subunit 4	-2.24
Q9Y2J2	E41L3	Band 4.1-like protein 3	-2.24
P23526	SAHH	Adenosylhomocysteinase	-2.24
P00505	AATM	Aspartate aminotransferase, mitochondrial	-2.24
P17174	AATC	Aspartate aminotransferase, cytoplasmic	-2.23
P54725	RD23A	UV excision repair protein RAD23 homolog A	-2.23
Q6YN16	HSDL2	Hydroxysteroid dehydrogenase-like protein 2	-2.23
P61981	1433G	14-3-3 protein gamma	-2.23
P09012	SNRPA	U1 small nuclear ribonucleoprotein A	-2.22
P50991	TCPD	T-complex protein 1 subunit delta	-2.22
P62258	1433E	14-3-3 protein epsilon	-2.22
P24752	THIL	Acetyl-CoA acetyltransferase, mitochondrial	-2.22
P05455	LA	Lupus La protein	-2.22
P49006	MRP	MARCKS-related protein	-2.21
P07195	LDHB	L-lactate dehydrogenase B chain	-2.21
O43707	ACTN4	Alpha-actinin-4	-2.20
P12268	IMDH2	Inosine-5'-monophosphate dehydrogenase 2	-2.20
O15294	OGT1	UDP-N-acetylglucosamine--peptide N-acetylglucosaminyltransferase 110 kDa subunit	-2.20
P52209	6PGD	6-phosphogluconate dehydrogenase, decarboxylating	-2.19
P55786	PSA	Puromycin-sensitive aminopeptidase	-2.19
P51649	SSDH	Succinate-semialdehyde dehydrogenase, mitochondrial	-2.18
Q08J23	NSUN2	tRNA (cytosine(34)-C(5))-methyltransferase	-2.18
P60174	TPIS	Triosephosphate isomerase	-2.18
P14866	HNRPL	Heterogeneous nuclear ribonucleoprotein L	-2.18
P50570	DYN2	Dynamin-2	-2.18
Q92841	DDX17	Probable ATP-dependent RNA helicase DDX17	-2.17
P30084	ECHM	Enoyl-CoA hydratase, mitochondrial	-2.17

P10809	CH60	60 kDa heat shock protein, mitochondrial	-2.16
P55884	EIF3B	Eukaryotic translation initiation factor 3 subunit B	-2.16
P05023	AT1A1	Sodium/potassium-transporting ATPase subunit alpha-1	-2.16
Q9BV20	MTNA	Methylthioribose-1-phosphate isomerase	-2.16
P17980	PRS6A	26S protease regulatory subunit 6A	-2.15
P61978	HNRPK	Heterogeneous nuclear ribonucleoprotein K	-2.15
Q9UKK9	NUDT5	ADP-sugar pyrophosphatase	-2.15
P27824	CALX	Calnexin	-2.15
P31150	GDIA	Rab GDP dissociation inhibitor alpha	-2.15
O15067	PUR4	Phosphoribosylformylglycinamidine synthase	-2.15
O95861	BPNT1	3'(2'),5'-bisphosphate nucleotidase 1	-2.15
P14625	ENPL	Endoplasmin	-2.14
Q14152	EF1G	Eukaryotic translation initiation factor 3 subunit A	-2.14
P26641	EIF3A	Elongation factor 1-gamma	-2.14
Q14974	IMB1	Importin subunit beta-1	-2.14
P67936	TPM4	Tropomyosin alpha-4 chain	-2.14
P12277	KCRB	Creatine kinase B-type	-2.14
P11021	GRP78	78 kDa glucose-regulated protein	-2.14
Q9P2J5	SYLC	Leucine--tRNA ligase, cytoplasmic	-2.14
Q99613	EIF3C	Eukaryotic translation initiation factor 3 subunit C	-2.14
Q7KZF4	SND1	Staphylococcal nuclease domain-containing protein 1	-2.14
P63104	1433Z	14-3-3 protein zeta/delta	-2.13
Q01105	SET	Protein SET	-2.13
Q86UP2	KTN1	Kinectin	-2.12
Q15393	SF3B3	Splicing factor 3B subunit 3	-2.12
P68371	TBB4B	Tubulin beta-4B chain	-2.12
Q9UBF2	COPG2	Coatomer subunit gamma-2	-2.12

P07910	HNRPC	Heterogeneous nuclear ribonucleoproteins C1/C2	-2.11
Q16186	ADRM1	Proteasomal ubiquitin receptor ADRM1	-2.11
P50395	GDIB	Rab GDP dissociation inhibitor beta	-2.11
O75643	U520	U5 small nuclear ribonucleoprotein 200 kDa helicase	-2.11
Q9UQ80	PA2G4	Proliferation-associated protein 2G4	-2.11
O15372	EIF3H	Eukaryotic translation initiation factor 3 subunit H	-2.11
Q99460	PSMD1	26S proteasome non-ATPase regulatory subunit 1	-2.10
Q92616	GCN1L	Translational activator GCN1	-2.10
Q9UNM6	PSD13	26S proteasome non-ATPase regulatory subunit 13	-2.10
P52907	CAZA1	F-actin-capping protein subunit alpha-1	-2.10
P23396	RS3	40S ribosomal protein S3	-2.09
P49411	EFTU	Elongation factor Tu, mitochondrial	-2.09
P07237	PDIA1	Protein disulfide-isomerase	-2.09
P53004	BIEA	Biliverdin reductase A	-2.09
P49419	AL7A1	Alpha-aminoadipic semialdehyde dehydrogenase	-2.09
O60763	USO1	General vesicular transport factor p115	-2.09
Q9BPU6	DPYL5	Dihydropyrimidinase-related protein 5	-2.08
P21281	VATB2	V-type proton ATPase subunit B, brain isoform	-2.08
P42704	LPPRC	Leucine-rich PPR motif-containing protein, mitochondrial	-2.08
P20073	ANXA7	Annexin A7	-2.07
P13010	XRCC5	X-ray repair cross-complementing protein 5	-2.07
Q15029	U5S1	116 kDa U5 small nuclear ribonucleoprotein component	-2.07
P54886	P5CS	Delta-1-pyrroline-5-carboxylate synthase	-2.07
Q10713	MPPA	Mitochondrial-processing peptidase subunit alpha	-2.07
O75390	CISY	Citrate synthase, mitochondrial	-2.06
O95831	AIFM1	Apoptosis-inducing factor 1, mitochondrial	-2.06
P38919	IF4A3	Eukaryotic initiation factor 4A-III	-2.06

Q15459	SF3A1	Splicing factor 3A subunit 1	-2.06
O75439	MPPB	Mitochondrial-processing peptidase subunit beta	-2.04
P78527	PRKDC	DNA-dependent protein kinase catalytic subunit	-2.04
Q9Y4L1	HYOU1	Hypoxia up-regulated protein 1	-2.03
P14324	FPPS	Farnesyl pyrophosphate synthase	-2.03
P00338	LDHA	L-lactate dehydrogenase A chain	-2.03
Q13200	PSMD2	26S proteasome non-ATPase regulatory subunit 2	-2.03
P35998	PRS7	26S protease regulatory subunit 7	-2.03
O00231	PSD11	26S proteasome non-ATPase regulatory subunit 11	-2.00
O00232	PSD12	26S proteasome non-ATPase regulatory subunit 12	-2.00
Q09028	RBBP4	Histone-binding protein RBBP4	-1.98
P06576	ATPB	ATP synthase subunit beta, mitochondrial	-1.98
P40926	MDHM	Malate dehydrogenase, mitochondrial	-1.97
Q8NBS9	TXND5	Thioredoxin domain-containing protein 5	-1.95
P27797	CALR	Calreticulin	-1.95
P22102	PUR2	Trifunctional purine biosynthetic protein adenosine-3	-1.94
P35232	PHB	Prohibitin	-1.93
P43686	PRS6B	26S protease regulatory subunit 6B	-1.93
P62195	PRS8	26S protease regulatory subunit 8	-1.93
P06748	NPM	Nucleophosmin	-1.92
P09104	ENOG	Gamma-enolase	-1.90
Q9Y262	EIF3L	Eukaryotic translation initiation factor 3 subunit L	-1.89
O14818	PSA7	Proteasome subunit alpha type-7	-1.89
P21333	FLNA	Filamin-A	-1.89
Q9Y265	RUVB1	RuvB-like 1	-1.88
P40939	ECHA	Trifunctional enzyme subunit alpha, mitochondria	-1.88
P09622	DLDH	Dihydrolipoyl dehydrogenase, mitochondrial	-1.87

P14735	IDE	Insulin-degrading enzyme	-1.86
P23246	SFPQ	Splicing factor, proline- and glutamine-rich	-1.85
P54136	SYRC	Arginine--tRNA ligase, cytoplasmic	-1.85
P68363	TBA1B	Tubulin alpha-1B chain	-1.84
Q99798	ACON	Aconitate hydratase, mitochondrial	-1.83
P04181	OAT	Ornithine aminotransferase, mitochondrial	-1.83
P27708	PYR1	CAD protein	-1.83
P25705	ATPA	ATP synthase subunit alpha, mitochondrial	-1.83
P26599	PTBP1	Polypyrimidine tract-binding protein 1	-1.83
Q8N163	CCAR2	Cell cycle and apoptosis regulator protein 2	-1.82
Q6P2E9	EDC4	Enhancer of mRNA-decapping protein 4	-1.81
O75369	FLNB	Filamin-B	-1.81
P60709	ACTB	Actin, cytoplasmic 1	-1.80
P31943	HNRH1	Heterogeneous nuclear ribonucleoprotein H	-1.79
Q00839	HNRPU	Heterogeneous nuclear ribonucleoprotein U	-1.78
P61163	ACTZ	Alpha-centractin	-1.77
Q7L576	CYFP1	Cytoplasmic FMR1-interacting protein 1	-1.76
P07814	SYEP	Bifunctional glutamate/proline--tRNA ligase	-1.76
Q04917	1433F	14-3-3 protein eta	-1.76
Q99623	PHB2	Prohibitin-2	-1.74
P52732	KIF11	Kinesin-like protein KIF11	-1.74
P47897	SYQ	Glutamine--tRNA ligase	-1.73
Q12906	ILF3	Interleukin enhancer-binding factor 3	-1.73
P56545	CTBP2	C-terminal-binding protein 2	-1.70
P31040	SDHA	Succinate dehydrogenase [ubiquinone] flavoprotein subunit, mitochondrial	-1.70
P67809	YBOX1	Nuclease-sensitive element-binding protein 1	-1.66
Q14839	CHD4	Chromodomain-helicase-DNA-binding protein 4	-1.66

P36957	ODO2	Dihydrolipoyllysine-residue succinyltransferase component of 2-oxoglutarate dehydrogenase complex, mitochondrial	-1.66
Q9Y5B9	SP16H	FACT complex subunit SPT16	-1.64
Q14203	DCTN1	Dynactin subunit 1	-1.61
Q96C19	EFHD2	EF-hand domain-containing protein D2	-1.60
P52272	HNRPM	Heterogeneous nuclear ribonucleoprotein M	-1.59
O75131	CPNE3	Copine-3	-1.59
Q9Y2Z0	SUGT1	Suppressor of G2 allele of SKP1 homolog	-1.58
P61247	RS3A	40S ribosomal protein S3a	-1.57
Q13561	DCTN2	Dynactin subunit 2	-1.57
P49448	DHE4	Glutamate dehydrogenase 2, mitochondrial	-1.55
P52597	HNRPF	Heterogeneous nuclear ribonucleoprotein F	-1.54
P22695	QCR2	Cytochrome b-c1 complex subunit 2, mitochondrial	-1.51
O75533	*SF3B1*	*Splicing factor 3B subunit 1*	*-1.50*
P41252	*SYIC*	*Isoleucine--tRNA ligase, cytoplasmic*	*-1.48*
P31930	*QCR1*	*Cytochrome b-c1 complex subunit 1, mitochondrial*	*-1.48*
P12236	*ADT3*	*ADP/ATP translocase 3*	*-1.48*
P14868	*SYDC*	*Aspartate--tRNA ligase, cytoplasmic*	*-1.45*
P05783	*K1C18*	*Keratin, type I cytoskeletal 18*	*-1.45*
Q16658	*FSCN1*	*Fascin*	*-1.43*
P19367	*HXK1*	*Hexokinase-1*	*-1.41*
Q14204	*DYHC1*	*Cytoplasmic dynein 1 heavy chain 1*	*-1.40*
P55084	*ECHB*	*Trifunctional enzyme subunit beta, mitochondrial*	*-1.40*
Q8NAG3	*Q8NAG3*	*highly similar to TROPOMYOSIN, CYTOSKELETAL TYPE*	*-1.39*
Q9Y2A7	*NCKP1*	*Nck-associated protein 1*	*-1.38*
P15880	*RS2*	*40S ribosomal protein S2*	*-1.33*
P48163	*MAOX*	*NADP-dependent malic enzyme*	*-1.30*

Q9UM54	*MYO6*	*Unconventional myosin-VI*	*-1.29*
Q02218	*ODO1*	*2-oxoglutarate dehydrogenase, mitochondrial*	*-1.29*
P08670	*VIME*	*Vimentin*	*-1.27*
P26196	*DDX6*	*Probable ATP-dependent RNA helicase DDX6*	*-1.27*
Q9BV38	*WDR18*	*WD repeat-containing protein 18*	*-1.25*
Q08211	*DHX9*	*ATP-dependent RNA helicase A*	*-1.23*
Q9UJZ1	*STML2*	*Stomatin-like protein 2, mitochondrial*	*-1.23*
Q5T4S7	*UBR4*	*E3 ubiquitin-protein ligase UBR4*	*-1.14*
Q00610	*CLH1*	*Clathrin heavy chain 1*	*-1.12*
Q13813	*SPTN1*	*Spectrin alpha chain, non-erythrocytic 1*	*-1.11*
Q96F07	*CYFP2*	*Cytoplasmic FMR1-interacting protein 2*	*-1.11*
Q01082	*SPTB2*	*Spectrin beta chain, non-erythrocytic 1*	*-1.11*
P62701	*RS4X*	*40S ribosomal protein S4, X isoform*	*-1.08*
P38646	*GRP75*	*Stress-70 protein, mitochondrial*	*-1.07*
P56192	*SYMC*	*Methionine--tRNA ligase, cytoplasmic*	*-1.06*
Q7Z417	*NUFP2*	*Nuclear fragile X mental retardation-interacting protein 2*	*-1.06*
Q9NZI8	*IF2B1*	*Insulin-like growth factor 2 mRNA-binding protein 1*	*-1.05*
P00390	*GSHR*	*Glutathione reductase, mitochondrial*	*-1.03*
Q9UMS4	*PRP19*	*Pre-mRNA-processing factor 19*	*-1.02*
Q02878	*RL6*	*60S ribosomal protein L6*	*-0.98*
Q99459	*CDC5L*	*Cell division cycle 5-like protein*	*-0.97*
P12270	*TPR*	*Nucleoprotein TPR*	*-0.94*
Q9NR30	*DDX21*	*Nucleolar RNA helicase 2*	*-0.94*
P39023	*P39023*	*60S ribosomal protein L3*	*-0.90*
P19338	*NUCL*	*Nucleolin*	*-0.89*
Q15075	*EEA1*	*Early endosome antigen 1*	*-0.88*
P62424	*RL7A*	*60S ribosomal protein L7a*	*-0.86*

P16403	*H12*	*Histone H1.2*	*-0.85*
P05388	*RLA0*	*60S acidic ribosomal protein P0*	*-0.79*
Q8WWM7	*ATX2L*	*Ataxin-2-like protein*	*-0.70*
P10515	*ODP2*	*Dihydrolipoyllysine-residue acetyltransferase component of pyruvate dehydrogenase complex, mitochondrial*	*-0.69*
Q14980	*NUMA1*	*Nuclear mitotic apparatus protein 1*	*-0.69*
P36578	*RL4*	*60S ribosomal protein L4*	*-0.68*
O00148	*DX39A*	*ATP-dependent RNA helicase DDX39A*	*-0.60*
Q9UQ35	*SRRM2*	*Serine/arginine repetitive matrix protein 2*	*-0.47*
P35580	*MYH10*	*Myosin-10*	*-0.47*
P35579	*MYH9*	*Myosin-9*	*-0.43*
P11498	*PYC*	*Pyruvate carboxylase, mitochondrial*	*-0.41*
Q12802	*AKP13*	*A-kinase anchor protein 13*	*-0.17*

APPENDIX II

List of putative Claspin interacting proteins identified by MAP-SILAC mass spectrometry analysis. Column 1 contains the Uniprot accession code, column 2 the gene name, column 3 the protein name and column 4 percentage of detection in the CRAPome. The data is listed by detection in the CRAPome from smallest to largest. Proteins detected in over 30% of CRAPome control experiments are displayed in italics, were eliminated from further analysis.

Protein ID	Gene Name	Protein name	Detection in CRAPome (%)
Q9HAW4	CLSPN	Claspin	0
P50995	ANX11	Annexin A11	1
Q9BV20	MTNA	Methylthioribose-1-phosphate isomerase	1
O95861	BPNT1	3'(2'),5'-bisphosphate nucleotidase 1	1
P54725	RD23A	UV excision repair protein RAD23 homolog A	2
Q00796	DHSO	Sorbitol dehydrogenase	2
P56545	CTBP2	C-terminal-binding protein 2	2
P17174	AATC	Aspartate aminotransferase, cytoplasmic	3
P53004	BIEA	Biliverdin reductase A	3
Q01581	HMCS1	Hydroxymethylglutaryl-CoA synthase, cytoplasmic	3
P28482	MK01	Mitogen-activated protein kinase 1	4
P15121	ALDR	Aldose reductase	4
Q6YN16	HSDL2	Hydroxysteroid dehydrogenase-like protein 2	4
P20073	ANXA7	Annexin A7	4
Q9UGI8	TES	Testin	4
P14324	FPPS	Farnesyl pyrophosphate synthase	4
P53041	PPP5	Serine/threonine-protein phosphatase 5	4
P14735	IDE	Insulin-degrading enzyme	4
P51649	SSDH	Succinate-semialdehyde dehydrogenase, mitochondrial	4
Q10713	MPPA	Mitochondrial-processing peptidase subunit alpha	5
Q9Y617	SERC	Phosphoserine aminotransferase	5

P06737	PYGL	Glycogen phosphorylase, liver form	5
Q9UHD1	CHRD1	Cysteine and histidine-rich domain-containing protein 1	5
P11413	G6PD	Glucose-6-phosphate 1-dehydrogenase	5
O75131	CPNE3	Copine-3	5
Q9BPU6	DPYL5	Dihydropyrimidinase-related protein 5	6
P38117	ETFB	Electron transfer flavoprotein subunit beta	6
P00505	AATM	Aspartate aminotransferase, mitochondrial	6
P55809	SCOT1	Succinyl-CoA:3-ketoacid coenzyme A transferase 1, mitochondrial	7
Q99798	ACON	Aconitate hydratase, mitochondrial	7
P45974	USP5	Ubiquitin carboxyl-terminal hydrolase 5	7
Q9UKK9	NUDT5	ADP-sugar pyrophosphatase	7
Q8NBS9	TXND5	Thioredoxin domain-containing protein 5	7
P30566	PUR8	Adenylosuccinate lyase	8
O75439	MPPB	Mitochondrial-processing peptidase subunit beta	8
Q96C19	EFHD2	EF-hand domain-containing protein D2	8
Q9BXJ9	NAA15	N-alpha-acetyltransferase 15, NatA auxiliary subunit	8
P12081	SYHC	Histidine--tRNA ligase, cytoplasmic	8
P35221	CTNA1	Catenin alpha-1	8
P55786	PSA	Puromycin-sensitive aminopeptidase	8
Q13867	BLMH	Bleomycin hydrolase	9
P49419	AL7A1	Alpha-aminoadipic semialdehyde dehydrogenase	9
P22695	QCR2	Cytochrome b-c1 complex subunit 2, mitochondrial	9
Q86UP2	KTN1	Kinectin	9
Q9Y2Z0	SUGT1	Suppressor of G2 allele of SKP1 homolog	9
P49189	AL9A1	4-trimethylaminobutyraldehyde dehydrogenase	10
P50570	DYN2	Dynamin-2	10
P30084	ECHM	Enoyl-CoA hydratase, mitochondrial	10

O15067	PUR4	Phosphoribosylformylglycinamidine synthase	10
P21281	VATB2	V-type proton ATPase subunit B, brain isoform	10
Q9UBT2	SAE2	SUMO-activating enzyme subunit 2	10
P37837	TALDO	Transaldolase	10
Q6IN85	P4R3A	Serine/threonine-protein phosphatase 4 regulatory subunit 3A	10
Q9UBE0	SAE1	SUMO-activating enzyme subunit 1	10
P51858	HDGF	Hepatoma-derived growth factor	10
P31040	SDHA	Succinate dehydrogenase [ubiquinone] flavoprotein subunit, mitochondrial	11
Q10567	AP1B1	AP-1 complex subunit beta-1	11
Q6P2E9	EDC4	Enhancer of mRNA-decapping protein 4	11
Q7L576	CYFP1	Cytoplasmic FMR1-interacting protein 1	11
Q9BT78	CSN4	COP9 signalosome complex subunit 4	12
Q9Y4L1	HYOU1	Hypoxia up-regulated protein 1	12
O43491	E41L2	Band 4.1-like protein 2	12
O00299	CLIC1	Chloride intracellular channel protein 1	12
P29401	TKT	Transketolase	12
P49588	SYAC	Alanine--tRNA ligase, cytoplasmic	13
P49006	MRP	MARCKS-related protein	13
P63010	AP2B1	AP-2 complex subunit beta	13
Q96AE4	FUBP1	Far upstream element-binding protein 1	13
Q8WUM4	PDC6I	Programmed cell death 6-interacting protein	13
Q9Y2J2	E41L3	Band 4.1-like protein 3	13
O15294	OGT1	UDP-N-acetylglucosamine--peptide N-acetylglucosaminyltransferase 110 kDa subunit	13
P62495	ERF1	Eukaryotic peptide chain release factor subunit 1	14
P18206	VINC	Vinculin	14
P36957	ODO2	Dihydrolipoyllysine-residue succinyltransferase component of 2-oxoglutarate dehydrogenase complex, mitochondrial	14

Q8N1F7	NUP93	Nuclear pore complex protein Nup93	14
O95433	AHSA1	Activator of 90 kDa heat shock protein ATPase homolog 1	14
Q99615	DNJC7	DnaJ homolog subfamily C member 7	14
P13667	PDIA4	Protein disulfide-isomerase A4	14
P06744	G6PI	Glucose-6-phosphate isomerase	15
P24752	THIL	Acetyl-CoA acetyltransferase, mitochondrial	15
P31150	GDIA	Rab GDP dissociation inhibitor alpha	15
O60763	USO1	General vesicular transport factor p115	15
Q13011	ECH1	Delta(3,5)-Delta(2,4)-dienoyl-CoA isomerase, mitochondrial	16
P26639	SYTC	Threonine--tRNA ligase, cytoplasmic	16
Q93008	USP9X	Probable ubiquitin carboxyl-terminal hydrolase FAF-X	16
O75534	CSDE1	Cold shock domain-containing protein E1	16
P17858	PFKAL	ATP-dependent 6-phosphofructokinase, liver type	16
P52209	6PGD	6-phosphogluconate dehydrogenase, decarboxylating	16
Q9UBF2	COPG2	Coatomer subunit gamma-2	16
Q16186	ADRM1	Proteasomal ubiquitin receptor ADRM1	16
P09012	SNRPA	U1 small nuclear ribonucleoprotein A	17
Q16181	SEPT7	Septin-7	17
P40939	ECHA	Trifunctional enzyme subunit alpha, mitochondria	18
P55036	PSMD4	26S proteasome non-ATPase regulatory subunit 4	18
O95757	HS74L	Heat shock 70 kDa protein 4L	18
Q7Z6Z7	MULE	E3 ubiquitin-protein ligase MULE	18
Q9Y5B9	SP16H	FACT complex subunit SPT16	18
Q08J23	NSUN2	tRNA (cytosine(34)-C(5))-methyltransferase	19
Q9UNM6	PSD13	26S proteasome non-ATPase regulatory subunit 13	19
Q16543	CDC37	Hsp90 co-chaperone Cdc37	19
P50395	GDIB	Rab GDP dissociation inhibitor beta	19

Q14839	CHD4	Chromodomain-helicase-DNA-binding protein 4	19
Q9Y490	TLN1	Talin-1	20
P25789	PSA4	Proteasome subunit alpha type-4	20
P50502	F10A1	Hsc70-interacting protein	20
P12268	IMDH2	Inosine-5'-monophosphate dehydrogenase 2	20
O15372	EIF3H	Eukaryotic translation initiation factor 3 subunit H	20
P49448	DHE4	Glutamate dehydrogenase 2, mitochondrial	20
O60256	KPRB	Phosphoribosyl pyrophosphate synthase-associated protein 2	20
P09622	DLDH	Dihydrolipoyl dehydrogenase, mitochondrial	20
Q01518	CAP1	Adenylyl cyclase-associated protein 1	21
P35232	PHB	Prohibitin	21
Q14203	DCTN1	Dynactin subunit 1	21
P00558	PGK1	Phosphoglycerate kinase 1	21
P25786	PSA1	Proteasome subunit alpha type-1	21
Q86VP6	CAND1	Cullin-associated NEDD8-dissociated protein 1	21
O14818	PSA7	Proteasome subunit alpha type-7	22
P60174	TPIS	Triosephosphate isomerase	22
O75390	CISY	Citrate synthase, mitochondrial	22
Q13561	DCTN2	Dynactin subunit 2	22
Q9Y262	EIF3L	Eukaryotic translation initiation factor 3 subunit L	22
P63151	2ABA	Serine/threonine-protein phosphatase 2A 55 kDa regulatory subunit B alpha isoform	23
P54886	P5CS	Delta-1-pyrroline-5-carboxylate synthase	23
P46821	MAP1B	Microtubule-associated protein 1B	23
P47897	SYQ	Glutamine--tRNA ligase	23
P49736	MCM2	DNA replication licensing factor MCM2	23
P46940	IQGA1	Ras GTPase-activating-like protein IQGAP1	23
P62191	PRS4	26S protease regulatory subunit 4	23

Q02790	FKBP4	Peptidyl-prolyl cis-trans isomerase FKBP4	23
P04181	OAT	Ornithine aminotransferase, mitochondrial	23
P61163	ACTZ	Alpha-centractin	23
Q99623	PHB2	Prohibitin-2	23
P60228	EIF3E	Eukaryotic translation initiation factor 3 subunit E	23
P33176	KINH	Kinesin-1 heavy chain	24
O00231	PSD11	26S proteasome non-ATPase regulatory subunit 11	24
O00232	PSD12	26S proteasome non-ATPase regulatory subunit 12	24
P43686	PRS6B	26S protease regulatory subunit 6B	24
P23526	SAHH	Adenosylhomocysteinase	24
Q9Y266	NUDC	Nuclear migration protein nudC	24
P26640	SYVC	Valine--tRNA ligase	24
Q14566	MCM6	DNA replication licensing factor MCM6	25
P34897	GLYM	Serine hydroxymethyltransferase, mitochondrial	25
O95831	AIFM1	Apoptosis-inducing factor 1, mitochondrial	25
Q04637	IF4G1	Eukaryotic translation initiation factor 4 gamma 1	25
P05455	LA	Lupus La protein	25
Q99460	PSMD1	26S proteasome non-ATPase regulatory subunit 1	25
P40926	MDHM	Malate dehydrogenase, mitochondrial	25
P30101	PDIA3	Protein disulfide-isomerase A3	25
Q9UQ80	PA2G4	Proliferation-associated protein 2G4	25
Q92616	GCN1L	Translational activator GCN1	25
P22102	PUR2	Trifunctional purine biosynthetic protein adenosine-3	25
Q14697	GANAB	Neutral alpha-glucosidase AB	26
P22234	PUR6	Multifunctional protein ADE2	26
P22314	UBA1	Ubiquitin-like modifier-activating enzyme 1	26
P55884	EIF3B	Eukaryotic translation initiation factor 3 subunit B	26

Q99613	EIF3C	Eukaryotic translation initiation factor 3 subunit C	27
P11586	C1TC	C-1-tetrahydrofolate synthase, cytoplasmic	27
P49321	NASP	Nuclear autoantigenic sperm protein	27
P54136	SYRC	Arginine--tRNA ligase, cytoplasmic	27
Q14152	EF1G	Eukaryotic translation initiation factor 3 subunit A	27
O43684	BUB3	Mitotic checkpoint protein BUB3	27
P17980	PRS6A	26S protease regulatory subunit 6A	27
P27797	CALR	Calreticulin	28
P07237	PDIA1	Protein disulfide-isomerase	28
P62195	PRS8	26S protease regulatory subunit 8	28
Q04917	1433F	14-3-3 protein eta	28
Q12931	TRAP1	Heat shock protein 75 kDa, mitochondrial	29
P53396	ACLY	ATP-citrate synthase	29
P05023	AT1A1	Sodium/potassium-transporting ATPase subunit alpha-1	29
Q7KZF4	SND1	Staphylococcal nuclease domain-containing protein 1	29
Q8N163	CCAR2	Cell cycle and apoptosis regulator protein 2	29
Q92598	HS105	Heat shock protein 105 kDa	29
P25205	MCM3	DNA replication licensing factor MCM3	29
P31948	STIP1	Stress-induced-phosphoprotein 1	29
Q14978	NOLC1	Nucleolar and coiled-body phosphoprotein 1	29
Q13200	PSMD2	26S proteasome non-ATPase regulatory subunit 2	30
P15924	*DESP*	*Desmoplakin*	*31*
P55060	*XPO2*	*Exportin-2*	*31*
P27824	*CALX*	*Calnexin*	*31*
P35998	*PRS7*	*26S protease regulatory subunit 7*	*31*
P67936	*TPM4*	*Tropomyosin alpha-4 chain*	*31*
Q13347	*EIF3I*	*Eukaryotic translation initiation factor 3 subunit I*	*31*

Q15084	*PDIA6*	*Protein disulfide-isomerase A6*	*31*
P42704	*LPPRC*	*Leucine-rich PPR motif-containing protein, mitochondrial*	*32*
P61981	*1433G*	*14-3-3 protein gamma*	*32*
Q9P2J5	*SYLC*	*Leucine--tRNA ligase, cytoplasmic*	*32*
P30153	*2AAA*	*Serine/threonine-protein phosphatase 2A 65 kDa regulatory subunit A alpha isoform*	*32*
P34932	*HSP74*	*Heat shock 70 kDa protein 4*	*32*
Q92945	*FUBP2*	*Far upstream element-binding protein 2*	*32*
P52907	*CAZA1*	*F-actin-capping protein subunit alpha-1*	*32*
P63244	*GBLP*	*Guanine nucleotide-binding protein subunit beta-2-like 1*	*33*
Q5VTE0	*EF1A3*	*Putative elongation factor 1-alpha-like 3*	*33*
Q15459	*SF3A1*	*Splicing factor 3A subunit 1*	*33*
Q13838	*DX39B*	*Spliceosome RNA helicase DDX39B*	*34*
P49411	*EFTU*	*Elongation factor Tu, mitochondrial*	*34*
P00338	*LDHA*	*L-lactate dehydrogenase A chain*	*34*
Q9Y230	*RUVB2*	*RuvB-like 2*	*34*
O43707	*ACTN4*	*Alpha-actinin-4*	*34*
P31946	*1433B*	*14-3-3 protein beta/alpha*	*36*
O75643	*U520*	*U5 small nuclear ribonucleoprotein 200 kDa helicase*	*36*
P38919	*IF4A3*	*Eukaryotic initiation factor 4A-III*	*36*
P27708	*PYR1*	*CAD protein*	*36*
Q09028	*RBBP4*	*Histone-binding protein RBBP4*	*36*
P07355	*ANXA2*	*Annexin A2*	*36*
Q01105	*SET*	*Protein SET*	*37*
O43175	*SERA*	*D-3-phosphoglycerate dehydrogenase*	*37*
Q9Y265	*RUVB1*	*RuvB-like 1*	*37*
P27348	*1433T*	*14-3-3 protein theta*	*37*
P07814	*SYEP*	*Bifunctional glutamate/proline--tRNA ligase*	*38*

Q12906	*ILF3*	*Interleukin enhancer-binding factor 3*	*38*
P08865	*RSSA*	*40S ribosomal protein SA*	*39*
Q14974	*IMB1*	*Importin subunit beta-1*	*39*
Q15029	*U5S1*	*116 kDa U5 small nuclear ribonucleoprotein component*	*39*
Q2VIR3	*IF2GL*	*Putative eukaryotic translation initiation factor 2 subunit 3-like protein*	*40*
P12277	*KCRB*	*Creatine kinase B-type*	*40*
P52732	*KIF11*	*Kinesin-like protein KIF11*	*40*
P07195	*LDHB*	*L-lactate dehydrogenase B chain*	*40*
P49368	*TCPG*	*T-complex protein 1 subunit gamma*	*40*
P49327	*FAS*	*Fatty acid synthase*	*41*
P55072	*TERA*	*Transitional endoplasmic reticulum ATPase*	*41*
P09104	*ENOG*	*Gamma-enolase*	*41*
O75369	*FLNB*	*Filamin-B*	*42*
Q99832	*TCPH*	*T-complex protein 1 subunit eta*	*42*
P04075	*ALDOA*	*Fructose-bisphosphate aldolase A*	*42*
P26599	*PTBP1*	*Polypyrimidine tract-binding protein 1*	*42*
Q15393	*SF3B3*	*Splicing factor 3B subunit 3*	*42*
Q8NC51	*PAIRB*	*Plasminogen activator inhibitor 1 RNA-binding protein*	*43*
O14744	*ANM5*	*Protein arginine N-methyltransferase 5*	*43*
P78527	*PRKDC*	*DNA-dependent protein kinase catalytic subunit*	*43*
P58107	*EPIPL*	*Epiplakin*	*43*
Q13263	*TIF1B*	*Transcription intermediary factor 1-beta*	*43*
P40227	*TCPZ*	*T-complex protein 1 subunit zeta*	*43*
P78371	*TCPB*	*T-complex protein 1 subunit beta*	*44*
P63104	*1433Z*	*14-3-3 protein zeta/delta*	*44*
P07910	*HNRPC*	*Heterogeneous nuclear ribonucleoproteins C1/C2*	*44*
P48643	*TCPE*	*T-complex protein 1 subunit epsilon*	*44*

P50990	*TCPQ*	*T-complex protein 1 subunit theta*	*45*
P17987	*TCPA*	*T-complex protein 1 subunit alpha*	*45*
P50991	*TCPD*	*T-complex protein 1 subunit delta*	*45*
P62258	*1433E*	*14-3-3 protein epsilon*	*45*
P14625	*ENPL*	*Endoplasmin*	*45*
Q15366	*PCBP2*	*Poly(rC)-binding protein 2*	*46*
P13010	*XRCC5*	*X-ray repair cross-complementing protein 5*	*46*
P60842	*IF4A1*	*Eukaryotic initiation factor 4A-I*	*46*
P14866	*HNRPL*	*Heterogeneous nuclear ribonucleoprotein L*	*46*
P26641	*EIF3A*	*Elongation factor 1-gamma*	*47*
Q15365	*PCBP1*	*Poly(rC)-binding protein 1*	*47*
B4DJ98	*B4DJ98*	*highly similar to Protein disulfide-isomerase A3*	*48*
P23246	*SFPQ*	*Splicing factor, proline- and glutamine-rich*	*49*
P61247	*RS3A*	*40S ribosomal protein S3a*	*49*
P13639	*EF2*	*Elongation factor 2*	*50*
P25705	*ATPA*	*ATP synthase subunit alpha, mitochondrial*	*51*
P06576	*ATPB*	*ATP synthase subunit beta, mitochondrial*	*51*
P52272	*HNRPM*	*Heterogeneous nuclear ribonucleoprotein M*	*54*
P06733	*ENOA*	*Alpha-enolase*	*54*
P21333	*FLNA*	*Filamin-A*	*55*
P10809	*CH60*	*60 kDa heat shock protein, mitochondrial*	*56*
P67809	*YBOX1*	*Nuclease-sensitive element-binding protein 1*	*57*
P62987	*RL40*	*Ubiquitin-60S ribosomal protein L40*	*57*
Q92841	*DDX17*	*Probable ATP-dependent RNA helicase DDX17*	*58*
P52597	*HNRPF*	*Heterogeneous nuclear ribonucleoprotein F*	*59*
P04406	*G3P*	*Glyceraldehyde-3-phosphate dehydrogenase*	*60*
P14618	*KPYM*	*Pyruvate kinase PKM*	*61*

P06748	*NPM*	*Nucleophosmin*	*61*
P22626	*ROA2*	*Heterogeneous nuclear ribonucleoproteins A2/B1*	*64*
P31943	*HNRH1*	*Heterogeneous nuclear ribonucleoprotein H*	*64*
P23396	*RS3*	*40S ribosomal protein S3*	*65*
P09651	*ROA1*	*Heterogeneous nuclear ribonucleoprotein A1*	*65*
P07900	*HS90A*	*Heat shock protein HSP 90-alpha*	*66*
P08238	*HS90B*	*Heat shock protein HSP 90-beta*	*67*
Q00839	*HNRPU*	*Heterogeneous nuclear ribonucleoprotein U*	*68*
P61978	*HNRPK*	*Heterogeneous nuclear ribonucleoprotein K*	*70*
P11021	*GRP78*	*78 kDa glucose-regulated protein*	*88*
P60709	*ACTB*	*Actin, cytoplasmic 1*	*88*
P68371	*TBB4B*	*Tubulin beta-4B chain*	*91*
P07437	*TBB5*	*Tubulin beta chain*	*93*
P68363	*TBA1B*	*Tubulin alpha-1B chain*	*95*
P08107	*HSP71*	*Heat shock 70 kDa protein 1A/1B*	*96*
P11142	*HSP7C*	*Heat shock cognate 71 kDa protein*	*96*

APPENDIX III

The final list of putative Claspin interacting proteins identified by MAP-SILAC mass spectrometry analysis and filtered by SILAC ratio and CRAPome detection. Column 1 contains the Uniprot accession code, column 2 the gene name, column 3 the protein name and column 4 the SILAC ratio expressed as the Log2 SILAC ratio of empty vector/Claspin. The data is listed by SILAC ratio from smallest to largest, with the most negative SILAC ratio representing the most enriched protein compared to the control.

Protein ID	Gene Name	Protein name	Log2 (EV/CLSPN)
Q9HAW4	CLSPN	Claspin	-5.82
Q92598	HS105	Heat shock protein 105 kDa	-3.92
Q9UGI8	TES	Testin	-3.35
O95433	AHSA1	Activator of 90 kDa heat shock protein ATPase homolog 1	-3.19
Q04637	IF4G1	Eukaryotic translation initiation factor 4 gamma 1	-3.18
P49588	SYAC	Alanine--tRNA ligase, cytoplasmic	-3.07
Q96AE4	FUBP1	Far upstream element-binding protein 1	-2.93
Q9UBE0	SAE1	SUMO-activating enzyme subunit 1	-2.90
P63151	2ABA	Serine/threonine-protein phosphatase 2A 55 kDa regulatory subunit B alpha isoform	-2.90
O75534	CSDE1	Cold shock domain-containing protein E1	-2.89
Q93008	USP9X	Probable ubiquitin carboxyl-terminal hydrolase FAF-X	-2.84
Q9Y490	TLN1	Talin-1	-2.82
P25205	MCM3	DNA replication licensing factor MCM3	-2.81
P53041	PPP5	Serine/threonine-protein phosphatase 5	-2.80
Q00796	DHSO	Sorbitol dehydrogenase	-2.76
Q10567	AP1B1	AP-1 complex subunit beta-1	-2.76
Q13011	ECH1	Delta(3,5)-Delta(2,4)-dienoyl-CoA isomerase, mitochondrial	-2.75
P51858	HDGF	Hepatoma-derived growth factor	-2.74
P06737	PYGL	Glycogen phosphorylase, liver form	-2.74
Q9BXJ9	NAA15	N-alpha-acetyltransferase 15, NatA auxiliary subunit	-2.74
P11586	C1TC	C-1-tetrahydrofolate synthase, cytoplasmic	-2.73
P45974	USP5	Ubiquitin carboxyl-terminal hydrolase 5	-2.72

Q14566	MCM6	DNA replication licensing factor MCM6	-2.72
P49736	MCM2	DNA replication licensing factor MCM2	-2.71
O43491	E41L2	Band 4.1-like protein 2	-2.67
P38117	ETFB	Electron transfer flavoprotein subunit beta	-2.65
Q9UHD1	CHRD1	Cysteine and histidine-rich domain-containing protein 1	-2.64
Q6IN85	P4R3A	Serine/threonine-protein phosphatase 4 regulatory subunit 3A	-2.63
P17858	PFKAL	ATP-dependent 6-phosphofructokinase, liver type	-2.62
O95757	HS74L	Heat shock 70 kDa protein 4L	-2.60
P62495	ERF1	Eukaryotic peptide chain release factor subunit 1	-2.60
P18206	VINC	Vinculin	-2.59
P46940	IQGA1	Ras GTPase-activating-like protein IQGAP1	-2.58
P50502	F10A1	Hsc70-interacting protein	-2.58
O00299	CLIC1	Chloride intracellular channel protein 1	-2.58
P62191	PRS4	26S protease regulatory subunit 4	-2.57
Q9Y266	NUDC	Nuclear migration protein nudC	-2.57
Q9UBT2	SAE2	SUMO-activating enzyme subunit 2	-2.57
P28482	MK01	Mitogen-activated protein kinase 1	-2.54
Q16543	CDC37	Hsp90 co-chaperone Cdc37	-2.54
P31948	STIP1	Stress-induced-phosphoprotein 1	-2.54
Q12931	TRAP1	Heat shock protein 75 kDa, mitochondrial	-2.53
P22314	UBA1	Ubiquitin-like modifier-activating enzyme 1	-2.53
Q01581	HMCS1	Hydroxymethylglutaryl-CoA synthase, cytoplasmic	-2.53
P37837	TALDO	Transaldolase	-2.52
Q14697	GANAB	Neutral alpha-glucosidase AB	-2.52
Q14978	NOLC1	Nucleolar and coiled-body phosphoprotein 1	-2.51
P22234	PUR6	Multifunctional protein ADE2	-2.50
P06744	G6PI	Glucose-6-phosphate isomerase	-2.49

Q9Y617	SERC	Phosphoserine aminotransferase	-2.48
P30566	PUR8	Adenylosuccinate lyase	-2.47
Q99615	DNJC7	DnaJ homolog subfamily C member 7	-2.47
P12081	SYHC	Histidine--tRNA ligase, cytoplasmic	-2.46
Q86VP6	CAND1	Cullin-associated NEDD8-dissociated protein 1	-2.45
P00558	PGK1	Phosphoglycerate kinase 1	-2.45
Q01518	CAP1	Adenylyl cyclase-associated protein 1	-2.45
O60256	KPRB	Phosphoribosyl pyrophosphate synthase-associated protein 2	-2.42
P49321	NASP	Nuclear autoantigenic sperm protein	-2.41
P13667	PDIA4	Protein disulfide-isomerase A4	-2.40
P63010	AP2B1	AP-2 complex subunit beta	-2.40
P34897	GLYM	Serine hydroxymethyltransferase, mitochondrial	-2.39
P30101	PDIA3	Protein disulfide-isomerase A3	-2.39
P15121	ALDR	Aldose reductase	-2.38
Q9BT78	CSN4	COP9 signalosome complex subunit 4	-2.38
Q16181	SEPT7	Septin-7	-2.37
P26640	SYVC	Valine--tRNA ligase	-2.34
O43684	BUB3	Mitotic checkpoint protein BUB3	-2.34
P35221	CTNA1	Catenin alpha-1	-2.33
P50995	ANX11	Annexin A11	-2.33
Q02790	FKBP4	Peptidyl-prolyl cis-trans isomerase FKBP4	-2.32
P26639	SYTC	Threonine--tRNA ligase, cytoplasmic	-2.31
P11413	G6PD	Glucose-6-phosphate 1-dehydrogenase	-2.31
P55809	SCOT1	Succinyl-CoA:3-ketoacid coenzyme A transferase 1, mitochondrial	-2.30
P25789	PSA4	Proteasome subunit alpha type-4	-2.30
Q13867	BLMH	Bleomycin hydrolase	-2.30
P60228	EIF3E	Eukaryotic translation initiation factor 3 subunit E	-2.30

Q8WUM4	PDC6I	Programmed cell death 6-interacting protein	-2.30
P46821	MAP1B	Microtubule-associated protein 1B	-2.30
P29401	TKT	Transketolase	-2.30
P25786	PSA1	Proteasome subunit alpha type-1	-2.30
P53396	ACLY	ATP-citrate synthase	-2.29
Q7Z6Z7	MULE	E3 ubiquitin-protein ligase MULE	-2.29
P33176	KINH	Kinesin-1 heavy chain	-2.28
Q8N1F7	NUP93	Nuclear pore complex protein Nup93	-2.28
P49189	AL9A1	4-trimethylaminobutyraldehyde dehydrogenase	-2.27
P55036	PSMD4	26S proteasome non-ATPase regulatory subunit 4	-2.24
Q9Y2J2	E41L3	Band 4.1-like protein 3	-2.24
P23526	SAHH	Adenosylhomocysteinase	-2.24
P00505	AATM	Aspartate aminotransferase, mitochondrial	-2.24
P17174	AATC	Aspartate aminotransferase, cytoplasmic	-2.23
P54725	RD23A	UV excision repair protein RAD23 homolog A	-2.23
Q6YN16	HSDL2	Hydroxysteroid dehydrogenase-like protein 2	-2.23
P09012	SNRPA	U1 small nuclear ribonucleoprotein A	-2.22
P24752	THIL	Acetyl-CoA acetyltransferase, mitochondrial	-2.22
P05455	LA	Lupus La protein	-2.22
P49006	MRP	MARCKS-related protein	-2.21
P12268	IMDH2	Inosine-5'-monophosphate dehydrogenase 2	-2.20
O15294	OGT1	UDP-N-acetylglucosamine--peptide N-acetylglucosaminyltransferase 110 kDa subunit	-2.20
P52209	6PGD	6-phosphogluconate dehydrogenase, decarboxylating	-2.19
P55786	PSA	Puromycin-sensitive aminopeptidase	-2.19
P51649	SSDH	Succinate-semialdehyde dehydrogenase, mitochondrial	-2.18
Q08J23	NSUN2	tRNA (cytosine(34)-C(5))-methyltransferase	-2.18
P60174	TPIS	Triosephosphate isomerase	-2.18

P50570	DYN2	Dynamin-2	-2.18
P30084	ECHM	Enoyl-CoA hydratase, mitochondrial	-2.17
P55884	EIF3B	Eukaryotic translation initiation factor 3 subunit B	-2.16
P05023	AT1A1	Sodium/potassium-transporting ATPase subunit alpha-1	-2.16
Q9BV20	MTNA	Methylthioribose-1-phosphate isomerase	-2.16
P17980	PRS6A	26S protease regulatory subunit 6A	-2.15
Q9UKK9	NUDT5	ADP-sugar pyrophosphatase	-2.15
P31150	GDIA	Rab GDP dissociation inhibitor alpha	-2.15
O15067	PUR4	Phosphoribosylformylglycinamidine synthase	-2.15
O95861	BPNT1	3'(2'),5'-bisphosphate nucleotidase 1	-2.15
Q14152	EF1G	Eukaryotic translation initiation factor 3 subunit A	-2.14
Q99613	EIF3C	Eukaryotic translation initiation factor 3 subunit C	-2.14
Q7KZF4	SND1	Staphylococcal nuclease domain-containing protein 1	-2.14
Q86UP2	KTN1	Kinectin	-2.12
Q9UBF2	COPG2	Coatomer subunit gamma-2	-2.12
Q16186	ADRM1	Proteasomal ubiquitin receptor ADRM1	-2.11
P50395	GDIB	Rab GDP dissociation inhibitor beta	-2.11
Q9UQ80	PA2G4	Proliferation-associated protein 2G4	-2.11
O15372	EIF3H	Eukaryotic translation initiation factor 3 subunit H	-2.11
Q99460	PSMD1	26S proteasome non-ATPase regulatory subunit 1	-2.10
Q92616	GCN1L	Translational activator GCN1	-2.10
Q9UNM6	PSD13	26S proteasome non-ATPase regulatory subunit 13	-2.10
P07237	PDIA1	Protein disulfide-isomerase	-2.09
P53004	BIEA	Biliverdin reductase A	-2.09
P49419	AL7A1	Alpha-aminoadipic semialdehyde dehydrogenase	-2.09
O60763	USO1	General vesicular transport factor p115	-2.09
Q9BPU6	DPYL5	Dihydropyrimidinase-related protein 5	-2.08

P21281	VATB2	V-type proton ATPase subunit B, brain isoform	-2.08
P20073	ANXA7	Annexin A7	-2.07
P54886	P5CS	Delta-1-pyrroline-5-carboxylate synthase	-2.07
Q10713	MPPA	Mitochondrial-processing peptidase subunit alpha	-2.07
O75390	CISY	Citrate synthase, mitochondrial	-2.06
O95831	AIFM1	Apoptosis-inducing factor 1, mitochondrial	-2.06
O75439	MPPB	Mitochondrial-processing peptidase subunit beta	-2.04
Q9Y4L1	HYOU1	Hypoxia up-regulated protein 1	-2.03
P14324	FPPS	Farnesyl pyrophosphate synthase	-2.03
Q13200	PSMD2	26S proteasome non-ATPase regulatory subunit 2	-2.03
O00231	PSD11	26S proteasome non-ATPase regulatory subunit 11	-2.00
O00232	PSD12	26S proteasome non-ATPase regulatory subunit 12	-2.00
P40926	MDHM	Malate dehydrogenase, mitochondrial	-1.97
Q8NBS9	TXND5	Thioredoxin domain-containing protein 5	-1.95
P27797	CALR	Calreticulin	-1.95
P22102	PUR2	Trifunctional purine biosynthetic protein adenosine-3	-1.94
P35232	PHB	Prohibitin	-1.93
P43686	PRS6B	26S protease regulatory subunit 6B	-1.93
P62195	PRS8	26S protease regulatory subunit 8	-1.93
Q9Y262	EIF3L	Eukaryotic translation initiation factor 3 subunit L	-1.89
O14818	PSA7	Proteasome subunit alpha type-7	-1.89
P40939	ECHA	Trifunctional enzyme subunit alpha, mitochondria	-1.88
P09622	DLDH	Dihydrolipoyl dehydrogenase, mitochondrial	-1.87
P14735	IDE	Insulin-degrading enzyme	-1.86
P54136	SYRC	Arginine--tRNA ligase, cytoplasmic	-1.85
Q99798	ACON	Aconitate hydratase, mitochondrial	-1.83
P04181	OAT	Ornithine aminotransferase, mitochondrial	-1.83

Q8N163	CCAR2	Cell cycle and apoptosis regulator protein 2	-1.82
Q6P2E9	EDC4	Enhancer of mRNA-decapping protein 4	-1.81
P61163	ACTZ	Alpha-centractin	-1.77
Q7L576	CYFP1	Cytoplasmic FMR1-interacting protein 1	-1.76
Q04917	1433F	14-3-3 protein eta	-1.76
Q99623	PHB2	Prohibitin-2	-1.74
P47897	SYQ	Glutamine--tRNA ligase	-1.73
P56545	CTBP2	C-terminal-binding protein 2	-1.70
P31040	SDHA	Succinate dehydrogenase [ubiquinone] flavoprotein subunit, mitochondrial	-1.70
Q14839	CHD4	Chromodomain-helicase-DNA-binding protein 4	-1.66
P36957	ODO2	Dihydrolipoyllysine-residue succinyltransferase component of 2-oxoglutarate dehydrogenase complex, mitochondrial	-1.66
Q9Y5B9	SP16H	FACT complex subunit SPT16	-1.64
Q14203	DCTN1	Dynactin subunit 1	-1.61
Q96C19	EFHD2	EF-hand domain-containing protein D2	-1.60
O75131	CPNE3	Copine-3	-1.59
Q9Y2Z0	SUGT1	Suppressor of G2 allele of SKP1 homolog	-1.58
Q13561	DCTN2	Dynactin subunit 2	-1.57
P49448	DHE4	Glutamate dehydrogenase 2, mitochondrial	-1.55
P22695	QCR2	Cytochrome b-c1 complex subunit 2, mitochondrial	-1.51